
Development of a Water Boil-Off Spent Fuel Calorimeter System

**J. M. Creer
J. W. Shupe, Jr.**

May 1981

**Prepared for the Hanford Engineering
Development Laboratory
under a Related Services Agreement
with the U.S. Department of Energy
Contract DE-AC06-76RLO 1830**

**Pacific Northwest Laboratory
Operated for the U.S. Department of Energy
by Battelle Memorial Institute**



NOTICE

This report was prepared as an account of work sponsored by the United States Government. Neither the United States nor the Department of Energy, nor any of their employees, nor any of their contractors, subcontractors, or their employees, makes any warranty, express or implied, or assumes any legal liability or responsibility for the accuracy, completeness or usefulness of any information, apparatus, product or process disclosed, or represents that its use would not infringe privately owned rights.

The views, opinions and conclusions contained in this report are those of the contractor and do not necessarily represent those of the United States Government or the United States Department of Energy.

PACIFIC NORTHWEST LABORATORY
operated by
BATTELLE
for the
UNITED STATES DEPARTMENT OF ENERGY
Under Contract DE-AC06-76RLO 1830

Printed in the United States of America
Available from
National Technical Information Service
United States Department of Commerce
5285 Port Royal Road
Springfield, Virginia 22151

Price: Printed Copy \$ _____ *; Microfiche \$3.00

*Pages	NTIS Selling Price
001-025	\$4.00
026-050	\$4.50
051-075	\$5.25
076-100	\$6.00
101-125	\$6.50
126-150	\$7.25
151-175	\$8.00
176-200	\$9.00
201-225	\$9.25
226-250	\$9.50
251-275	\$10.75
276-300	\$11.00

3 3679 00054 4983

DEVELOPMENT OF A
WATER BOIL-OFF SPENT FUEL
CALORIMETER SYSTEM

J. M. Creer
J. W. Shupe, Jr.

May 1981

Prepared for the Hanford Engineering
Development Laboratory
under a Related Services Agreement
with the U.S. Department of Energy
Contract DE-AC06-76RL0 1830

Pacific Northwest Laboratory
Richland, Washington 99352



ACKNOWLEDGMENTS

This report presents the results of a spent fuel calorimeter development project conducted by the Pacific Northwest Laboratory (PNL) under contract to the Hanford Engineering Development Laboratory (HEDL). The Office of Nuclear Waste Isolation (ONWI) sponsored this project as part of the overall effort to develop spent fuel disposal technology. The authors would like to acknowledge those from PNL, HEDL, ONWI, and Westinghouse Advanced Energy Systems Division (AESD) who contributed to the project.

The authors wish to identify F. R. Zaloudek of PNL for being the major contributor to the basic conceptual design of the water boil-off calorimeter system. Appreciation is extended to G. E. Zima and W. J. Apley for assistance during conceptual design, A. J. Anthony for design and drafting, K. D. Hinkle for procurement, fabrication, and assembly, A. G. Dunbar, R. A. Scoggin, and H. M. Woods for instrumentation design, procurement, and installation, T. J. Doherty and G. H. Beeman for seismic analysis, P. M. Crawford for manuscript typing, and S. W. Matsumoto for editing.

The authors would like to thank the HEDL project manager, D. M. Bosi, for his support and suggestions throughout the project. Appreciation is extended to D. A. Cantley, HEDL Manager of Spent Fuel R&D, for selection of PNL to conduct the Spent Fuel Calorimeter Project. The help provided by J. C. Krogness in verifying the data reduction method is greatly appreciated.

The authors are indebted to J. A. Carr of ONWI for his support as program manager and for his input during design and management review meetings.

The authors wish to acknowledge the efforts of the following Westinghouse AESD, Nevada personnel for their efforts on the project: D. C. Durrill, A. P. Weber, and C. B. Dimmerling for management support; J. C. Dobbins and K. G. Garey for installation; B. L. Robbins, R. A. McClure, and their staff for installation and operations; and D. L. Weeks for Technical Operating Procedure preparation. A special thanks is extended to J. B. DeLee for the many hours he spent becoming familiar with the calorimeter and operating the system during acceptance testing and during measurement of the heat generation rate of the first spent fuel assembly.

The authors would like to thank T. E. Cross of Westinghouse AESD, Pittsburgh, for his diligent preparation of the Safety Assessment Document, and his critical review of the control system design and the Technical Operating Procedure.

SUMMARY

A calorimeter system was developed to measure decay heat generation rates of unmodified spent fuel assemblies from commercial nuclear reactors. The system was designed, fabricated, and successfully tested using the following criteria:

- Capacity: one boiling water or one pressurized water reactor spent fuel assembly
- Decay Heat Generation Range: 0.1 to 2.5 kW
- Measurement Time: <12 hr
- Accuracy: $\pm 10\%$ or better.

The system was installed and tested in the engine, maintenance, and disassembly hot bay facility located on the Nevada Test Site and operated by Westinghouse Advanced Energy Systems Division. The decay heat generation rate was measured for a spent fuel assembly from the Turkey Point pressurized water reactor operated by Florida Power and Light.

The calorimeter system uses a water boil-off principle to permit measurements of heat generation rates. Before a spent fuel assembly is inserted in the calorimeter, an internal reference heater is used to boil water and produce steam. The vaporizaton rate in this initial step is determined by condensing the steam and measuring the condensate mass accumulation rate. The product of the mass accumulation rate and the latent heat of vaporizaton of the water is equal to the heat generated in the heater minus heat losses. This procedure is repeated at the same heater power with a spent fuel assembly inserted in the calorimeter. In the final step, the product of the mass accumulated rate and latent heat is a measure of the unknown heat generated in the spent fuel assembly, plus the heat generated in the reference heater, minus system heat losses. The decay heat generation rate of spent fuel assemblies is determined by differencing the final and initial products of mass accumulation rates and latent heats.

The calorimeter system consists of five major subsystems. These subsystems are the calorimeter vessel and support structure, the water supply/storage tank and fill pump, the steam condenser, the condensate collection apparatus, and the control and data acquisition instrumentation. The 20-in.-dia, 18-ft-long stainless steel calorimeter vessel contains an inner pipe which supports lead rings required to absorb radiated gamma energy associated with spent fuel assemblies. The vessel also contains four heaters required to boil water and a lid fitted with a hook to support spent fuel assemblies during calorimetry. The calorimeter weighs approximately five tons when filled with ~200 gal of water. The water supply/storage tank is located directly below the vessel to provide make-up water and to permit the vessel to be completely drained. The condenser and condensate collection apparatus are used to condense steam generated in the calorimeter vessel, to collect subcooled condensate over a recorded period of time, and to measure both the volume and the weight of the condensate. The collection time and condensate measurements result in determinations of mass accumulation rates. Instrumentation required to control the system and record necessary data from sensors is located in an operating gallery adjacent to the hot bay.

The system was acceptance tested using a dc reference heater to simulate spent fuel assembly heat generation rates. Results of these tests indicated that the system could be used to measure heat generation rates between 0.5 and 2.5 kW within $\pm 5\%$. Measurements of heat generation rates of ~0.1 kW were obtained within $\pm 15\%$. Other significant results obtained during acceptance testing were:

- The water boil-off spent fuel calorimeter concept was verified.
- A procedure was developed to obtain acceptable mass accumulation rate data critical in the determination of heat generation rates.
- The calorimeter system has excellent stability, and the system time constant is sufficiently short to permit completion of calorimetry of a spent fuel assembly in one eight hour period.
- The calorimeter system has the potential to permit measurements of heat generation rates of spent fuel assemblies and other devices in the 12- to 14-kW range.

- The system design is compatible with hot cell operations and should be used as a prototype for future spent fuel packaging facilities.

Results of calorimetry of a Turkey Point spent fuel assembly indicated that the assembly was generating ~1.55 kW. Once the fuel assembly had been immersed in the calorimeter and a steady-state condition had been obtained (~4-1/2 hr), four consecutive data runs resulted in an average measured heat generation rate of 1.55 kW. The data scatter of these runs was $^{+2\%}_{-1\%}$. A prediction of the spent fuel assembly heat generation rate obtained with the ORIGEN2 computer program compared within 6% to this measured value. It was concluded that the calorimeter system performance satisfied the intent of the design criteria.

CONTENTS

ACKNOWLEDGMENTS	iii
SUMMARY	v
FIGURES	xi
TABLES	xii
NOMENCLATURE	xiii
1.0 INTRODUCTION	1.1
2.0 CONCLUSIONS AND RECOMMENDATIONS FOR FUTURE SYSTEMS	2.1
2.1 CONCLUSIONS	2.1
2.2 RECOMMENDATIONS FOR FUTURE SYSTEMS	2.2
3.0 SELECTION AND EVALUATION OF CANDIDATE CALORIMETER METHODS	3.1
3.1 SELECTION CRITERIA	3.1
3.2 CONTACT BOIL-OFF	3.2
3.3 NON-CONTACT BOIL-OFF	3.6
3.4 FLOWING WATER	3.7
3.5 STATIC AIR	3.9
3.6 FLOWING AIR	3.10
3.7 RECOMMENDED CALORIMETER METHOD FOR FURTHER DEVELOPMENT	3.11
4.0 EXPERIMENTAL METHOD	4.1
4.1 FACILITY AND EQUIPMENT	4.1
4.1.1 EMAD Hot Bay Facility	4.1
4.1.2 Calorimeter System	4.2
4.2 EXPERIMENTAL PROCEDURE AND DATA	4.23
4.2.1 Acceptance Test Procedure	4.23
4.2.2 Spent Fuel Assembly Heat Generation Rate Measurement Procedure	4.25

4.2.3 Data Presentation	4.29
4.2.4 Data Reduction Method	4.29
4.2.5 Data Accuracy	4.30
5.0 EXPERIMENTAL RESULTS AND DISCUSSION	5.1
5.1 ACCEPTANCE TEST	5.1
5.1.1 Comparison of Head and Weight Mass Accumulation Measurements	5.1
5.1.2 System Heat Losses	5.2
5.1.3 Evaluation of Accuracy	5.6
5.1.4 Calorimeter Sensitivity	5.9
5.1.5 General Observations	5.9
5.1.6 Recommended Criteria for Acceptable Mass Accumulation Rate Data	5.11
5.2 SPENT FUEL ASSEMBLY HEAT GENERATION RATE MEASUREMENT	5.12
REFERENCES	Ref.1
APPENDIX A--DESIGN DRAWINGS	A.1
APPENDIX B--RAW DATA	B.1
APPENDIX C--DATA REDUCTION METHOD	C.1
APPENDIX D--UNCERTAINTY ANALYSIS	D.1

FIGURES

1	Contact Boil-Off Calorimeter	3.2
2	Boil-Off Calorimeter System	3.3
3	Non-Contact Boil-Off Calorimeter	3.7
4	Water Flow Calorimeter	3.8
5	Static Air Calorimeter	3.9
6	Air Flow Calorimeter	3.10
7	Calorimeter System Installed in the EMAD Calorimeter Pit (Courtesy Westinghouse AESD, Pittsburgh)	4.3
8	Contact Boil-Off Calorimeter Cross Section	4.4
9	Outer Calorimeter Vessel (Courtesy HEDL)	4.5
10	Closure Lid and HEDL Fuel Handling Fixture During Load Testing (Courtesy HEDL)	4.6
11	Calorimeter Vessel Top Flange (Courtesy HEDL)	4.7
12	Half Couplings for Heater Insertion (Courtesy HEDL)	4.9
13	Inner Calorimeter Vessel (Courtesy HEDL)	4.10
14	Vertical Support Beams and Columns (Courtesy Westinghouse AESD, Nevada)	4.12
15	Calorimeter System Schematic	4.13
16	Condenser/Fan Unit (Courtesy Westinghouse AESD, Nevada)	4.15
17	Instrumentation and Control Panels (Courtesy Westinghouse AESD, Nevada)	4.18
18	Remote Removal of the Insulation Cap (Courtesy Westinghouse AESD, Nevada)	4.26
19	Remote Removal of the Temporary Lid (Courtesy Westinghouse AESD, Nevada)	4.27
20	Remote Spent Fuel Assembly Insertion (Courtesy Westinghouse AESD, Nevada)	4.28

FIGURES

21	Comparison of Mass Accumulation Rate Measurements Using the Head and the Weight Methods	5.2
22	System Heat Losses Determined from Head Measurements	5.3
23	System Heat Losses Determined from Weight Measurements	5.3
24	Average System Heat Losses Determined from Head Measurements	5.5
25	Average System Heat Losses Determined from Weight Measurements	5.5
26	Typical Hot Bay Ambient Temperature History During a Testing Day	5.6
27	Comparisons of Calorimeter Differential Heat Generation Rate Measurements with Differential Heater Power Levels Using Runs 37 and 38 and Runs 28, 29, and 30 as References	5.8
28	Comparisons of Calorimeter Differential Heat Generation Rate Measurements with Differential Heater Power Levels Using Runs 7 through 9 as a Reference	5.8
29	Mass Accumulation Rates at Heater Power Levels Near 1 kW	5.10
30	Calorimeter Heat Generation Rate Measurements at a Heater Power Level Near 1 kW	5.10
31	Desired Condenser Outlet Temperature History During Approach to a Steady-State Condition	5.12

TABLES

1	Typical Uncertainty Values	4.30
2	Comparison of Differential Calorimeter Heat Generation Rate Measurements with Differential Heater Power Levels	5.7
3	Spent Fuel Assembly (D-34) Measured Heat Generation Rate	5.14

NOMENCLATURE

A	- area, in. ²
c_p	- heat capacity, Btu/(lb °F)
d	- diameter, in.
H	- head, in. H ₂ O @ 68°F
HH	- high high level
HF	- high fill level
h_{fg}	- latent heat of vaporization, Btu/lb
ΔH	- differential head, in. H ₂ O @ 68°F
Δh_{fg}	- differential latent heat, Btu/lb
I	- current, amperes
K	- conversion constant
LL	- low low level
\dot{m}	- mass accumulation rate, lb/hr
OH	- operating high level
OL	- operating low level
P	- pressure, psia or psig
q	- heat transfer or heat generation rate, kW
R	- resistance, ohms
s	- standard deviation
SL	- safe low level
T	- temperature, °F or °C
t	- time, sec
ΔT	- temperature difference, °F or °C
Δt	- differential time, sec
V	- voltage, volts
W	- weight, g
ΔW	- differential weight, g
ω	- uncertainty interval of 95%

SUBSCRIPTS

a	- ambient
A_T	- total area
B	- buoyancy
c	- condensate
cal	- calorimeter
DT	- dip tube
f	- final
h	- heater
H	- head
ΔH	- differential head
h_{fg}	- latent heat
i	- initial
I_h	- heater current
In	- inlet condition
L	- loss
\dot{m}_H	- mass accumulation rate measured with head (pressure) transmitter
\dot{m}_W	- mass accumulation rate measured with weigh scale
$\dot{m}_{f,H}$	- final mass accumulation rate measured with head method
$\dot{m}_{f,W}$	- final mass accumulation rate measured with weigh scale
$\dot{m}_{R,H}$	- reference mass accumulation rate measured with head method
$\dot{m}_{R,W}$	- reference mass accumulation rate measured with weigh scale
Out	- outlet condition
q_h	- heater power
$q_{L,H}$	- heat loss determined using head measurement
$q_{L,W}$	- heat loss determined using weight measurement
$q_{SF,H}$	- spent fuel assembly heat generation rate using head measurement
$q_{SF,W}$	- spent fuel assembly heat generation rate using weight measurement
$q_{L,f,H}$	- final run heat loss from head measurement
$q_{L,f,W}$	- final run heat loss from weight measurement
$q_{L,R,H}$	- reference run heat loss from head measurement
$q_{L,R,W}$	- reference run heat loss from weight measurement
R	- reference, resistor, or resistance
SF	- spent fuel

T	- total
Δt	- differential time
V_R	- resistor voltage drop
W	- weight
W_f	- final weight
W_i	- initial weight
ΔW	- differential weight
1	- first run in a series
2	- second run in a series
11	- differential head of 11 in. H_2O
16	- differential head of 16 in. H_2O
32	- differential head of 32 in. H_2O
0.25	- outside diameter of dip tube, in.
1.18	- internal diameter of collection tube, in.



DEVELOPMENT OF A WATER BOIL-OFF SPENT FUEL CALORIMETER SYSTEM

1.0 INTRODUCTION

One objective of the National Waste Terminal Storage Program is to determine the potential geologic disposal integrity of unprocessed spent fuel assemblies from light water reactors (LWRs). As part of this effort, heat transfer analyses are required to support assessments of spent fuel assembly isolation integrity. An important input parameter required for detailed heat transfer predictions is the decay heat generation rates of individual spent fuel assemblies. Because analytical predictions cannot be completely relied upon, experimentally determined decay heat generation rates of spent fuel assemblies dedicated to the program were needed.

Up to this time small calorimeters have been used to measure heat generation rates of sections of spent fuel rods, and computer codes such as ORIGIN (Bell 1973) have been used to estimate the heat generation rates of complete spent fuel assemblies. It is important that the accuracy of extrapolating partial rod heat generation measurements to total assembly heat generation values be evaluated. Likewise, computer codes should be evaluated using experimental data and improved to provide accurate predictive capabilities for design and analysis. Therefore, a spent fuel calorimeter was developed to provide decay heat generation rates of complete pressurized water reactor (PWR) and boiling water reactor (BWR) spent fuel assemblies.

The objectives of this Spent Fuel Calorimeter Development Project were to select a concept, evaluate the concept, design a complete system, fabricate components, and test the system. This report documents the project and the experimental effort conducted by the Pacific Northwest Laboratory (PNL) under contract to the Hanford Engineering Development Laboratory (HEDL). The selection and evaluation process, the experimental method, the results, and the conclusions and recommendations are discussed.



2.0 CONCLUSIONS AND RECOMMENDATIONS FOR FUTURE SYSTEMS

This spent fuel calorimeter development project resulted in a number of conclusions and recommendations. The following sections identify the major conclusions and important recommendations for future calorimeter systems.

2.1 CONCLUSIONS

- The water boil-off spent fuel calorimeter concept was verified. The existing calorimeter should continue to be used to obtain decay heat generation rate measurements of spent fuel assemblies when desired, but its use need not be limited to this application. Heat generation rates of other devices that can be positioned inside a 14-in. (inner diameter), 16-ft-long pipe can also be measured with the calorimeter system.
- The calorimeter system has excellent stability and the system time constant is sufficiently short to permit calorimetry during an eight-hour period. The system is compatible with hot cell operations and should be used as a prototype for future packaging facilities.
- A procedure was developed to obtain acceptable mass accumulation rate data critical to the determination of spent fuel heat generation rate values. The condensate head accumulation measurements should be used as primary data, and the condensate weight accumulation measurements should be used as secondary (back-up) measurements. Before weight measurements are used as primary data, the collection tube mounting design should be modified to provide better support and to ensure that solenoid drain valve actuation does not adversely affect weight accumulation measurements.
- Heat generation rate measurement accuracies within $\pm 5\%$ of true values can be obtained with the calorimeter in the range between 0.5 and 2.5 kW. Accuracies within $\pm 5\%$ to $\pm 10\%$ can be expected at power levels from 0.1 to 0.5 kW.

- The heat loss from the calorimeter system at a hot bay temperature of $\sim 66^{\circ}\text{F}$ was ~ 0.6 kW. An uncertainty analysis indicated that heat loss measurement uncertainties contributed significantly to the overall measurement accuracy. If better calorimeter measurement accuracies are desired, additional heat loss data at power levels of 1, 1.5, 2, 2.5, and 3 kW should be obtained to unconditionally verify that the system heat loss is essentially constant over this heat generation range.
- Reference calorimeter runs are as important to measurement accuracy as runs with an unknown heat generating device in the calorimeter. Until sufficient operating experience is gained, references runs should be performed before and after actual runs made with heat generating devices installed in the calorimeter.
- The calorimeter system has the potential to permit measurements of heat generation rates of spent fuel assemblies and other devices in the 12- to 14-kW range. Measurements of accurately known reference heat generation rates up to 12-14 kW should be obtained prior to attempting measurements of unknown heat generating devices in this range.
- Approximately four hours are required to bring the calorimeter water to a boiling condition from room temperature. Once the system reaches boiling, a steady-rate condition can be obtained in two to six hours at constant heater power.
- If 4 or 5 gallons of cold water from the supply/storage tank are injected into the calorimeter after attaining a steady-state condition, approximately one to two hours are required to regain a steady-state condition.
- The decay heat generation rate of a Turkey Point PWR spent fuel assembly as measured with the calorimeter system was 1.55 kW.
- Predictions of the decay heat generation rate (1.64 kW) of a Turkey Point PWR spent fuel assembly obtained with the ORIGEN2 (Coff 1980) computer program compared within 6% to values measured with the calorimeter system.

2.2 RECOMMENDATIONS FOR FUTURE SYSTEMS

- Calorimeter vessels should be 6-12 in. longer in systems built in the future. This will permit optimum distances between critical liquid level alarm setpoints near the top of the vessel and prevent water carry-over to the condenser, due to surface agitation during boiling.
- An additional liquid level sensing system should be installed on the upper 50 in. of future calorimeter vessels to increase the sensitivity of the level measurements and alarm setpoints.
- Calorimeter fluid temperatures should be measured with direct-contact temperature sensors in future systems.
- For ease of monitoring, future instrumentation consoles should include continuous digital readouts of vessel and supply/storage tank liquid levels, vessel fluid temperature, heater power, condensate head values, and condenser outlet temperature.
- As recommended in initial system conceptual designs, condensers in future systems should be liquid cooled to permit accurate heat balances to be obtained throughout the calorimeter system.



3.0 SELECTION AND EVALUATION OF CANDIDATE CALORIMETER METHODS

During the initial effort of this project several candidate calorimeter methods were selected and evaluated for further development:

- Contact Boil-Off (spent fuel assembly in contact with working fluid)
- Non-Contact Boil-Off (spent fuel assembly not in contact with working fluid)
- Flowing Water
- Static Air
- Flowing Air

The selection criteria and details of the evaluation analysis performed for each candidate method are presented in the following sections.

3.1 SELECTION CRITERIA

Before initiation of the analytical evaluation process, selection criteria were identified. The selection criteria most pertinent to the selection process were

- Capacity: one BWR or one PWR spent fuel assembly
- Potential decay heat generation range: 0.1 to 2.5 kW^(a)
- Measurement time: <30 hours
- Accuracy: $\pm 10\%$ or better

Requirements for system safety, operability, maintainability, simplicity, and costs were also considered in the evaluation.

(a) It is important that the term "potential decay heat generation" be understood. It is defined as the decay heat generation rate of a spent fuel assembly, plus the heat generation that would result from escaping radiation particles; i.e., alpha, beta, and gamma. In BWR and PWR spent fuel assemblies, gamma particles are the significant source of escaping radiation energy. In this report, heat generation will mean potential heat generation.

3.2 CONTACT BOIL-OFF CALORIMETER

The cross section of a conceptual contact boil-off calorimeter is shown in Figure 1. The calorimeter would be similar to a small cryogenic boil-off calorimeter developed at Los Alamos (Yarnell and Bendt 1977) and would consist of an inner pipe, lead radiation-absorbing liners, a cooling annulus, an outer containment pipe, and insulation. A spent fuel assembly would be placed in the inner pipe in contact with a boiling fluid. Note that the spent fuel assembly was modeled as one fuel rod in this analysis because all rods in an assembly will generate approximately the same amount of heat and have the same time constants.

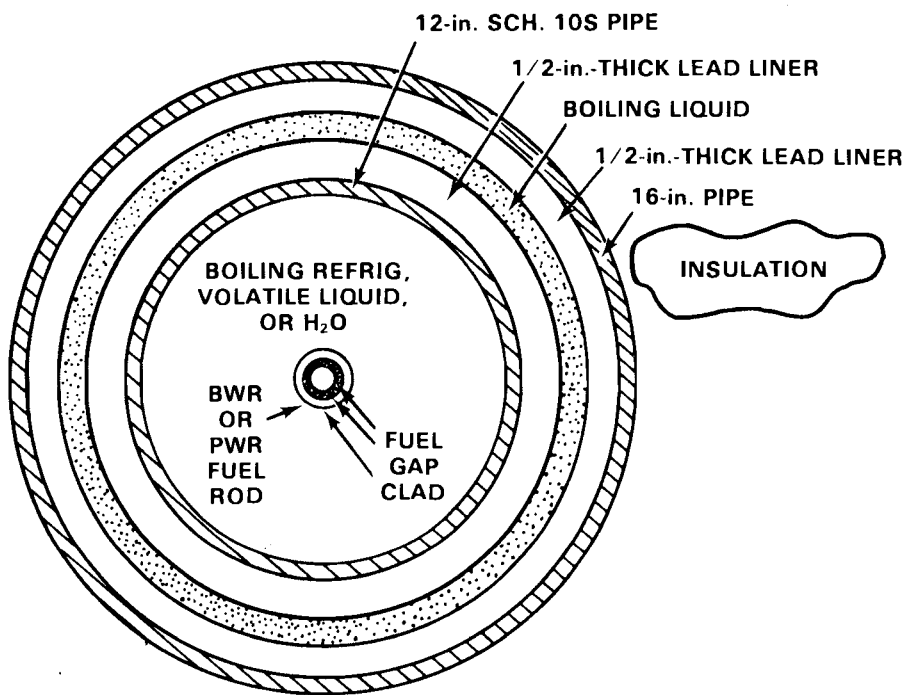


FIGURE 1. Contact Boil-Off Calorimeter

The purpose of the inner pipe would be to contain a spent fuel assembly and to support one lead liner. The lead liners would absorb gamma radiation and generate a proportional amount of thermal energy. The cooling annulus would permit boiling fluid to contact the maximum surface area and reduce the thermal time constant of the calorimeter. The outer vessel would support another lead liner and act as a final container. The insulation would reduce heat losses from the calorimeter.

The contact boil-off calorimeter could be installed in a system similar to that shown in Figure 2. The system would consist of a liquid supply/storage tank, a fill pump, the calorimeter, a condenser, and a condensate measuring tube.

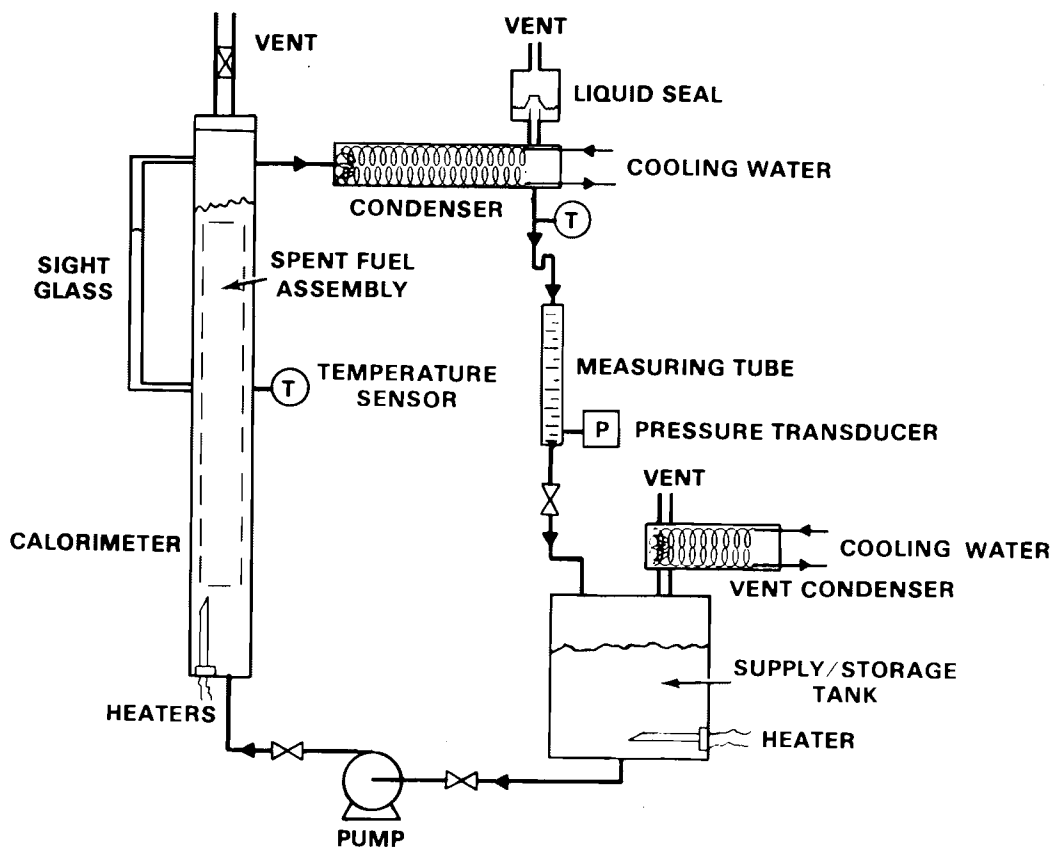


FIGURE 2. Boil-off Calorimeter System

The supply/storage tank would be used for filling and draining the calorimeter. A small pump would be used to fill the calorimeter with liquid. A pump bypass line would permit the calorimeter to be drained.

In addition to those parts shown in Figure 1, the calorimeter would be provided with heaters and a sight glass as shown in Figure 2. The purpose of the heaters would be to initially heat the liquid to boiling and to provide accurate reference vapor generation rates. The sight glass would enable the operator to readily assure that an adequate liquid level is maintained at all times. An absolute pressure transducer located near the bottom of the calorimeter could also be used to measure liquid levels and provide automatic shutdown capability.

A condenser connected to the calorimeter via a pipe could be used to condense the vapor. The condensate would be collected in a measuring tube. The product of the condensate mass accumulation rate (\dot{m}_c) and the latent heat of vaporization (h_{fg}) would be equal to the heat being generated in the calorimeter (q_{cal}) minus heat losses (q_L); i.e., $q_{cal} - q_L = \dot{m}_c h_{fg}$.

The boil-off calorimeter system could be operated using the following procedure:

1. Without a spent fuel assembly in the calorimeter, the calorimeter would be filled with liquid and the heater set at a predetermined power level.
2. After the system reached a steady state condition, the initial condensate mass accumulation rate (\dot{m}_i) would result from the heat being generated by the calorimeter heater (q_h) less any heat losses (q_L) from the system; i.e., $q_i = q_h - q_L = \dot{m}_i h_{fg}$.
3. A spent fuel assembly would be positioned in the calorimeter, and the system would be refilled with liquid to a desired level.
4. After steady-state conditions were attained, the final condensate mass accumulation rate (\dot{m}_f) would be measured. Note that the final condensate mass accumulation rate would result from that measured in step 2, plus the heat being generated in the spent fuel assembly and

the lead liners (q_{SF}). The difference between the final and initial condensate accumulation rates would be that resulting from the heat being generated in the bundle and lead; i.e., the potential decay heat generation rate of the assembly $q_{SF} = (\dot{m}_f - \dot{m}_i)h_{fg}$.

A transient thermal analysis was performed with the HEATING 5 computer code (Turner, Elrod, and Siman-Tov 1977) using the geometry model shown in Figure 1. Both water and ethyl acetate boil-off calorimeters were investigated. Ethyl acetate was considered because it has a latent heat of vaporization of ~ 185 Btu/lb compared to water at ~ 970 Btu/lb. The lower latent heat would permit more condensate mass to be accumulated during a given period of time for the same heat generation rate, thus enhancing measurement accuracy.

Results of the analysis indicated that the type of fluid used did not significantly affect the measurement time, i.e., the time to reach steady-state conditions.^(a) Both BWR and PWR fuel rods were predicted to reach steady-state conditions in less than 30 min. Two 0.5-in.-thick lead liners would attain steady-state conditions from an initial temperature of $\sim 160^{\circ}\text{F}$ in approximately 10 hours, when subjected to boiling water. In an actual case, the lead liners and piping would be very near the boiling temperature of the working fluid after an initial (reference) run using the system reference heater was completed. Therefore, with a spent fuel assembly immersed in the calorimeter, the measurement time was estimated to be more on the order of three to four hours, a value which satisfied the design criteria.

A sensitivity analysis was performed to determine the effects of changes in atmospheric pressure and ambient temperature on the heat of vaporization of water and calorimeter component temperatures. An assumed large change in atmospheric pressure of ± 1 in. Hg at constant temperature was predicted to correspond to a change in the heat of vaporization of water of $\sim \pm 0.1\%$, which is

(a) Steady state was assumed to be the condition at which a temperature was within 0.01°F of the predicted steady-state temperature.

insignificant in the calculation of heat generation rates. A thermal analysis using the HEATING 5 computer program indicated that an ambient temperature change of 20°F, over a 5-min time period, would result in a maximum internal calorimeter temperature change of ~0.01°F during a six-hour measurement period. This small temperature variation would not detectably contribute to calorimeter inaccuracies.

From the above results, it was preliminarily concluded that a contact boil-off calorimeter was a promising method to measure decay heat generation rates of spent fuel assemblies. Accuracies within $\pm 5\%$ were predicted to be feasible. Water has definite advantages over refrigerants and volatile liquids because corrosion and flammability problems are minimized.^(a)

3.3 NON-CONTACT BOIL-OFF CALORIMETER

A conceptual schematic of a non-contact boil-off calorimeter is shown in Figure 3. A typical LWR spent fuel assembly was modeled as a lumped circular mass. The bundle was assumed to be in a pipe containing air or helium. Boiling refrigerant, volatile liquid, or water in contact with the outer surface of the containment pipe would provide a heat sink. Note that the boiling fluid would not contact the spent fuel assembly, as the calorimeter name indicates. Calorimeter parts beyond the inner container, such as a lead absorbing liner, outer containment pipe, and insulation, were not considered in the evaluation of this concept.

The non-contact boil-off calorimeter could be installed in a system identical to that discussed in section 3.2. The operating procedure would also be the same; however, the measurement times were predicted to be longer than the contact concept because of the insulative gas gap.

A transient thermal analysis of the non-contact boil-off concept using freon and air resulted in excessively long measurement times. The temperature of a typical BWR spent fuel bundle generating 0.1 kW at an assumed initial

(a) More than 25 refrigerants and volatile liquids were considered as potential calorimeter working fluids.

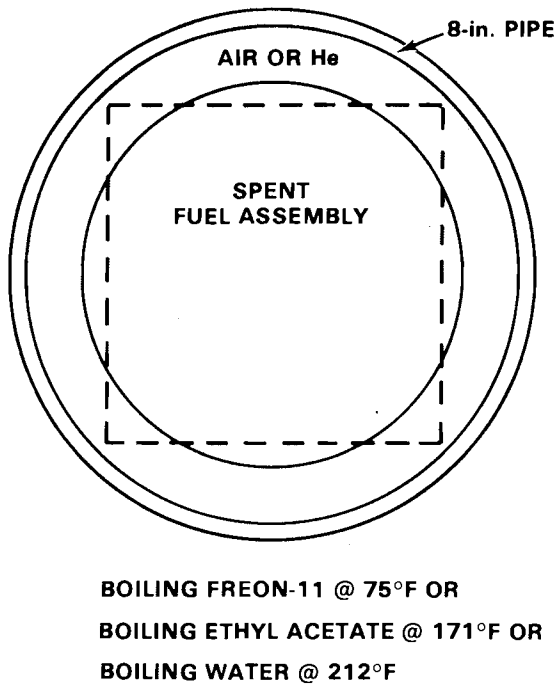


FIGURE 3. Non-Contact Boil-Off Calorimeter

temperature of $\sim 300^{\circ}\text{F}$ required ~ 12 hours to decrease by $\sim 20^{\circ}\text{F}$. The steady-state temperature of the bundle was predicted to be $\sim 223^{\circ}\text{F}$. By linearly extrapolating the temperature history to 223°F , it was predicted that ~ 46 hours would be required to reach a steady-state condition. An additional thermal analysis revealed that it would require ~ 12 hours to reduce the bundle temperature from 225 to 223°F . It was concluded that the measurement time of a non-contact boil-off calorimeter would be excessively long and that the method was not practical.

3.4 FLOWING WATER CALORIMETER

A flowing water calorimeter system, shown schematically in Figure 4, was considered in the selection process. The system would consist of a pump, a flowmeter, a calorimeter instrumented with inlet and outlet temperature sensors, a cooldown heat exchanger, and a heater. The calorimeter would be essentially the same as the contact boil-off calorimeter previously presented in Figure 1, but the boiling fluid would be replaced with flowing water. The cooldown heat exchanger and heater would be required to select and control desired inlet

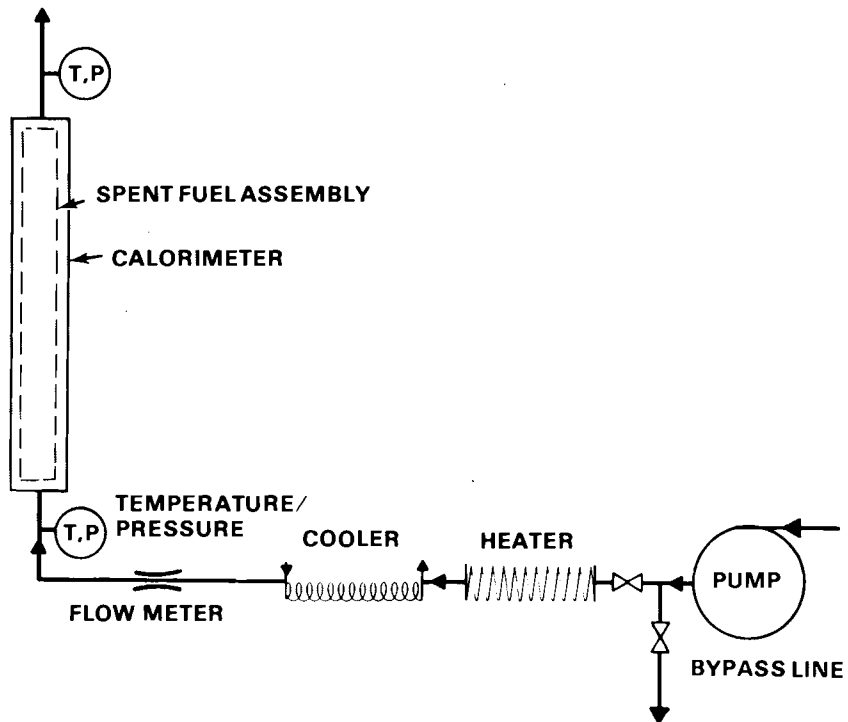


FIGURE 4. Water Flow Calorimeter

calorimeter temperatures during isothermal runs. Isothermal runs would be required to accurately determine heat losses from the calorimeter between the inlet and outlet temperature sensors.

During the operation of the water flow calorimeter, the flow rate (\dot{m}) and inlet temperature (T_{In}) would be set at desired values. The flow rate would be selected to produce a significant temperature gradient ($\geq 10^{\circ}\text{F}$) across the length of the calorimeter. The magnitude of the temperature gradient is important for accuracy requirements. A heat balance across the calorimeter would yield the heat being generated in the spent fuel assembly and lead liner; i.e., $q_{SF} = \dot{m}c_p(T_{Out} - T_{In}) + q_L$.

The flowing water calorimeter was eliminated as a potential method because the contact boil-off calorimeter appeared to be a faster, more accurate method of measuring decay heat generation rates. Also, a flowing water system would be extremely difficult to operate remotely in a hot bay facility.

3.5 STATIC AIR CALORIMETER

A typical static air calorimeter, shown in Figure 5, would consist of a spent fuel assembly, an inner containment pipe filled with air or gas, a heater, a lead liner to absorb escaping radiation energy, a gas gap, an outer containment pipe, and insulation. This calorimeter concept is similar to the technique reported by Beyer, Perry, and Lewis (1976). During the operation of the calorimeter, without a spent fuel assembly in place, power would be applied to the heater. After steady-state conditions are attained, temperature measurements at three or four axial locations would be obtained across the gas gap. A spent fuel assembly would be inserted in the calorimeter and the heater power reduced until the same temperature differences existed across the gas gap. The amount the heater power is reduced would be equal to the heat being generated in the assembly and lead liner.

A detailed thermal analysis of the static air calorimeter concept was not performed. It was obvious from the previous analyses that the time constant of the static air calorimeter would be longer than that of the non-contact boil-off calorimeter. Because the time to reach steady-state conditions was excessively long, it was concluded that the static air concept was unsatisfactory.

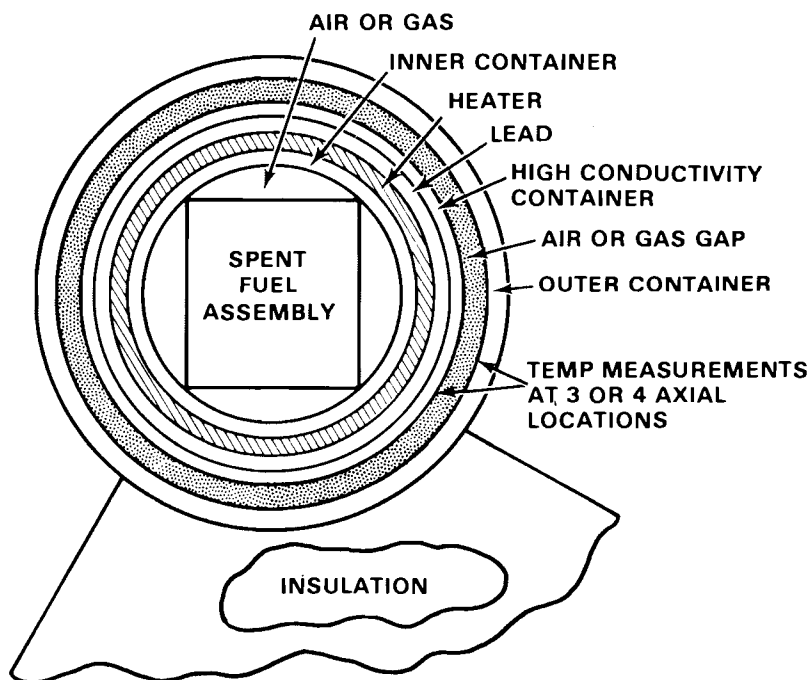


FIGURE 5. Static Air Calorimeter

3.6 FLOWING AIR CALORIMETER

A flowing air calorimeter operates on the same heat balance principle as the flowing water calorimeter. A typical flowing air calorimeter system is shown in Figure 6. A high-head blower would be required to supply air to the calorimeter. A heater and cooler would be required to select and control desired inlet air temperatures during isothermal heat loss runs. A flowmeter and temperature/pressure instruments would be necessary to permit heat balances to be obtained across the calorimeter.

Results of the transient thermal analysis of the flowing air calorimeter at relatively high air flows (11 ft/sec) indicated BWR and PWR fuel rods would reach steady-state conditions in ~3 hours. At low air flow rates (0.5 ft/sec) required to obtain satisfactory axial temperature differences ($>10^{\circ}\text{F}$) across the calorimeter, the time for the fuel rods to reach steady-state conditions increased to ~10 hours. A significant axial temperature difference across the calorimeter is desirable because it increases measurement accuracy. Velocity

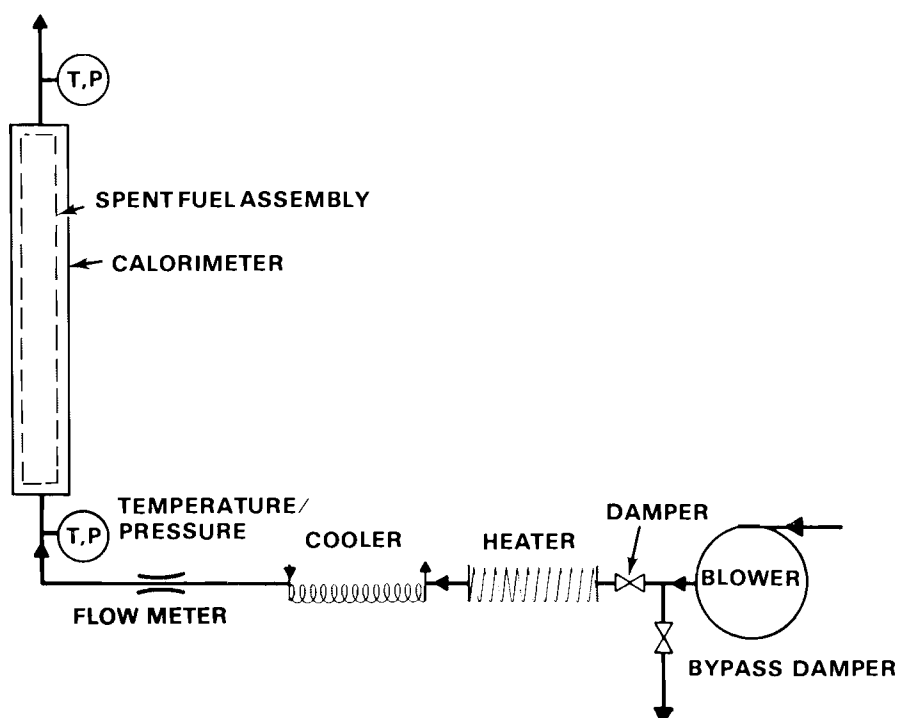


FIGURE 6. Air Flow Calorimeter

magnitudes (~0.5 ft/sec) associated with desired air flow rates would be of the order of magnitude of free convection currents. It was judged that very unstable outlet calorimeter temperatures could be encountered if the flow velocities are not an order of magnitude greater than the free convection currents. This judgment is based on past experience with low-flow air facilities.

Although the air flow calorimeter appears to be satisfactory for measurement time and accuracy ($\pm 8\%$), it was eliminated as a prospective method because of the unknown problems associated with the system instabilities. In addition, the difficulties associated with operating a flowing system in a limited access hot bay do not appear to be justifiable.

3.7 RECOMMENDED CALORIMETER METHOD FOR FURTHER DEVELOPMENT

From the results of this initial effort on the project, it was concluded that the contact water boil-off calorimeter met the selection criteria presented in section 3.1 better than the other candidate methods. The remaining sections of this report discuss the detailed design of a contact water boil-off calorimeter system that evolved from the concepts presented in section 3.2. The calorimeter system was fabricated and ultimately installed in the EMAD hot bay facility. Results of an acceptance test and actual calorimeter measurements of a spent fuel assembly are also presented.



4.0 EXPERIMENTAL METHOD

The following sections discuss the development of a contact water boil-off calorimeter system. Facility and equipment designs are presented, and the procedures used to perform the acceptance test and measure the decay heat generation rate of a Turkey Point PWR spent fuel assembly are discussed. The data, the data reduction method, and the estimated accuracy of the data are presented.

4.1 FACILITY AND EQUIPMENT

The calorimeter system was designed and fabricated by PNL and shipped to the Nevada test site for installation and operation in the EMAD hot bay facility. A description of the EMAD facility and a discussion of the calorimeter equipment design are presented.

4.1.1 EMAD Hot Bay Facility

The EMAD facility is a large complex which contains a hot bay approximately 140 ft long, 66 ft wide, and 74 ft high. The walls are constructed of 5- to 6-ft-thick reinforced concrete with lead glass viewing windows located at various work stations. The hot bay contains standard gauge railroad tracks which allow railroad transport system vehicles to enter and exit the bay with radioactive materials. A shielded air lock pass-through for personnel entry from a change room is provided.

The hot bay is equipped with a 40-ton overhead crane with a 10-ton auxiliary hook which is remotely operated from portable controllers located in the operating gallery near window work stations. Maximum hook heights of ~62 ft are possible.

In addition, the bay is equipped with a wall-mounted handling system, an overhead positioning system, and a floor-mounted handling system, which are all remotely operated from portable controllers located in the gallery. These handling systems have special tools and fixtures to facilitate remote assembly and disassembly operations. Master slave manipulators and inspection tables are located at window work stations. Periscopes at various work stations provide inspection and photographic capabilities.

The hot bay contains a pit ~13-1/2 ft deep, ~4-1/2 ft wide, and ~26-1/3 ft long. The calorimeter system was installed in the north end of the pit in full view of a window work station. The hot bay is described in depth by the EMAD Capabilities Manual (refer to references).

4.1.2 Calorimeter System

The calorimeter system consists of five major subsystems. These subsystems are the calorimeter vessel and support structures, the water supply/storage tank and fill pump, the steam condenser, the condensate collection apparatus, and the control and data acquisition instrumentation. In addition to these subsystems, a fuel handling fixture designed and fabricated by the Hanford Engineering Development Laboratory (HEDL) was required to support a Turkey Point PWR spent fuel assembly within the calorimeter vessel during decay heat generation rate measurements.

The calorimeter vessel and the water supply/storage tank for the system were installed in the calorimeter pit located in the EMAD hot bay facility, as shown in Figure 7. The steam condenser and the condensate collection apparatus were located on the hot bay floor adjacent to the calorimeter pit. The controls for the calorimeter system and the data acquisition system were located in the operating gallery adjacent to, but isolated from, the hot bay area.

Detailed discussions of each calorimeter subsystem are included in the following sections. Appendix A provides detailed design drawings of the calorimeter system.

4.1.2.1 Calorimeter Vessel and Supports

The calorimeter vessel consists of an outer vessel, an inner vessel, lead absorption rings, closure lids, and insulation as shown in Figures 7 and 8. The outer calorimeter vessel (Figure 9) was fabricated from an 18-ft-long section of 304 stainless steel pipe with a 20-in. outer diameter and a 1/2-in. wall thickness. The bottom head of the vessel was fabricated from 1/2-in.-thick 304 stainless steel plate. A 2-1/2-in. by 1-in. concentric reducer, which serves as a drain sump, and four 3/4-in.-dia hold-down studs were welded to the bottom head.

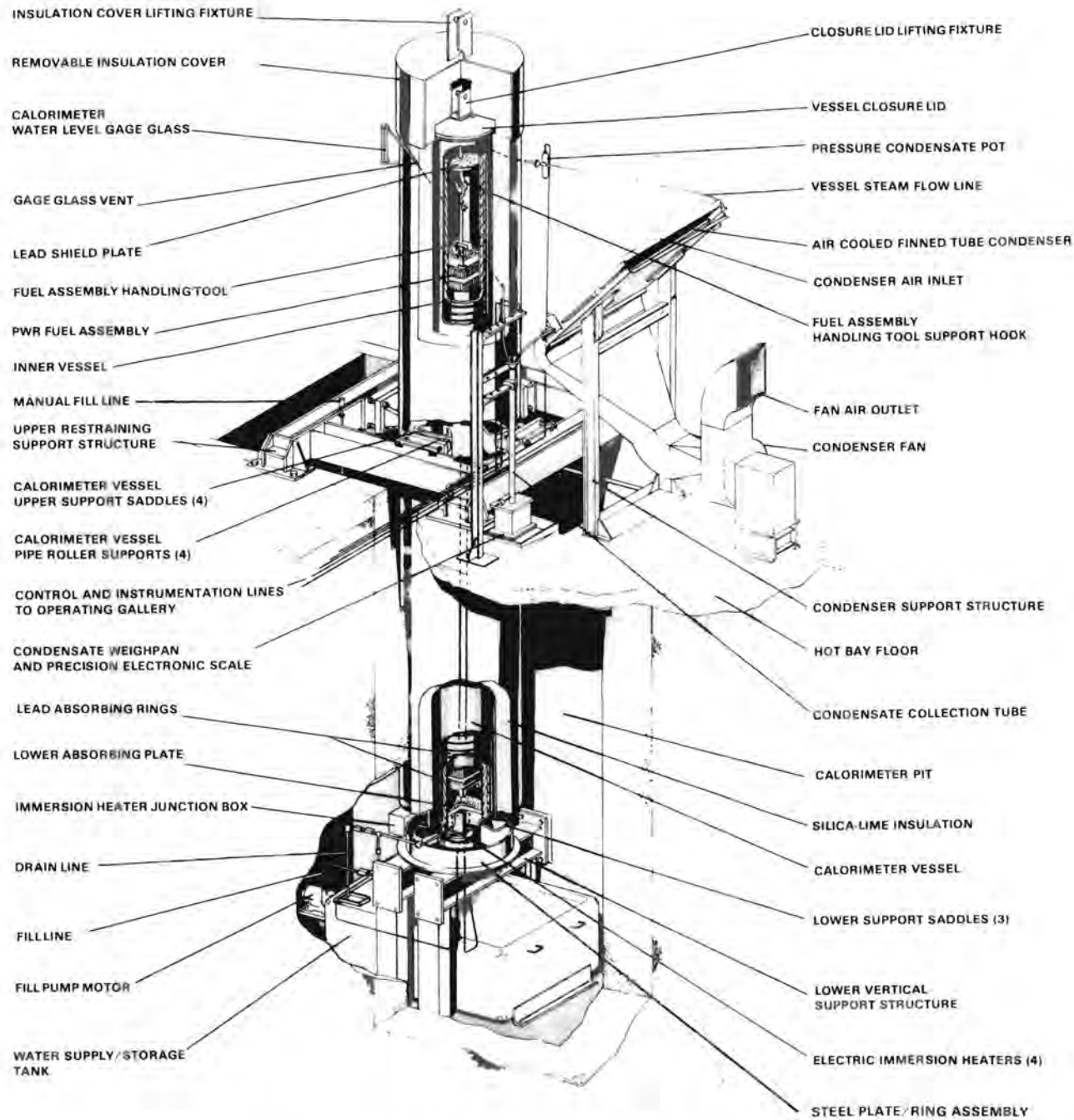


FIGURE 7. Calorimeter System Installed in the EMAD Calorimeter Pit
(Courtesy Westinghouse AESD, Pittsburgh)

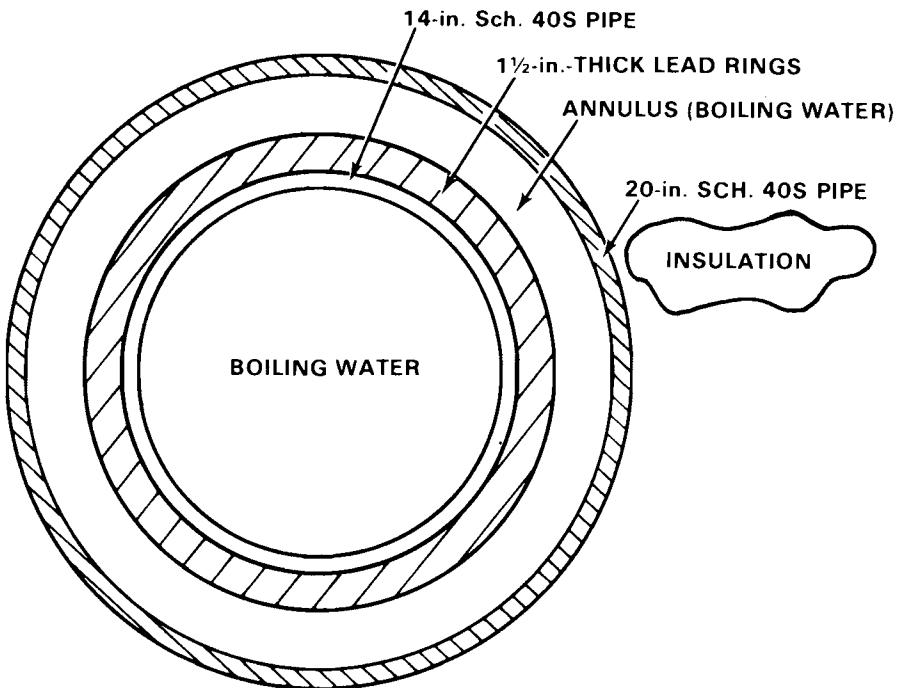


FIGURE 8. Contact Boil-Off Calorimeter Cross Section

Two closure lids are provided for the calorimeter. One serves as a calorimeter vessel lid/lifting fixture and is used both to lift and position the outer vessel during installation and to seal it during heatup operations with no fuel assembly. The second lid (Figure 10) serves as a lid/support when an assembly is in the calorimeter vessel. Both lids were constructed of 1-in.-thick 304 stainless steel plate, 24 in. in diameter, and mate with an O-ring inserted in the calorimeter vessel top flange (Figure 11). The lid/lifting fixture is similar to the lid/support except that the lid support has no lid hook. During decay heat generation measurements, the weight of the spent fuel assembly suspended from the lid/support hook is sufficient to maintain a steam-tight seal against the vessel flange O-ring. When no fuel assembly is suspended from the lid/support or when the vessel lid/lifting fixture is used during heatup operations, the closure seal is made by screw locks that compress the lids against the O-ring seal (see Appendix A for details of the locking spider).

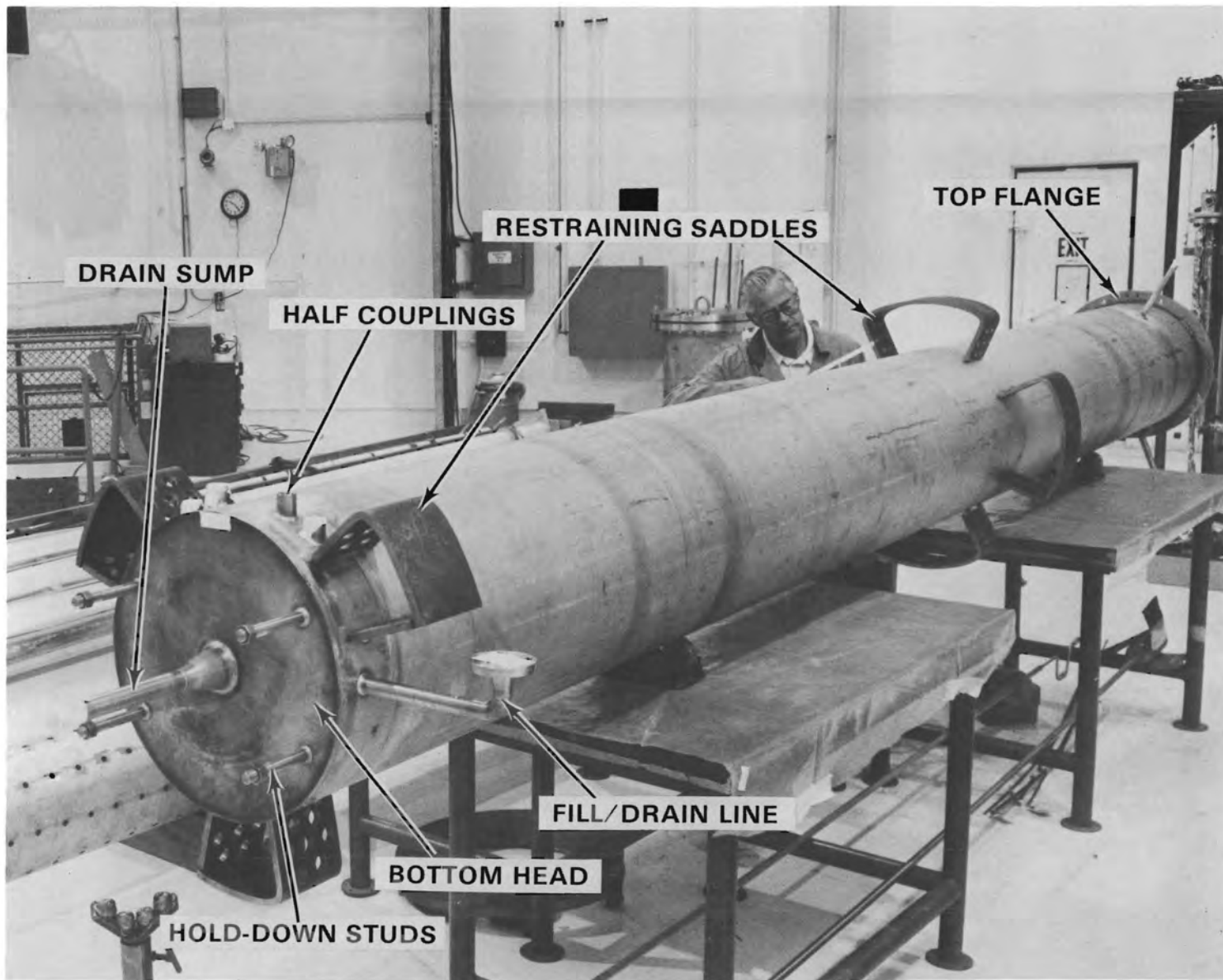


FIGURE 9. Outer Calorimeter Vessel (Courtesy HEDL)

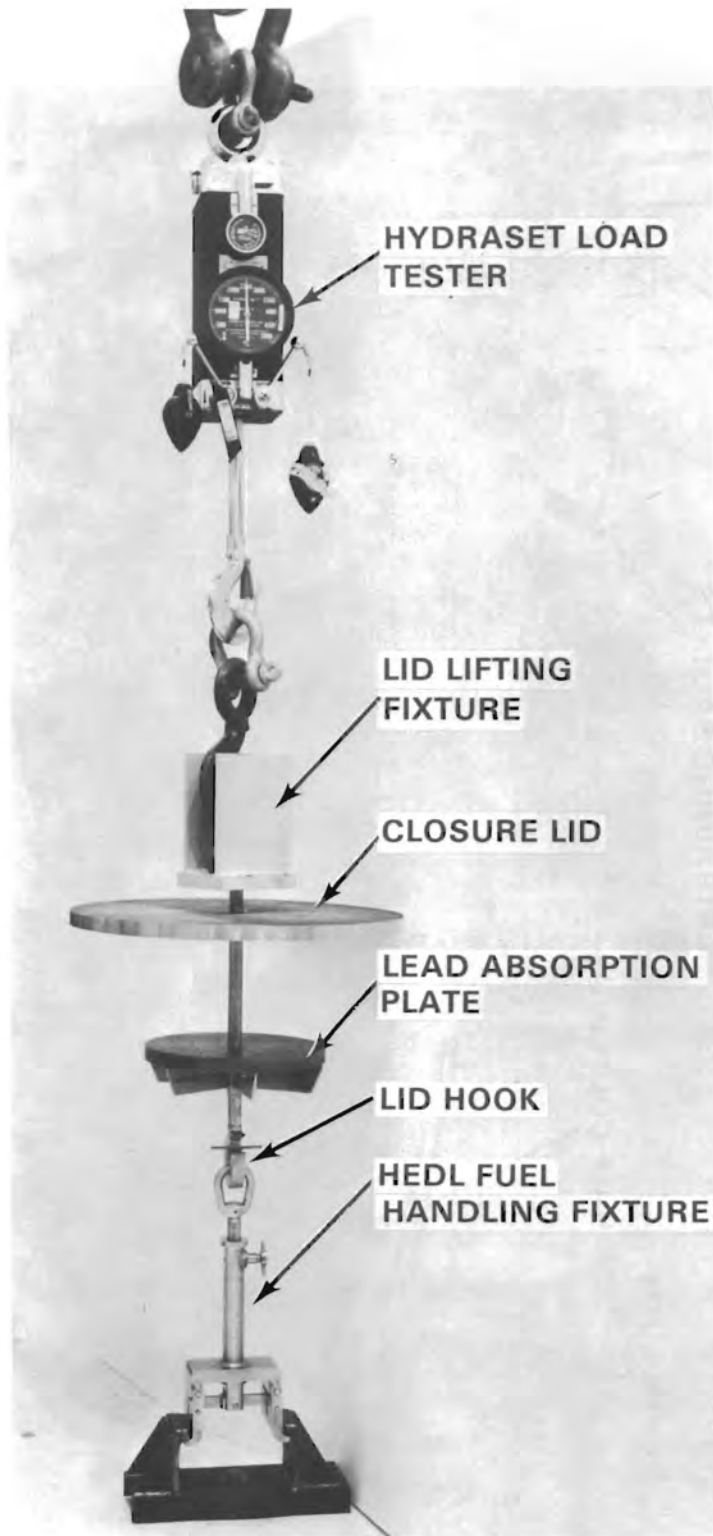


FIGURE 10. Closure Lid and HEDL Fuel Handling Fixture During Load Testing (Courtesy HEDL)



FIGURE 11. Calorimeter Vessel Top Flange (Courtesy HEDL)

Three piping penetrations were welded into the calorimeter vessel, in addition to the reducer welded to the bottom head. A 3/4-in. Schedule 40 pipe, which functions as a fill/drain line, enters the vessel 2-1/2 in. above the bottom head (Figure 9). A 3/4-in. Schedule 40 pipe, located 2-1/2 in. below the vessel top flange (Figure 11), provides a steam discharge path to the condenser and acts as a vessel pressure relief vent to the hot bay atmosphere through the open end of the condenser discharge line. The third vessel penetration, a 1/2-in. Schedule 40 pipe, provides a connection for the water level sight glass and a second pressure relief vent path to the hot bay atmosphere (Figure 11).

A 1-in. Schedule 40 drain line was welded to the reducer penetration in the bottom head of the vessel (Figure 9). The drain line branches below the vessel support structure elevation. One branch of the drain line contains a connection for the calorimeter vessel level detection system and two manual ball valves. The other branch of the vessel drain line extends to the east operating gallery to provide an auxiliary water fill system.

In addition to the calorimeter vessel piping penetrations described above, four half-pipe couplings were welded to the vessel 3-1/2 in. above the bottom head as shown in Figure 12. The couplings were threaded to accept immersion electric heaters that are used to heat the water in the vessel to boiling conditions and to maintain system thermal equilibrium.

The calorimeter outer vessel was insulated with a nominal 8.5-in.-thick layer of silica-lime block-type insulation. The top closure insulation "hat" was constructed of a stainless steel sheet metal can covered with insulation and is removable for access to the vessel lid (Figure 7).

During decay heat generation measurements, a spent fuel assembly is positioned within an inner vessel fabricated from 14-in.-dia Schedule 40 type 304 stainless steel pipe (Figure 13). Holes were drilled in the pipe to reduce the thermal time constant and permit water to flow in the annulus formed by the inner and outer vessels. The principal purpose of the inner vessel is to support lead rings which absorb gamma radiation emitted by spent fuel assemblies

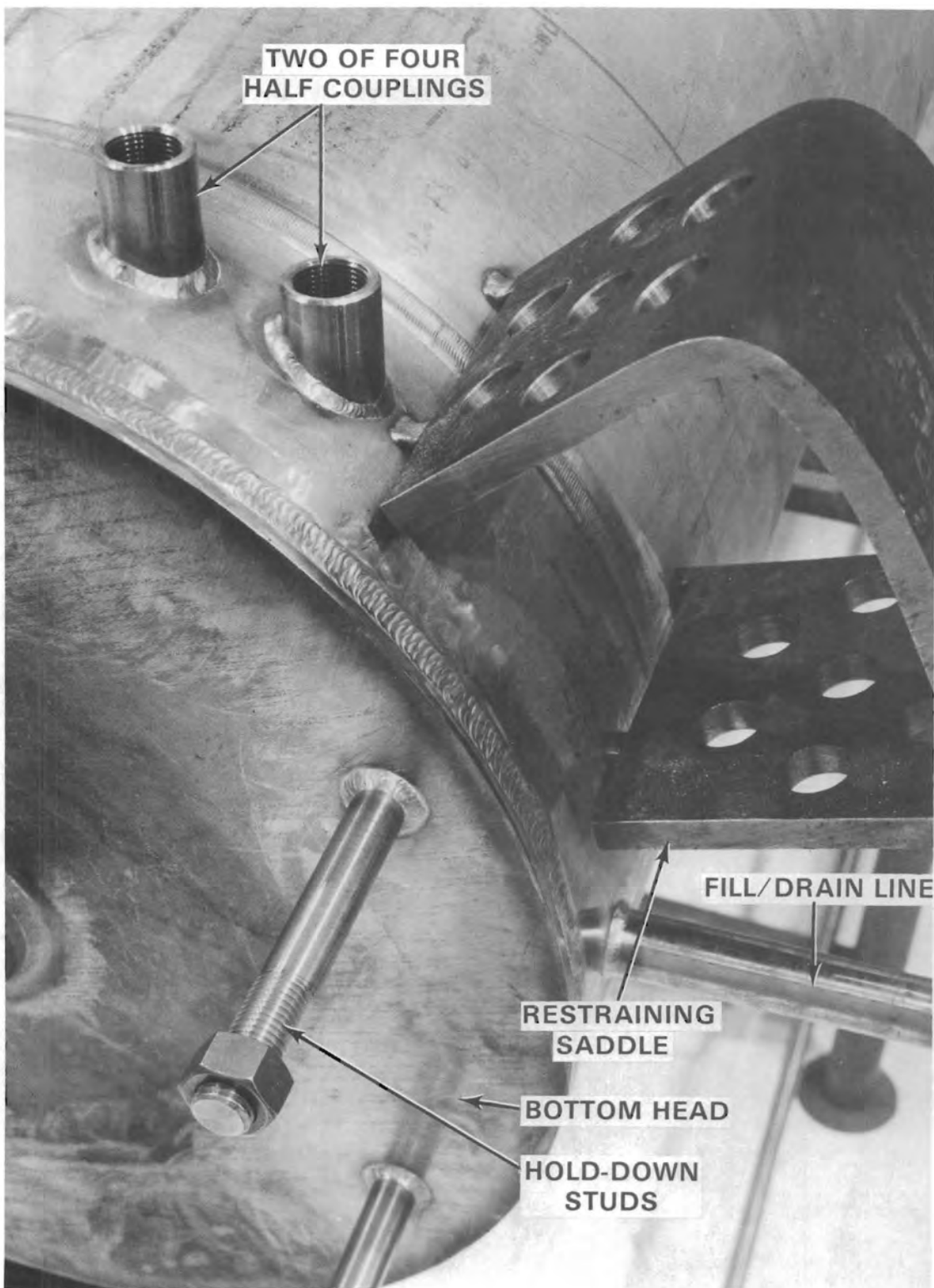


FIGURE 12. Half Couplings for Heater Insertion (Courtesy HEDL)

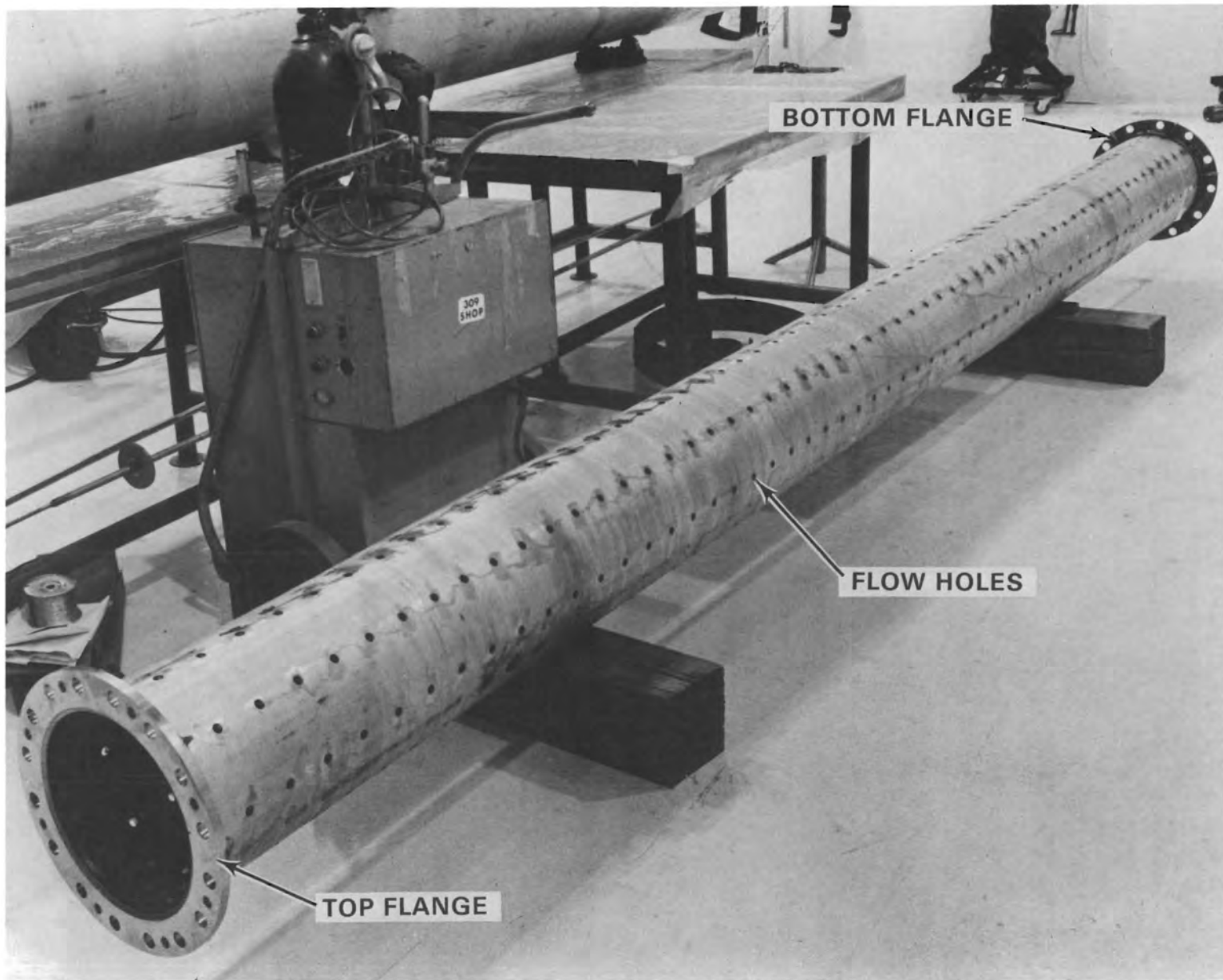


FIGURE 13. Inner Calorimeter Vessel (Courtesy HEDL)

The lead rings, which are attached to the outer surface of the pipe, have a nominal absorption thickness of 1.25 in. The rings were estimated to be 99 % effective in absorbing the gamma energy emitted from typical spent fuel assemblies. Water flow slots were machined in the rings to reduce their thermal time constant.

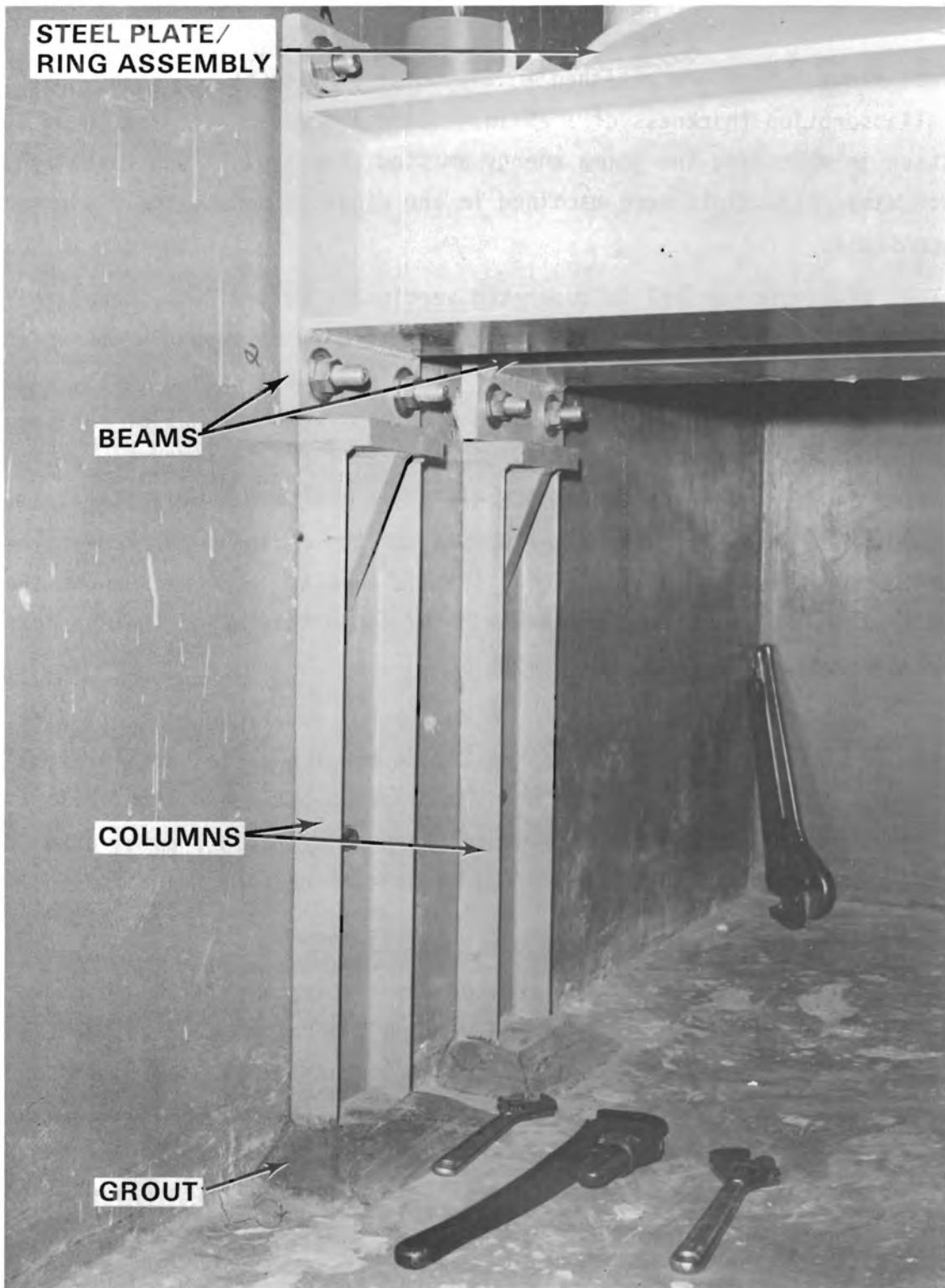
The calorimeter vessel is supported vertically by two 8-in. beams that span the width of the calorimeter pit (Figure 14). The support beams were anchored into the calorimeter pit walls with 3/4-in.-dia anchor bolts. Additional support is provided by columns that extend from the ends of each beam to the pit floor. Restraining saddles, welded to the calorimeter vessel near the bottom end as shown in Figures 9 and 12, are restrained by a steel plate/-ring (shown in Figure 7) that was welded to the top of the 8-in. support beams to provide horizontal stability during seismic events. Spacers support the bottom head of the vessel approximately 3 in. above the top of the support beams and provide clearance for insulation.

A welded steel structure, anchored to the hot bay floor at the top of the calorimeter pit, provides horizontal restraint for the vessel at approximately mid-height (Figure 7). The restraint is provided by standard pipe rollers that react against saddles welded to the vessel. The pipe rollers allow unrestrained thermal growth of the vessel during vessel heatup.

4.1.2.2 Water Supply/Storage Tank and Fill Pump

The water supply/storage tank for the calorimeter system was anchored to the floor of the calorimeter pit directly below the calorimeter vessel. The tank was fabricated from 1/8-in.-thick 300-series stainless steel and is 60 in. long by 48 in. wide by 22 in. high. The top of the tank is recessed approximately 2 in. below the side walls to form a catch basin. The approximate internal volume of the tank is 250 gallons, excluding the catch basin, which holds approximately 25 gallons.

A simplified schematic diagram of the calorimeter system piping and instrumentation is provided in Figure 15. The tank fill line and the air line for the pneumatic level instrumentation enter the supply/storage tank through



WA 878 INSTALLATION OF NEW BOTTOM SUPPORT LEGS BETWEEN CALORIMETER LOWER FRAME AND CALORIMETER PIT FLOOR

FIGURE 14. Vertical Support Beams and Columns (Courtesy Westinghouse AESD, Nevada)

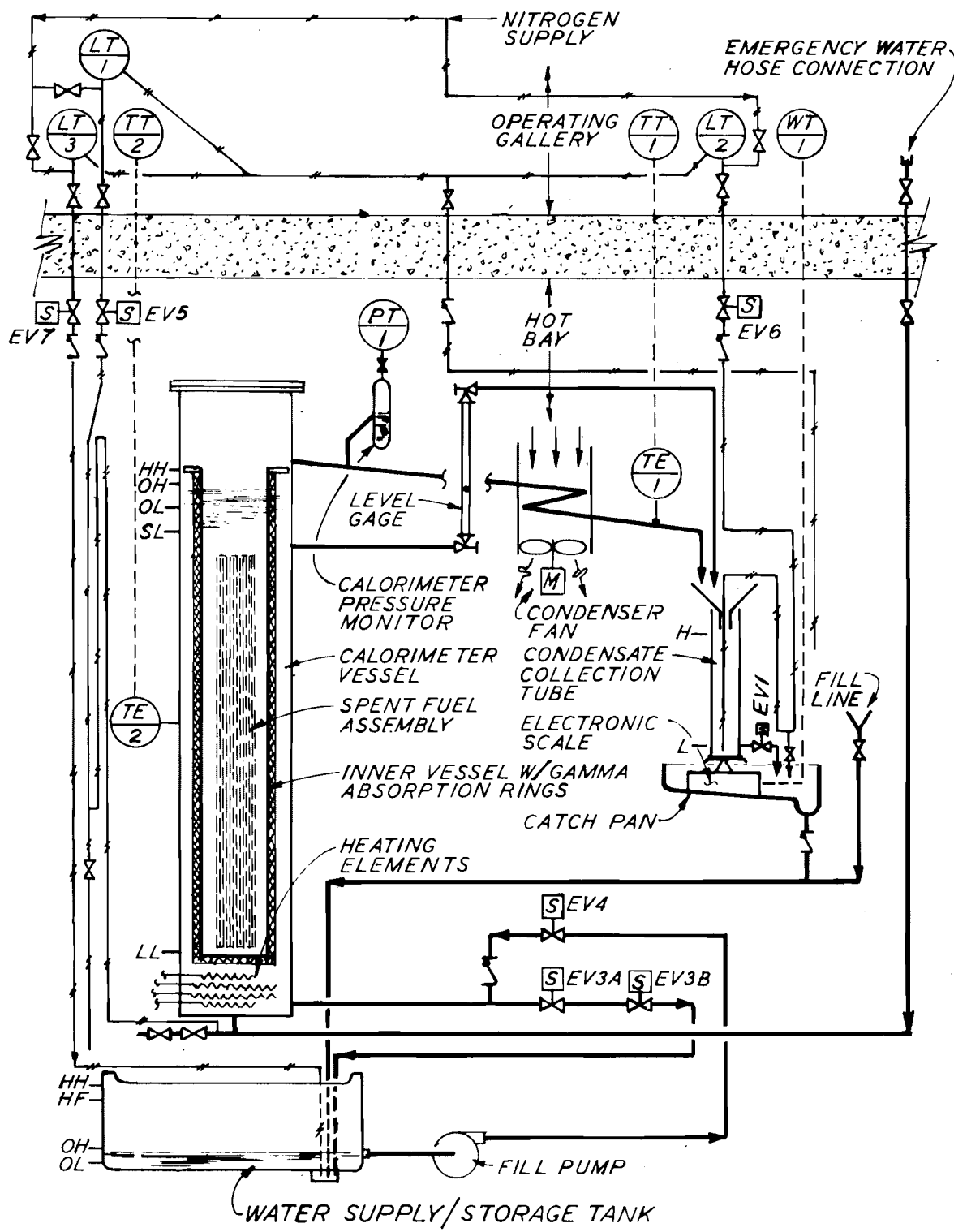


FIGURE 15. Calorimeter System Schematic

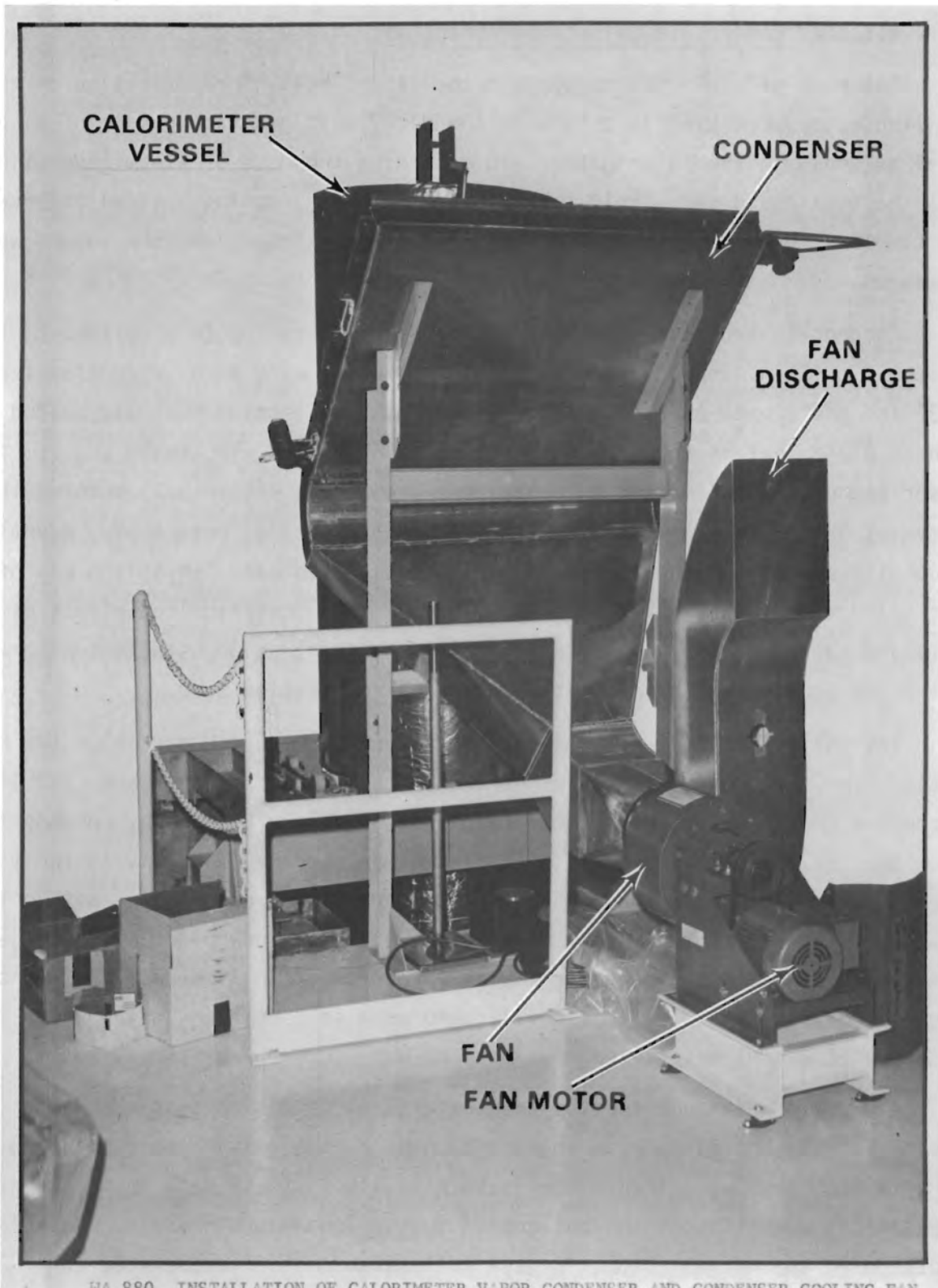
an opening in the bottom of the catch basin. The all-brass fill pump was bolted to the floor, and the 1-1/4-in. suction line was attached to the tank near the bottom. The pump has a capacity of 10 gal/min, operating against a water head of 58 ft. The pump is close-coupled to a 1/2-hp motor that is energized from a regulated 120-V single-phase source. The fill line extends from the supply/storage tank to the hot bay floor elevation, where demineralized water can be added from portable containers. A manual ball valve isolates the fill line after the supply/storage tank is filled.

A normally closed solenoid valve (EV4, Figure 15) and a check valve installed in the fill pump discharge line isolate the fill line from the calorimeter vessel. The two normally closed solenoid valves, EV3A and EV3B, isolate the calorimeter vessel from the supply/storage tank and provide a means to remotely drain the vessel if required.

4.1.2.3 Steam Condenser

Steam generated within the calorimeter vessel is directed from the vessel to a condenser (Figure 16) located on the hot bay floor outside the perimeter of the calorimeter pit. The 3/4-in. steam pipe from the vessel enters the condenser through a manifold where the flow is divided into two parallel paths. Each of the parallel paths through the condenser was fabricated from 3/4-in.-dia (0.035-in. wall thickness) 304 stainless steel tubing fitted with spiral-wound aluminum fins to enhance heat transfer. The total length of each flow path is ~12 ft. Condensate flows from the condenser through a manifold where the two flow paths are combined and directed to the condensate collection tube.

The condenser is air-cooled by a squirrel cage blower rated at 1300 scfm. A sheet metal shroud channels the air flow through the finned tube condenser to the fan inlet located below the condenser. The fan, driven by a 1-hp single-phase electric motor, discharges directly into the hot bay. A switch to sense air flow through the condenser is located in the fan outlet duct. The condenser and the associated air flow equipment were conservatively designed to condense and subcool all the steam generated in the calorimeter vessel by a 2.5-kW spent fuel assembly plus 1 kW from a dc reference heater.



WA 880 INSTALLATION OF CALORIMETER VAPOR CONDENSER AND CONDENSER COOLING FAN

FIGURE 16. Condenser/Fan Unit (Courtesy Westinghouse AESD, Nevada)

4.1.2.4 Condensate Collection Apparatus

The rate of steam generation and the latent heat of vaporization of the boiling water were used to determine the decay heat generation rate of a spent fuel assembly in the calorimeter. To determine the rate of steam generation, all the steam produced within the calorimeter vessel during a known interval of time was condensed, subcooled, collected, and weighed, and the volume was measured.

Condensate from the condenser discharge was directed to a collection tube, which is a 41-in.-long section of precision tubing with an outside diameter of 1.25 in. and a wall thickness of 0.035 in. The collection tube was welded to a base plate that is mounted on the pan of a precision electronic scale. The upper end of the collection tube is supported with a linear ball bushing that provides lateral support for the tube with minimal axial restraint. A drain line with a solenoid shut-off valve (EV1) was welded near the bottom end of the collection tube (Figure 15). To minimize the eccentric load effect of the solenoid valve and drain line on scale measurements, an adjustable counter-weight is located on the opposite side of the collection tube.

The collection tube drain line discharges into a catch pan below the scale. The catch pan drain is connected to the supply/storage tank fill line through a check valve. With the solenoid drain valve (EV1) open, condensate from the collection tube flows to the catch pan and then directly to the tank. The lip of the catch pan projects over the edge of the calorimeter pit so that any overflow is directed into the pit drain gutter. Such overflow could be the result of drain stoppage or flow in excess of drain line capacity, which might occur, for example, if the fill pump were to continue running after the calorimeter vessel was filled.

A 0.25-in.-dia tube for the pneumatic level detection system extends inside the collection tube to an elevation below the drain line connection. Signals from the level transmitter automatically initiate data logger scans and control operation of the collection tube solenoid drain valve, EV1. In addition to the normal automatic data collection mode, the operator can

remotely initiate a data scan without draining the collection tube or can initiate drainage of the collection tube, which automatically initiates a data scan.

4.1.2.5 Control and Data Acquisition Instrumentation

Instrumentation provided with the calorimeter system is used principally to monitor and control water level, pressure, and temperature, and to facilitate data acquisition. The main instrumentation and control panels are shown in Figure 17. Power for the instrumentation, control panels, and fill pump is isolated from facility voltage transients (up to $\pm 15\%$) by an ac voltage regulator.

Water Level Instrumentation and Control. Water levels in the calorimeter vessel, supply/storage tank, and condensate collection tube are measured pneumatically (Figure 15). Air is introduced through a small diameter tube until a finite flow (~10% of full scale) is indicated on an air rotameter located in the control panel (Figure 17). The pressure required to sustain air flow, as sensed by a pressure transmitter (Figure 17), is equal to the head of water in the vessel above the open end of the tube. The advantage of using this "bubble" technique for hot bay applications is that the pressure transducers could be located outside the bay for easy maintenance and calibration.

There are five water level set points in the calorimeter vessel: high high (HH), operating high (OH), operating low (OL), safe low (SL), and low low (LL). The LL limit was established to assure that the electric heaters located in the bottom of the calorimeter vessel cannot be energized unless there is sufficient water in the vessel to cover them. At or below the LL level, the electric heaters cannot be operated and an alarm on the annunciator panel is activated. The LL limit interlock on heater operation cannot be bypassed by any manual switch on the control panel.

The SL limit in the calorimeter vessel was established to assure that spent fuel assemblies are completely immersed in water. At or below the SL level, all electric heaters are deactivated, and an annunciator alarm is activated in the control panel. The SL limit can be adjusted for different types

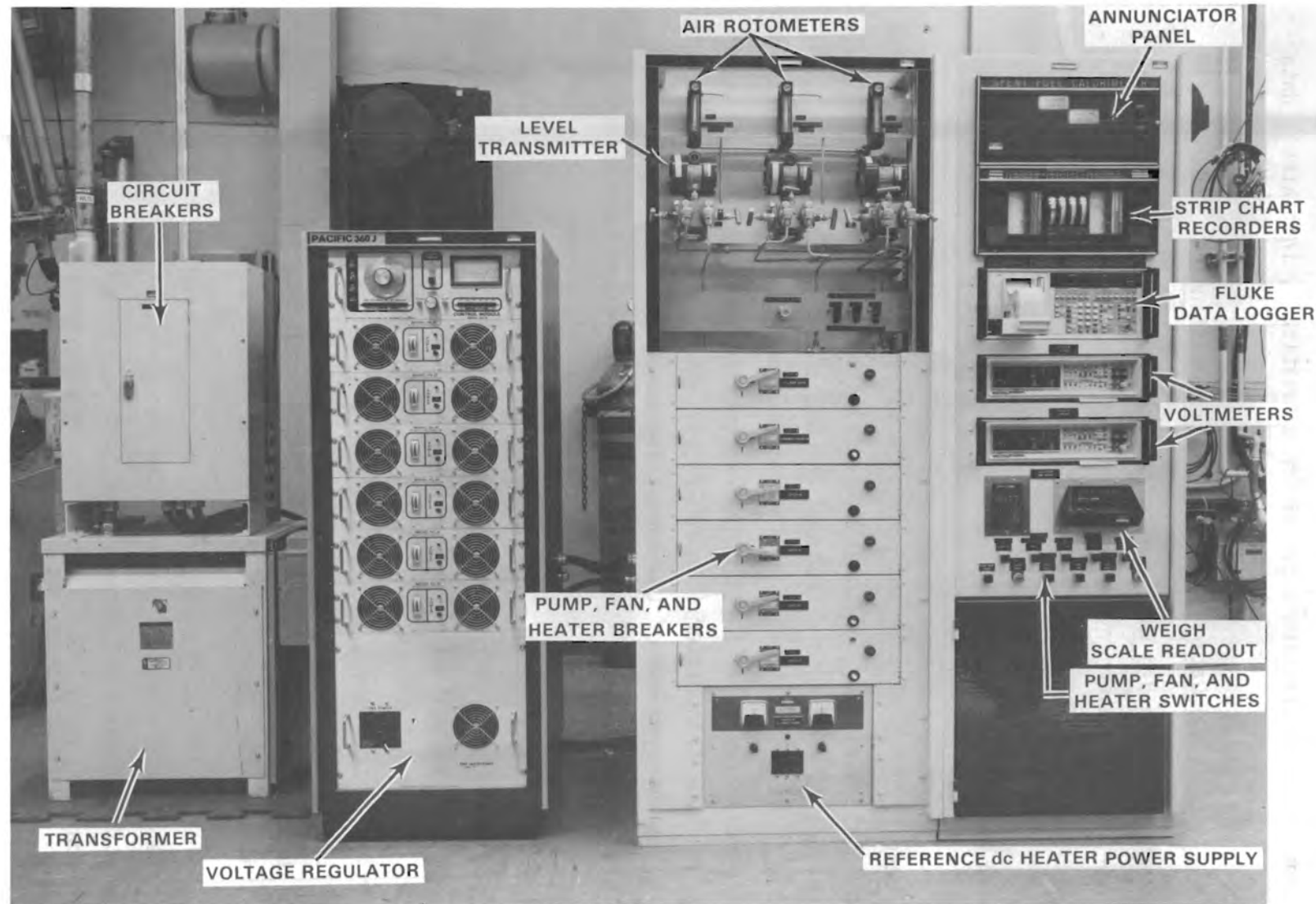


FIGURE 17. Instrumentation and Control Panels (Courtesy Westinghouse AESD, Nevada)

of fuel assemblies and support equipment. Conservatively, it is recommended that the SL limit be set approximately 8 in. above the top of a fuel assembly.

The OL and OH set points establish the normal water level range. At the OL level, the OL alarm activates on the annunciator panel, and the fill pump automatically starts to refill the calorimeter vessel. The pump continues to fill the vessel until the level reaches the OH level or a data scan is initiated through the condensate collection control circuit. Pump operation can be initiated manually whenever the water level in the vessel is below OH and a data scan is not in progress. At the OH level, an alarm activates on the control panel and the fill pump automatically shuts off.

If the pump fails to shut off, the water level would continue to increase until the HH level is reached. At the HH level, an alarm would sound, and the operator must shut the pump off to avoid excess water from flowing out the steam discharge line, through the condenser, into the collection tube, and to the supply/storage tank. Remote drainage of the calorimeter vessel can be initiated by activating a key switch on the control to avoid the HH level.

There are five water level set points in the supply/storage tank: high high (HH), operating high (OH), operating low (OL), high fill (HF), and a safe low (SL2), which is a backup for the calorimeter safe low condition. The HH, OH, OL, and HF levels are monitored by alarms on the annunciator panel, and a storage tank level meter is located on the control panel. The SL2 level is set to sense an increase in storage tank water level above the OH level, a condition that can be indicative of inadvertent drainage from the calorimeter vessel. The storage tank SL2 level is connected in series with the SL calorimeter level in the electric heater control circuit to shut off the electric heaters if the supply/storage tank safe low level is exceeded.

There are two water level set points, low and high, associated with the condensate collection tube. Air for the pneumatic level detection system is introduced through a dip tube that passes through the open end of the collection tube and extends to an elevation below the drain connection (Figure 15).

When the level of condensate reaches the high limit, a data scan is automatically obtained with the data acquisition system. After the data scan is completed, the collection tube drain valve is automatically opened and the tube is drained to the low level. The system has a built-in time delay that can be adjusted so the data scan can be completed before the drain valve opens. The pump control circuit was designed so the pump cannot be operated during a data scan.

A momentary push button switch can be used to initiate a data scan and dump the condensate collection tube at any time. Another momentary push button switch can be used to initiate a data scan without dumping the collection tube. When the water level in the collection tube drains to the low level, the solenoid drain valve closes, and the system is ready for the next condensate collection cycle. Both the high and low level conditions in the collection tube initiate alarms on the annunciator panel.

Pressure Instrumentation. An absolute pressure transducer (25 psia) located in the hot bay measures and records the steam pressure in the calorimeter vessel (Figure 15). A condensate collection pot connected to the calorimeter steam discharge line minimizes condensate accumulation in the pressure sensing line. Measurement of the absolute pressure in the calorimeter vessel is necessary to determine the latent heat of vaporization from the steam tables.

Temperature Instrumentation and Control. Two resistance temperature detectors (RTDs) are included in the calorimeter system--one to measure the outer calorimeter vessel wall temperature and one to measure the temperature of the condensate discharged from the condenser. These temperature signals are transmitted to a strip chart recorder on the control panel and to the data logger. The calorimeter vessel "skin" temperature is provided to aid the operator during the heat-up phase of testing. The condensate temperature is necessary to assure adequate subcooling and to determine if the system has attained a steady-state condition; i.e., a constant, stable outlet temperature is an indication that a steady-state condition exists. The condenser cooling fan circuit was designed such that if the fan is not turned on, it would automatically come on if the condenser outlet temperature reaches $\sim 150^{\circ}\text{F}$.

Four thermocouples (TCs) are located near the calorimeter to measure hot bay ambient temperatures. These temperatures were recorded several times during each testing day to verify that the hot bay temperature was essentially constant. A constant or near constant hot bay temperature leads to the conclusion that the heat loss from the calorimeter is constant because this heat loss is directly proportional to the differential temperature between the boiling water and the hot bay.

Electric Heater Control. Four electric immersion heaters were installed near the bottom of the calorimeter vessel. All four immersion heaters provide a total of 22 kW and are used for initial heatup of the system. Two 8-kW heaters and one 3-kW heater are energized from individual 240-V single-phase breakers. The fourth electric heater has a 3-kW nominal rating and is used to stabilize the calorimeter system at boiling conditions prior to fuel immersion and to serve as a reference heater during decay heat generation rate measurements. The variable power for the fourth heater is supplied from a precision dc power controller. The dc heater voltage and current are monitored by voltmeters on the control panel and are recorded by the data acquisition system. The dc heater power is determined by measuring the voltage across the heater and by measuring the voltage across a precision shunt resistor placed in series with the heater. With the shunt resistance and voltage, the current passing through both the heater and shunt can be calculated.

An interlock in the heater control circuit is provided to prevent energizing the heaters if the water level in the calorimeter vessel is below the LL limit. The heater control circuit also de-energizes the heaters if the calorimeter vessel water level falls below the SL limit, if there is no airflow through the condenser, or if the water level in the storage tank exceeds the safe low (SL2) level.

Data Acquisition and Recording. A data scan is initiated on a data logger (Figure 17) by a high level in the condensate collection tube or by activating a push button switch. During a data scan, the following system parameters are recorded:

- Collection tube weight
- Collection tube water level

- dc electric heater power
- dc electric heater voltage
- dc electric heater amperage
- Condenser outlet temperature
- Calorimeter "skin" temperature
- Calorimeter absolute pressure
- Storage tank water level
- Calorimeter water level
- Start and stop times for collection cycle
- Date.

Two multi-pen analog recorders mounted in the control panel (Figure 17) provide a continuous record of these test parameters:

- Calorimeter vessel water level
- Calorimeter "skin" temperature
- dc electric heater power
- Condensate collection tube level
- Condensate collection tube weight
- Condenser outlet temperature.

Analog indicating meters mounted on the control panel (Figure 17) continuously monitor the following parameters:

- dc electric heater power
- dc electric heater voltage
- dc electric heater amperage
- Storage tank level.

A digital display of the following parameters is furnished on the control panel:

- Preselected data logger channel parameters
- dc electric heater voltage
- dc electric heater amperage
- Condensate collection tube weight.

Annunciator Panel. An annunciator panel (Figure 17) installed in the control panel provides the operator with an audible and visual indication of

the following system conditions:

- Calorimeter high high level
- Calorimeter operational high level
- Calorimeter operational low level
- Calorimeter safe low level
- Calorimeter low low level
- Collection tube high level
- Collection tube low level
- Condenser discharge high temperature
- Storage tank operational low level
- Storage tank high high level
- Calorimeter safe low level and condenser air flow by-pass
- Calorimeter drain switch
- Storage tank high fill level
- Loss of condenser cooling air flow.

4.2 EXPERIMENTAL PROCEDURE

After the calorimeter system was installed in the EMAD hot bay, checked out, and calibrated, an acceptance test was performed. After adequate operating experience was achieved, the decay heat generation rate of a Turkey Point PWR spent fuel assembly was measured. The following sections briefly present the procedures used to conduct the testing and measurement efforts.

4.2.1 Acceptance Test

The purpose of the acceptance test was to verify the operability of the system, to check system accuracy, and to estimate the overall system heat loss. During acceptance testing, important operating parameters such as the time required for cold start-up, the time to reach equilibrium, and the effects of injecting cold water into the calorimeter during equilibrium were investigated. Safety considerations, such as determining the approximate amount of additional heat loss that can be expected if the calorimeter insulating cap is removed, were determined.

The acceptance test was performed by bringing the water in the calorimeter vessel to boiling with power from the available heaters. The time to reach

boiling and attain equilibrium was recorded. The three ac heaters were turned off, and the dc heater was used to simulate the power generated by a spent fuel assembly. Nominal heater power settings of 0.9, 1.0, 1.5, 2.0, 2.5, and 3.0 kW were selected and accurately measured. At each of these settings, condensate accumulation rates were measured with the calorimeter collection apparatus. The run at 1 kW was repeated three times to determine system repeatability. The calorimeter insulation cap was removed during one 3-kW run to determine the additional heat loss that can be expected.

The data were used to check the accuracy of the calorimeter for measuring heat generation rates. This was achieved by utilizing the data from any two runs in the following relationships:

$$q_{h,1} = q_{cal,1} + q_{L,1} = \dot{m}_1 h_{fg} + q_{L,1}$$

$$q_{h,2} = q_{cal,2} + q_{L,2} = \dot{m}_2 h_{fg} + q_{L,2}$$

$$q_{h,1} - q_{h,2} = q_{cal,1} - q_{cal,2} + q_{L,1} - q_{L,2} = \dot{m}_1 h_{fg} - \dot{m}_2 h_{fg} + q_{L,1} - q_{L,2}$$

Assuming the hot bay ambient temperature and the temperature of the boiling water are constant, heat losses from the system during run #1 and run #2 are equal, therefore

$$\Delta q_h = \Delta q_{cal} = \dot{m}_1 h_{fg} - \dot{m}_2 h_{fg}$$

where

q_h --actual heat generated in the calorimeter by the heater for runs #1 and #2

q_{cal} --measured heat generation rate in the calorimeter using the mass accumulation collection system for runs #1 and #2

Δq_{cal} --difference in heat generation rates for runs #1 and #2 measured with the calorimeter system

Δq_h --difference in heat generation rate of the dc heater for runs #1 and #2

\dot{m}_1 --mass accumulation rate for run #1

\dot{m}_2 --mass accumulation rate for run #2

h_{fg} —latent heat of vaporization for water at calorimeter pressure.

In this manner, the difference in heat generation rates determined from measuring the condensate accumulation rate could be checked against actual heat generation rate differences based on the heater settings. Results of the acceptance test are discussed in detail in section 5.0.

4.2.2 Spent Fuel Assembly Heat Generation Measurement

The procedure used to measure the decay heat generation rate of a Turkey Point PWR spent fuel assembly was as follows:

- 1) The day prior to inserting the fuel assembly in the calorimeter, a reference run with the dc heater at ~1 kW was performed using the procedure in section 4.2.1. Measurements using the collection tube apparatus, weigh scale, and head transmitter provided the initial mass accumulation rate, \dot{m}_i . Note that this mass accumulation rate resulted from the heat generated by the heater (q_h) minus the heat loss ($q_{L,i}$) from the system.
- 2) The day the spent fuel assembly was inserted, the water in the calorimeter was heated to boiling using the heaters. After boiling was established, the dc heater was set at the value that the reference run was performed at in step 1.
- 3) The water level in the calorimeter was dropped to the SL setpoint, the insulation cap and temporary lid removed (Figures 18 and 19), and the fuel assembly was inserted in the calorimeter (Figure 20). The lid/support and the insulation cap were reinstalled, and the water level was increased to the OH level.
- 4) Data runs were obtained by letting the collection tube fill and dump automatically. After approximately 4-1/2 hours, the condenser outlet temperature was constant and four consecutive data runs had been obtained in which the times to accumulate fixed heads of water were constant within $\pm 1\%$ of the average time. With the mass accumulated and the accumulation time, the final mass accumulation rate (\dot{m}_f) was determined. Note that this mass accumulation rate resulted from

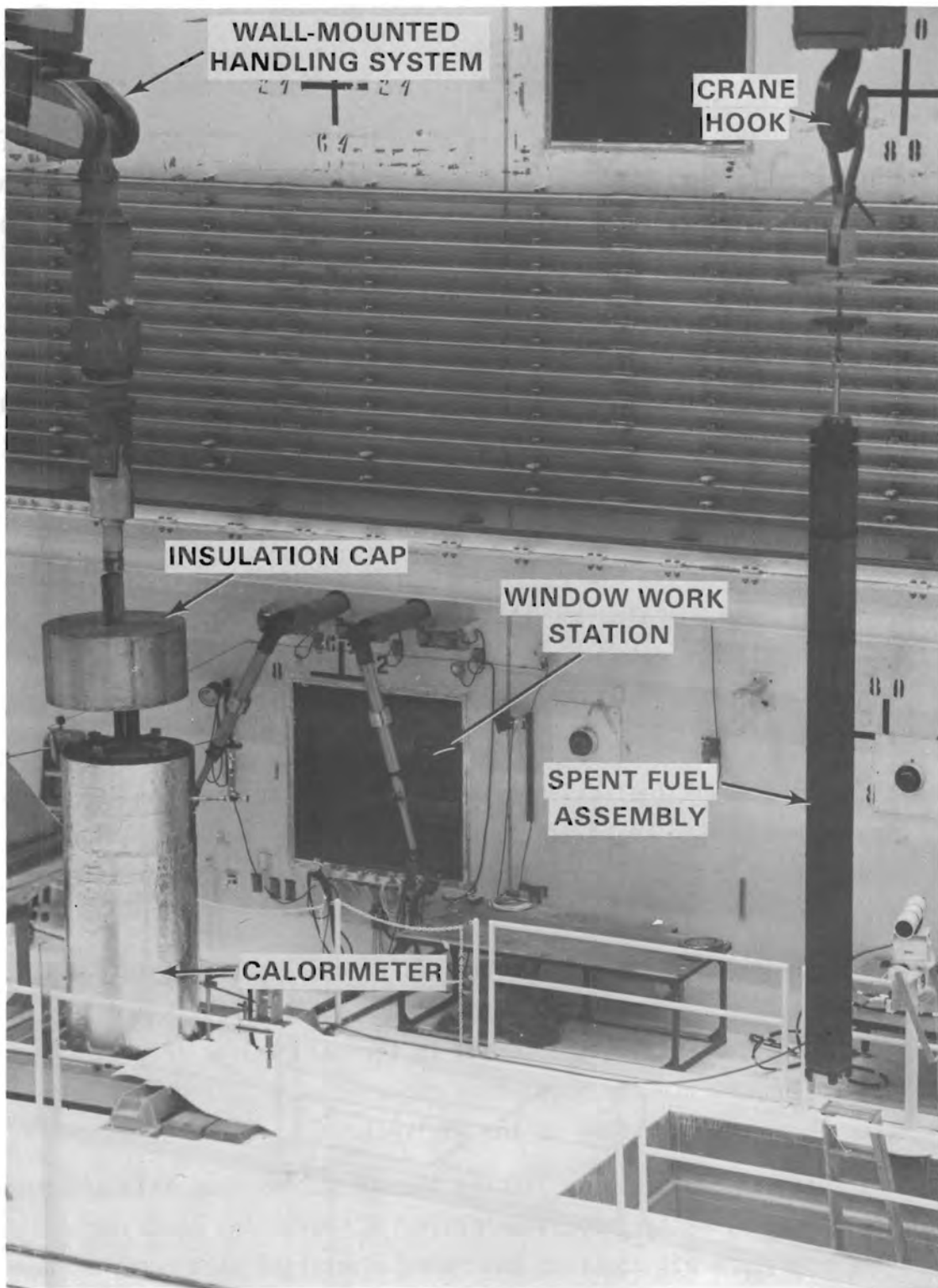


FIGURE 18. Remote Removal of the Insulation Cap
(Courtesy Westinghouse AESD, Nevada)

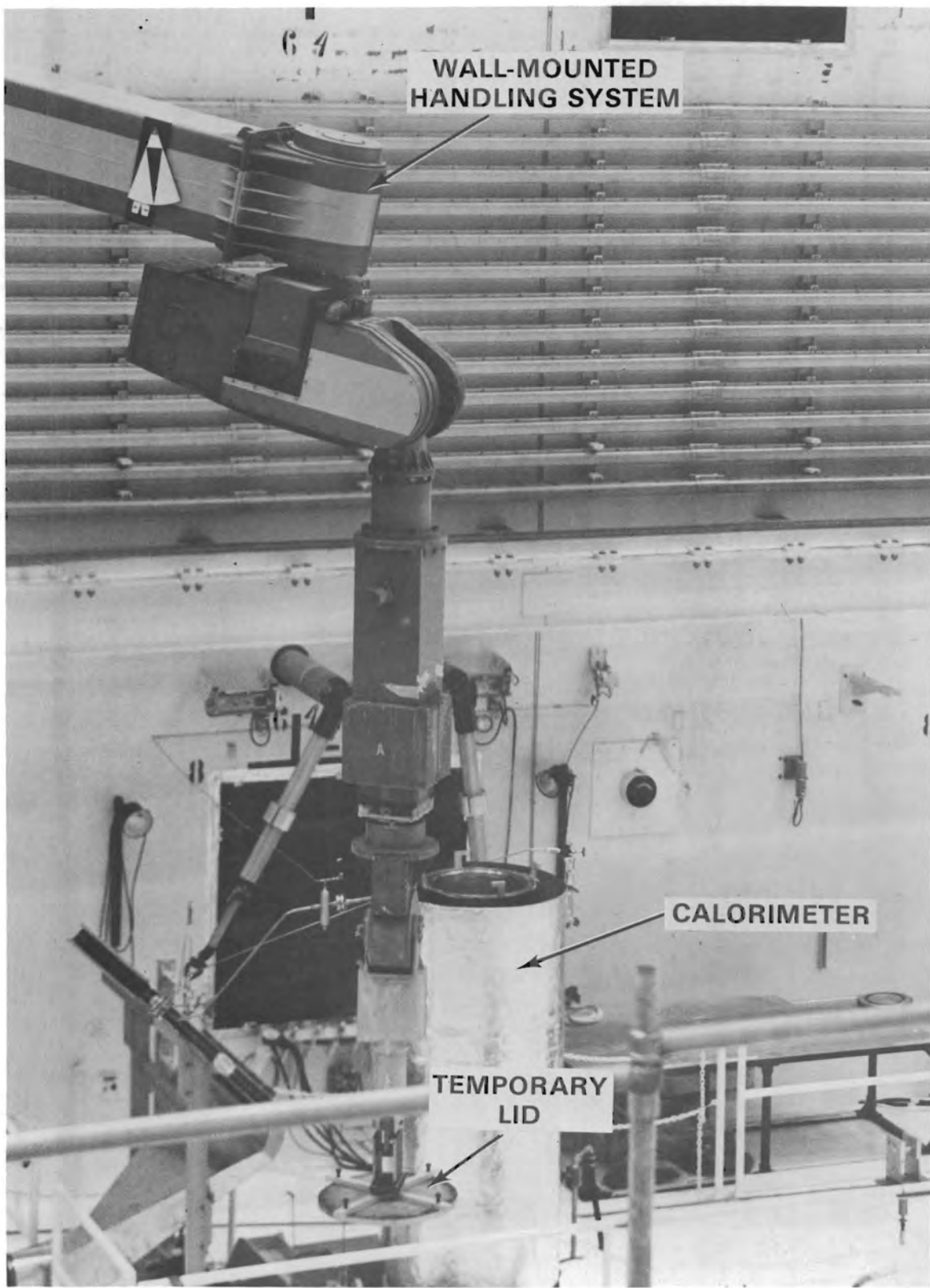


FIGURE 19. Remote Removal of Temporary Lid (Courtesy Westinghouse AESD, Nevada.)

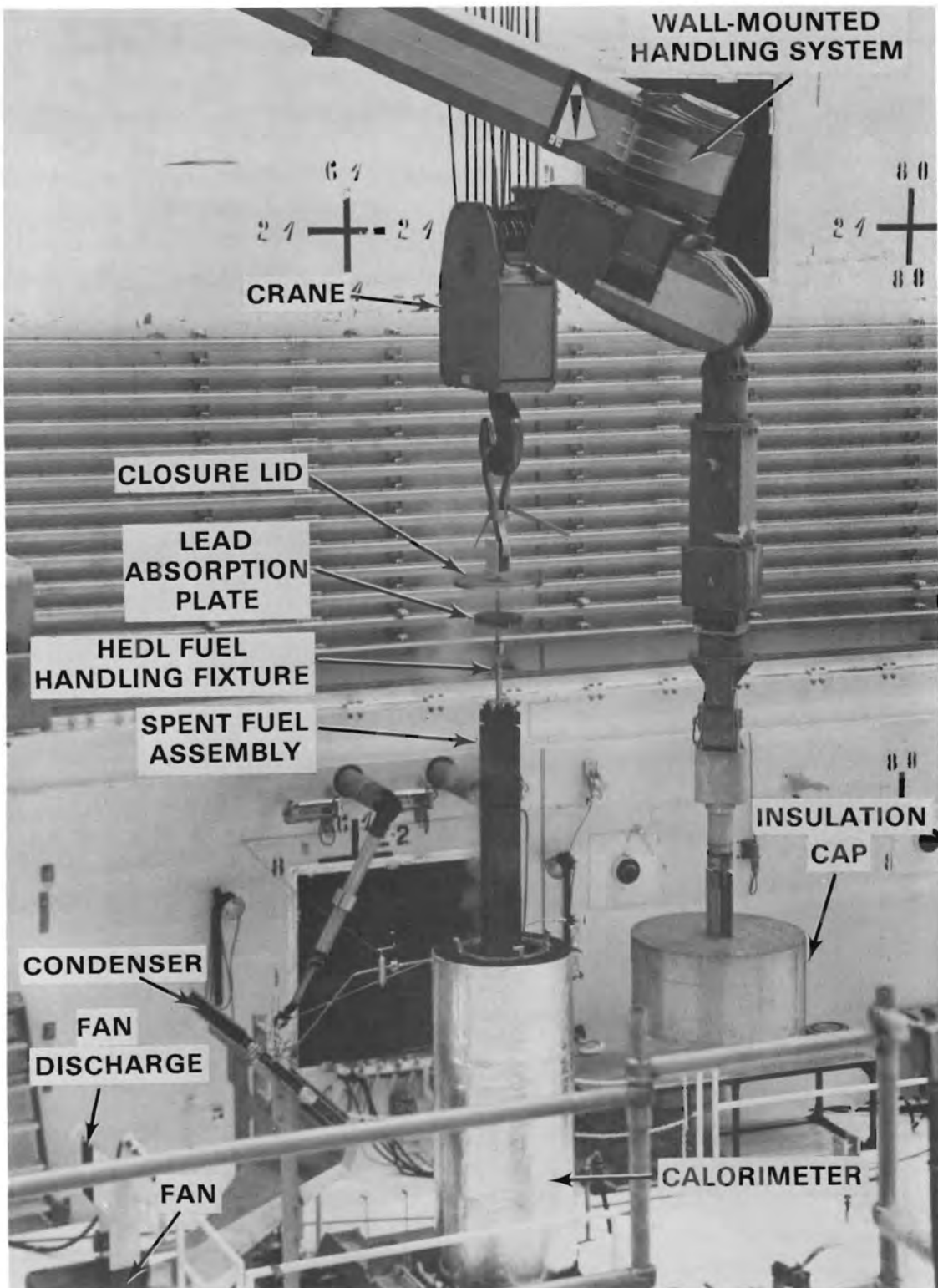


FIGURE 20. Remote Spent Fuel Assembly Insertion
(Courtesy Westinghouse AESD, Nevada)

the heat generated by the assembly and lead liner (q_{SF}) plus the heat generated by the heater (q_h) minus the heat loss from the system ($q_{L,f}$). The difference between the step 4 and step 2 mass accumulation rates ($\dot{m}_f - \dot{m}_i$) was that resulting from the decay heat generated by the spent fuel assembly and lead liner as shown below:

$$\begin{aligned}\dot{m}_i \alpha q_h - q_{L,i} \\ \dot{m}_f \alpha q_{SF} + q_h - q_{L,f} \\ \dot{m}_f - \dot{m}_i \alpha q_{SF} + q_h - q_{L,f} - (q_h - q_{L,i})\end{aligned}$$

The missing proportionality constant is the latent heat of vaporization and the heat generation rate of the spent fuel assembly was determined using the following expression assuming constant pressure (h_{fg}):

$$q_{SF} = (\dot{m}_f - \dot{m}_i)h_{fg} + q_{L,f} - q_{L,i}$$

Assuming the heat losses from the system were constant between the initial and final steps yields:

$$q_{SF} = (\dot{m}_f - \dot{m}_i)h_{fg}$$

- 5) The spent fuel assembly was removed from the calorimeter and another reference run was obtained the following day.

4.2.3 Data Presentation

Raw data obtained during acceptance testing and measurement of the decay heat generation rate of the Turkey Point spent fuel assembly are presented in Appendix B. A detailed discussion of the results obtained from analysis of the data is presented in section 5.0.

4.2.4 Data Reduction Method

The method used to reduce experimental data to engineering units is presented in Appendix C. It is important to note that not all recorded data values were important to the data reduction process. Many data were obtained for operations and backup purposes only.

4.2.5 Data Accuracy

An uncertainty analysis using Schenck's (1961) error and uncertainty method was performed to estimate important data accuracies. The method and analysis are presented and described in detail in Appendix D. Table 1 summarizes the results of the uncertainty analysis.

From Table 1 it is obvious that values obtained using head measurements have lower uncertainties than those using weight measurements. Lower uncertainties are a result of more accurate differential head measurements during condensate accumulation. Uncertainties in weight measurements of the condensate are higher because of uncertainties resulting from contact between the dip tube and collection tube, the resistance to scale platform movement caused by the collection tube alignment bearing, and the uneven loading on the scale platform caused by vibration from the collection tube solenoid drain valve during actuation.

TABLE 1. Typical Uncertainty Values

<u>Parameter</u>	<u>Nominal Value</u>	<u>Uncertainty</u>	
		<u>Value</u>	<u>Percent</u>
A_T	1.045 in. ²	± 0.0039 in. ²	$\pm 0.4\%$
P_{cal}	13.8 psia	± 0.125 psia	$\pm 1.0\%$
Δt	525 sec	± 1.4 sec	$\pm 0.27\%$
h_{fg}	974.8 Btu/lb	± 0.3 Btu/lb	$\pm 0.03\%$
q_h	3 kW	± 0.03 kW	$\pm 1.0\%$
ΔH	11 in. H ₂ O	± 0.35 in. H ₂ O	$\pm 3.2\%$
ΔW	185 g	± 12.0 g	$\pm 6.5\%$
\dot{m}_H	1.41 lb/hr	± 0.046 lb/hr	$\pm 3.2\%$
\dot{m}_W	1.45 lb/hr	± 0.092 lb/hr	$\pm 6.3\%$
$q_{cal,H}$	0.386 kW	± 0.013 kW	$\pm 3.3\%$
$q_{cal,W}$	0.386 kW	± 0.026 kW	$\pm 6.8\%$
$q_{L,H}$	0.596 kW	± 0.034 kW	$\pm 5.6\%$
$q_{L,W}$	0.553 kW	± 0.040 kW	$\pm 7.2\%$
$q_{SF,H}$	1.55 kW	± 0.058 kW	$\pm 3.7\%$
$q_{SF,W}$	1.55 kW	± 0.091 kW	$\pm 5.8\%$

The most significant uncertainty values presented in Table 1 are those of measurements of decay heat generation rates of the spent fuel assembly, i.e., $q_{SF,H}$ and $q_{SF,W}$. Uncertainty values of $\pm 3.7\%$ and $\pm 5.8\%$ were estimated for measured assembly heat generation rates obtained with the head and weight methods, respectively. These uncertainty values are less than the $\pm 10\%$ identified in the selection criteria discussed in section 3.1.



5.0 EXPERIMENTAL RESULTS AND DISCUSSION

The results of the calorimeter system acceptance test and measurement of the decay heat generation rate of a Turkey Point PWR spent fuel assembly are presented in this section. The measured value of the heat generation rate of the fuel assembly is compared with predictions obtained with the ORIGEN2 computer program (Croff 1980).

5.1 ACCEPTANCE TEST

The purpose of the acceptance test was to verify system operability, check accuracy, measure overall system heat losses, determine times for initial startup, estimate times to reach equilibrium after initiating boiling, and investigate the effects of injecting cold water into the bottom of the calorimeter during equilibrium. The additional heat loss that can be expected if the calorimeter insulating cap is removed was also determined. These topics are discussed in detail in the following subsections.

5.1.1 Comparison of Head and Weight Mass Accumulation Measurements

The primary measurement obtained with the calorimeter system was the condensate mass accumulation rate. The mass accumulation rate was used to calculate effective heat generation rates within the calorimeter using the equation

$$q_{cal} = \left(\dot{m}_c h_{fg} / 3412 \right) \text{ kW}$$

Two methods of measuring mass accumulation rates were used to assure accurate, reliable results. The primary method utilized a pressure transducer and a precision tube to measure head (volume) accumulation over a period of time. The secondary, or back-up, method was the measurement of weight accumulation using a precision scale. These methods have been discussed in detail in sections 4.1.2 and 4.2.4.

Figure 21 presents the ratios of weight-to-head mass accumulation rates. The mass accumulation rates obtained with the weigh scale are consistently ~2% less than those obtained with the head measurement. Possible reasons for this slight disagreement other than instrument calibration uncertainties are:

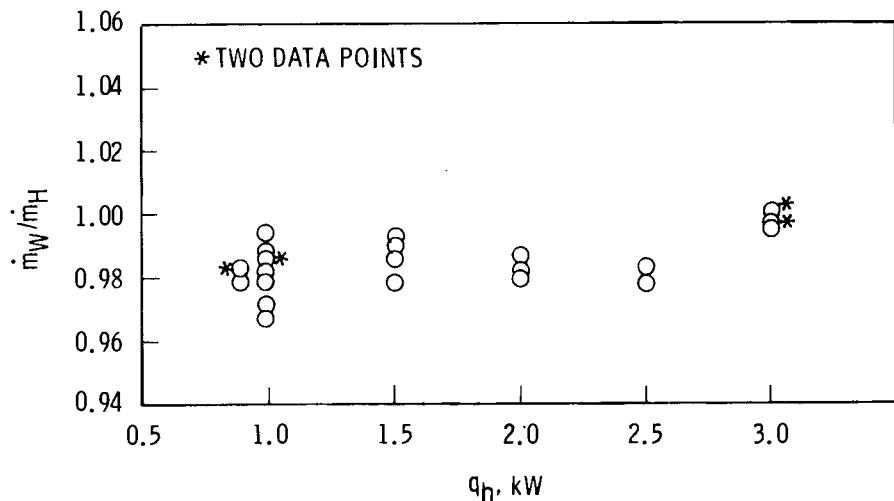


FIGURE 21. Comparison of Mass Accumulation Rate Measurements Using the Head and the Weight Methods

- The bubble tube used in the head method may have contacted the wall of the collection tube and caused resistance to movement of the scale platform.
- The vibration created by actuation of the collection tube drain valve may have caused eccentric loading of the tube on the scale platform.
- Binding between the collection tube and alignment bearing may have resulted from tube movement caused by drain valve vibration.

Agreement within 2% between measurements obtained with the two methods is considered satisfactory. Therefore, results from both head and weight measurements are presented in sections that follow.

5.1.2 System Heat Loss

As previously discussed in section 4.2.1, the evaluation of system heat loss was important, especially if it was determined to be relatively stable and constant. The loss was determined by taking the difference between the accurately measured reference heater power and the effective heat generated in the calorimeter measured with the condensate collection apparatus; i.e., $q_L = q_h - q_{cal}$. Figures 22 and 23 present heat loss data determined from individual condensate collection runs; i.e., collection tube fill-ups.

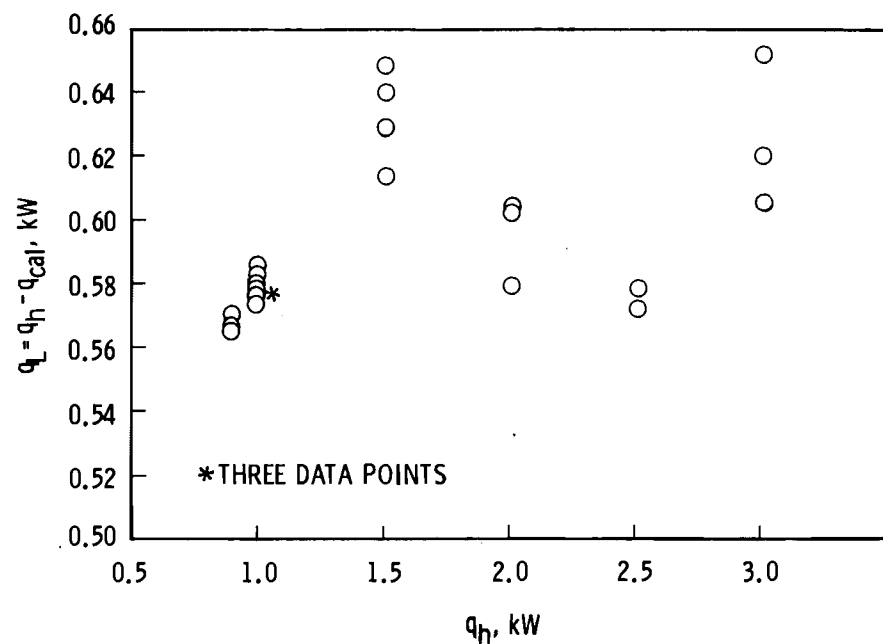


FIGURE 22. System Heat Losses Determined from Head Measurements

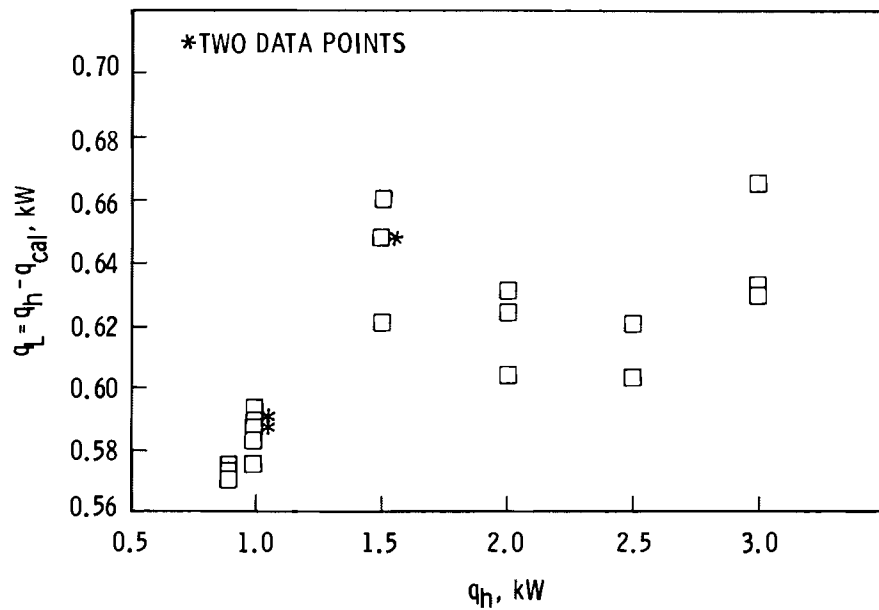


FIGURE 23. System Heat Losses Determined from Weight Measurements

Heat loss values ranging from ~ 0.56 to ~ 0.66 kW were calculated from the mass accumulation rate data obtained with the head and weight methods. Figures 22 and 23 indicate that heat loss values at reference heater powers of 1.5, 2.0, and 3.0 kW were slightly higher (~ 0.05 kW) than values at 1.0 and 2.5 kW. Note that more data points were obtained near $q_h = 1$ kW than at other heater power levels. Also, the scatter in data obtained near 1 kW was less than at other heater power levels.

The averaged data of Figures 24 and 25 show the same trends as the individual data points of Figures 22 and 23. Linear curve fits of the averaged data indicate slightly higher (~ 0.05 kW) heat loss values at the higher heater powers. Slightly higher heat losses at higher heater powers appear reasonable because the heater element operated at a higher temperature, which increased conduction losses along the body of the heater. Mathematical averages of the averaged data resulted in constant system heat losses of 0.602 kW and 0.621 kW, using the head and weight measurements, respectively.

During initial testing, it was believed that acceptable mass accumulation data were constituted by two consecutive condensate collection runs in which the times to collect a preselected head of condensate were within $\pm 1\%$ of one another. As operating experience was gained and during the completion of initial runs at reference heater powers of 1.5, 2.0, 2.5, and 3.0 kW, it became obvious that two runs were not sufficient to assure that steady-state conditions had been obtained. It was concluded that four consecutive runs with collection times agreeing within ± 1 to $\pm 1-1/2\%$ of their average time were required to assure that steady-state conditions existed and to constitute an acceptable series of runs. Most of the data acquired at a heater power of ~ 1 kW were obtained using this criterion. It is obvious from Figures 22 and 23 that the scatter in the data at 1 kW is much less than at the other power levels.

Data obtained at 1.5, 2.0, and 3.0 kW may be in slight error as a result of incorrect testing methods. Figures 22 through 25 indicate that the data at these three power levels were slightly high (~ 0.05 kW). It was preliminarily concluded that the heat loss from the system was essentially constant (~ 0.58 kW)

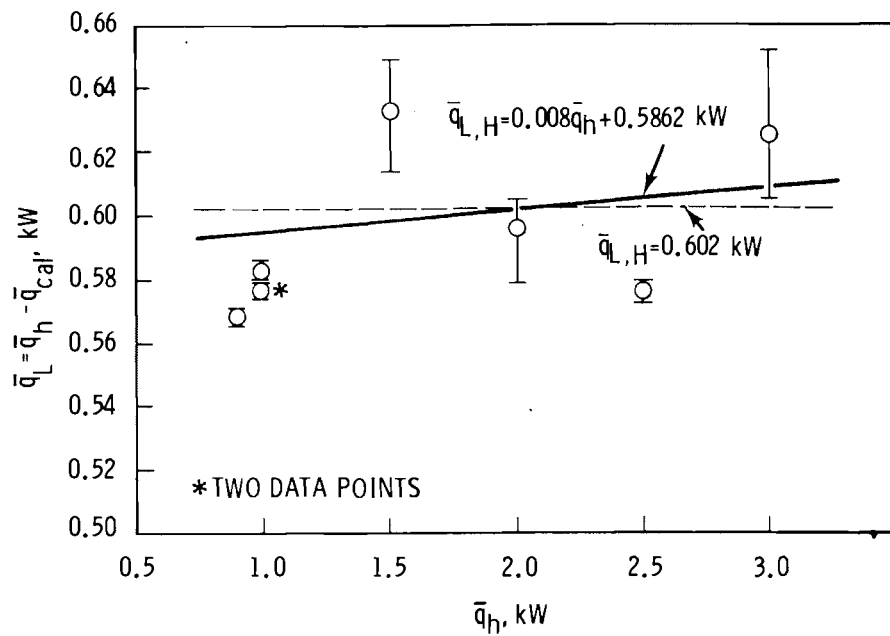


FIGURE 24. Average System Heat Losses Determined from Head Measurements

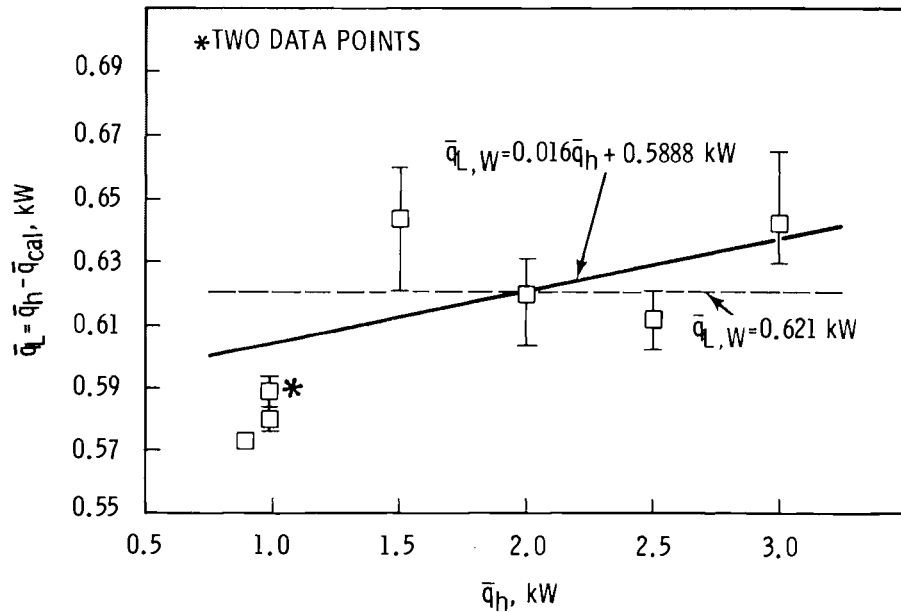


FIGURE 25. Average System Heat Losses Determined from Weight Measurements

at all power levels. This preliminary conclusion is partly confirmed by the hot bay ambient temperature history presented in Figure 26. As indicated, the temperature was essentially constant throughout a typical testing day. Because the temperature of the boiling water in the calorimeter was also constant, the difference between the water and ambient temperatures was constant. Therefore, the heat loss from the calorimeter system should have been constant.

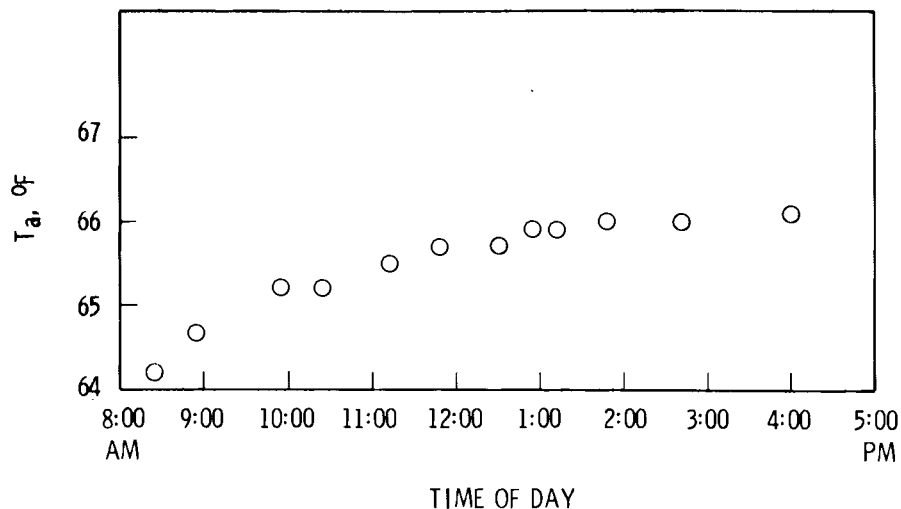


FIGURE 26. Typical Hot Bay Ambient Temperature History During a Testing Day.

The opportunity to repeat some of the heat loss runs did not present itself during acceptance testing. Therefore, if better calorimeter measurements accuracies are desired in the future, it is recommended that the data runs in Figures 22 and 23 be repeated to verify that the heat loss is constant.

5.1.3 Evaluation of Accuracy

An indication of the accuracy of the calorimeter system was evaluated by comparing differential calorimeter heat generation rate measurements with differential reference heater power levels. Table 2 and Figures 27 and 28 present the results of such a comparison.

Figure 27 presents differential heat generation values using the averaged data obtained in runs 37 and 38 as a reference value ($\bar{q}_h = 0.990 \text{ kW}$). As shown, the measurements obtained with the calorimeter at differential heat generation rates of 1 kW and above compare within ~4% of the corresponding

TABLE 2. Comparison of Differential Calorimeter Heat Generation Rate Measurements With Differential Heater Power Levels

Run Numbers ^(a)	$\bar{\Delta}q_h$ kW	$\bar{\Delta}q_{cal}$ kW	$\bar{\Delta}q_{cal}/\bar{\Delta}q_h$
(5,6) - (37,38)	2.500 - 0.990 = 1.510	1.888 - 0.411 = 1.477 1.925 - 0.415 = 1.510	0.978 (W) ^(b) 1.000 (H) ^(b)
(7,8,9) - (37,38)	2.011 - 0.990 = 1.021	1.391 - 0.411 = 0.980 1.415 - 0.415 = 1.000	0.960 (W) 0.979 (H)
(12,13,14) - (37,38)	3.000 - 0.990 = 2.010	2.357 - 0.411 = 1.946 2.374 - 0.415 = 1.959	0.968 (W) 0.975 (H)
(18,19,20,21) - (37,38)	1.493 - 0.990 = 0.503	0.848 - 0.411 = 0.437 0.860 - 0.415 = 0.445	0.869 (W) 0.885 (H)
(37,38) - (28, 29,30)	0.990 - 0.893 = 0.097	0.411 - 0.319 = 0.092 0.415 - 0.325 = 0.090	0.948 (W) 0.928 (H)
(24,25,26,27) - (28,29,30)	0.987 - 0.893 = 0.094	0.397 - 0.319 = 0.078 0.404 - 0.325 = 0.079	0.830 (W) 0.840 (H)
(C1,C2) - (28,29,30)	0.989 - 0.893 = 0.096	0.399 - 0.319 = 0.080 0.413 - 0.325 = 0.088	0.833 (W) 0.917 (H)
(5,6) - (7,8,9)	2.500 - 2.011 = 0.489	1.888 - 1.391 = 0.497 1.925 - 1.415 = 0.510	1.016 (W) 1.043 (H)
(12,13,14) - (7,8,9)	3.000 - 2.011 = 0.989	2.357 - 1.391 = 0.966 2.374 - 1.415 = 0.959	0.977 (W) 0.970 (H)

(a) See Appendix B for data associated with individual run numbers.

(b) (W) Weight Measurements, (H) Head Measurements

accurately measured heater power differentials. This compares favorably with the uncertainty estimates determined in section 4.2.5. At a differential power of ~ 0.5 kW ($\Delta\bar{q}_h = 1.493 - 0.990$ kW), the comparison falls outside the desired design criteria of $\pm 10\%$. However, it should be noted that this differential involves the runs at 1.5 kW, which are thought to be in slight error. Comparisons at a low differential power level of 0.1 kW fell both inside and outside the desired accuracy range.

The credibility of the 1.5-kW runs can be further investigated by taking the difference between other runs to obtain a differential power of 0.5 kW. Figure 28 presents differential heat generation rates using the average of

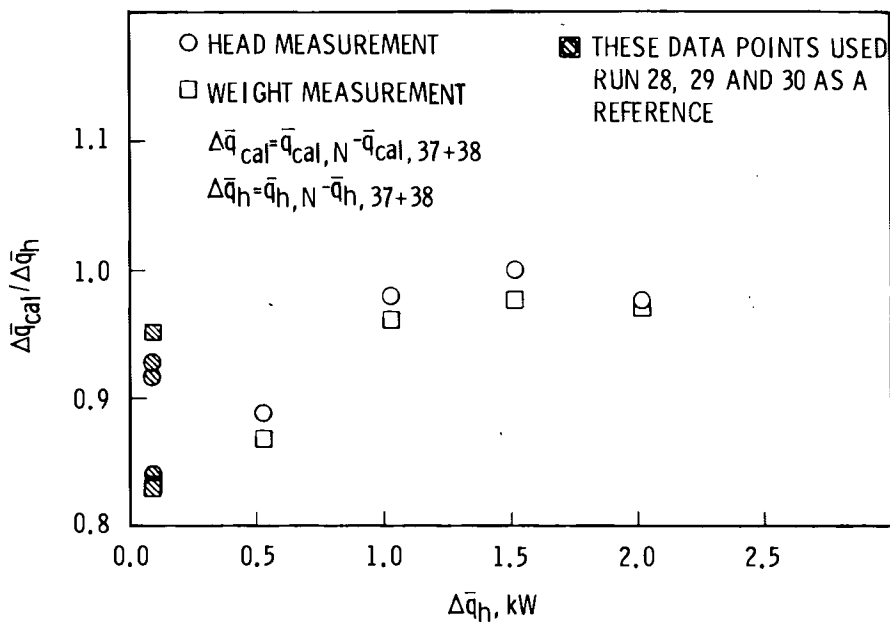


FIGURE 27. Comparisons of Calorimeter Differential Heat Generation Rate Measurements with Differential Heater Power Levels Using Runs 37 and 38 and 28, 29, and 30 as References

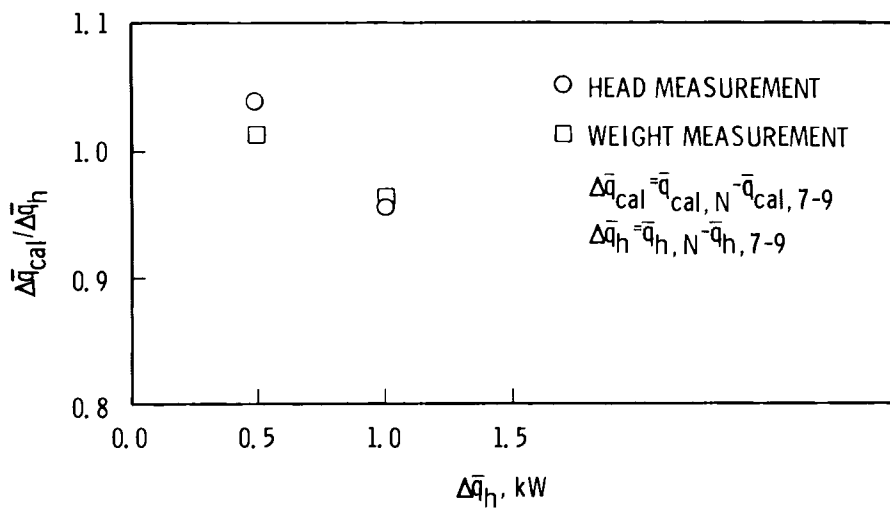


FIGURE 28. Comparisons of Calorimeter Differential Heat Generation Rate Measurements with Differential Heater Power Levels Using Runs 7 through 9 as a Reference

Runs 7 through 9 ($\bar{q}_h = 2.0$ kW) as a reference run. The comparison at $\bar{\Delta}q_h = 0.5$ kW (2.5-2.0 kW) between the heater and calorimeter differential heat generation rates are within 5%. This result is reasonable confirmation that the 1.5-kW run is slightly in error. Note that at $\bar{\Delta}q_h = 1$ kW (3.0 - 2.0 kW), the ratios of $\Delta\bar{q}_{cal}/\Delta\bar{q}_h$ are essentially the same as those in Figure 27 using $\bar{q}_h = 1$ kW as a reference.

5.1.4 Calorimeter Sensitivity

Three sets of data were obtained near $\bar{q}_h \sim 1$ kW. Figures 29 and 30 present mass accumulation rates and corresponding calorimeter heat generation rate measurements at heater powers of 0.987, 0.989, and 0.990 kW. These data show that the calorimeter system was sensitive to a change of 0.001 kW (1 watt) in heater power. However, the data in Figure 30 indicate that the calorimeter is not accurate to 1 watt because the differences in calorimeter heat generation rate measurements do not equal corresponding heater power differentials. Therefore, it cannot be concluded that the calorimeter has an accuracy of 1 watt. Discussions of accuracy were presented in the previous section and in section 4.2.5.

5.1.5 General Observations

During operation of the calorimeter system, the following observations were made:

- Approximately 4 to 5 hours were required to heat the water in the calorimeter from a cold condition (~65°F) to boiling.
- Approximately 3 to 6 hours were required to attain steady-state conditions after boiling was initiated.
- Once steady-state conditions existed, the addition of 4 or 5 gallons of cold water to the calorimeter required 1 to 2 hours to reestablish steady-state conditions.
- The difference in system heat losses with and without the insulation cap installed on the calorimeter vessel was ~0.23 kW (0.85 - 0.62 kW) at a reference heater power of 3 kW.

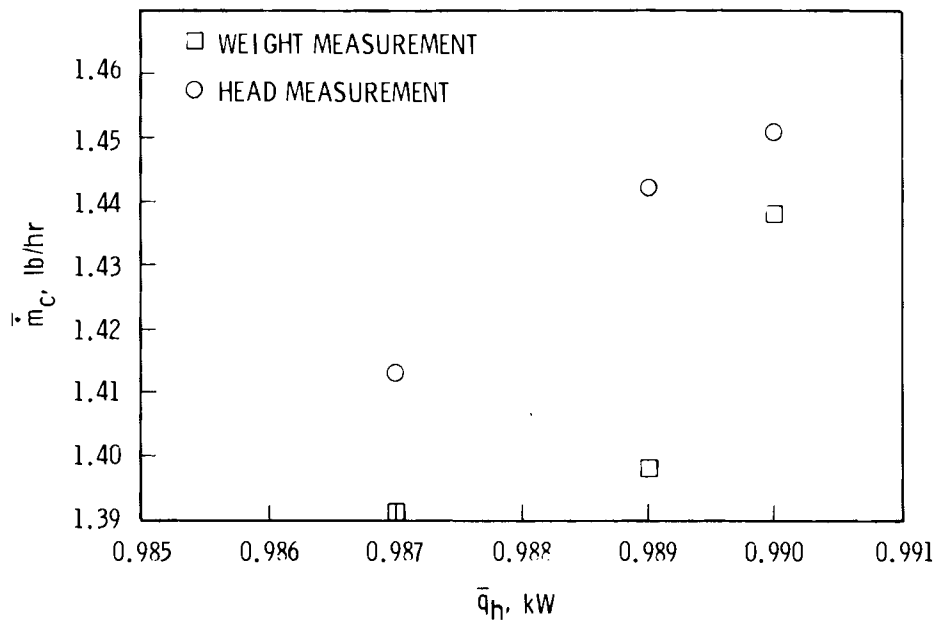


FIGURE 29. Mass Accumulation Rates at Heater Power Levels Near 1 kW

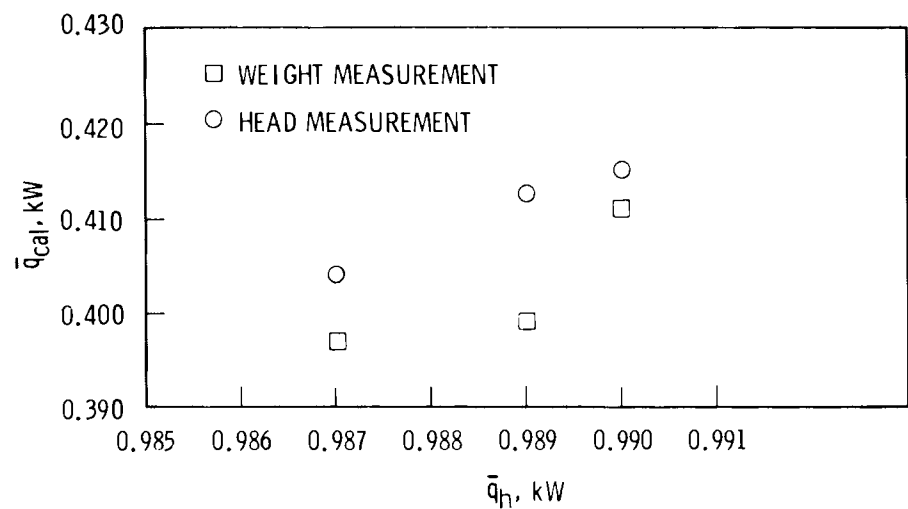


FIGURE 30. Calorimeter Heat Generation Rate Measurements at Heater Power Levels Near 1 kW

- Even though the system was designed for 3 or 4 kW, it has the potential to permit heat generation measurements in the 12- to 14-kW range. This was demonstrated by collecting condensate at ~14 kW without overloading the condenser/fan unit.

5.1.6 Recommended Criteria for Acceptable Mass Accumulation Data

The most important result of the acceptance test was the experience gained in operating the calorimeter system and determining what constituted acceptable condensate accumulation runs. It is recommended that the following procedure be used to attain boiling and assure that reliable, accurate mass accumulation data are obtained:

- When approaching boiling with 22 kW of heater power, the power should be reduced to 11 to 14 kW when the calorimeter vessel skin temperature (TE-2) reaches 84 or 85°C. This will minimize the chance of overloading the condenser or overflowing the steam and sight glass discharge lines.
- When boiling is initiated, the reference dc heater should be set at the desired power and the total heater power should be reduced to 4 to 8 kW. This power level should be maintained for 30 min to 1 hour. This will permit the system temperatures to attain steady-state values.
- The necessary ac heaters should be turned off, and the history of the condenser outlet temperature should be similar to that shown in Figure 31. The temperature should decay down to a steady-state value. If the temperature decays below the steady-state value and begins to increase, 3 to 8 kW of power from the ac heaters should be applied to the system for a short period of time (15 to 30 min). The ac heaters should be turned off and the condenser outlet temperature should decay similar to that shown in Figure 31. This procedure should be repeated until Figure 31 is approximated. Note, this procedure reduces the time required to attain a steady-state condition and makes it relatively easy to recognize that a steady-state condition has been reached.

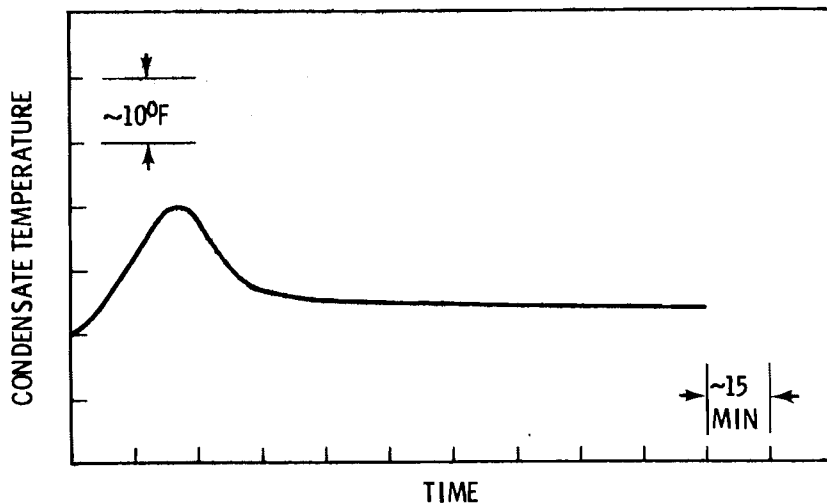


FIGURE 31. Desired Condenser Outlet Temperature History During Approach to a Steady-State Condition

- Once steady-state conditions exist, the power being generated by the dc reference heater should be checked for correctness. Four consecutive full-length collection tube runs should be obtained. The times to collect a specific head (weight) of condensate in the tube should compare within ± 1 to $\pm 1-1/2$ % of their average time.

5.2 SPENT FUEL ASSEMBLY HEAT GENERATION RATE MEASUREMENT

The decay heat generation rate of a Turkey Point PWR spent fuel assembly (ID # D-34) was measured with the calorimeter system. The day prior to performing calorimetry on the spent fuel assembly, a reference run with the dc heater generating 0.989 kW was performed (Runs C1 and C2 of Appendix B). Prior to inserting the fuel assembly in the calorimeter, the calorimeter water was brought to boiling and the reference heater was reset at 0.989 kW. The assembly was immersed in the calorimeter vessel, and approximately 4-1/2 hours were required to establish steady-state conditions and obtain acceptable mass accumulation rate data.

Results of the four data runs are presented in Table 3. The data reduction method discussed in section 4.2.4 was used to determine spent fuel assembly

decay heat generation values from measured mass accumulation rates. Heat losses from the system were assumed to be constant at any heat generation rate. Results from measurements obtained with both the head and weight methods indicate the Turkey Point PWR spent fuel assembly was generating 1.55 kW. Three different sets of reference runs obtained on different days were used to determine the fuel assembly decay heat generation rate. The three sets of data permitted an evaluation of uncertainties introduced by reference runs. A comparison of the average heat generation values in Table 3 indicates repeatability of $\pm 1\%$ is possible as long as the hot bay ambient temperature is reasonably constant ($\pm 2^{\circ}\text{F}$). Data of individual runs used to obtain average heat generation rates indicate a scatter of $\sim 2\%$, which is within the uncertainty values estimated in section 4.2.5.

An initial prediction of the decay heat generation rate of spent fuel assembly D-34 was performed by HEDL, using the ORIGEN computer program (Cross, Haese and Gove 1976). A value of 1.77 kW was predicted which agrees within 14% of the measured value of 1.55 kW. A subsequent prediction using the ORIGEN2 code, the latest version of the ORIGEN code (Croff 1980), resulted in a prediction of 1.64 kW, which compares within 5.8% of the measured value.

TABLE 3. Spent Fuel Assembly (D-34) Measured Heat Generation Rate

Run Number	Reference		$q_{D-34,W}, \text{kW}$	$\bar{q}_{D-34,W}, \text{kW}$	$q_{D-34,H}, \text{kW}$	$\bar{q}_{D-34,H}, \text{kW}$
	Date	Run Number				
C3	4/01/80	24 - 27	3/25/80	1.543	1.547	
C4		24 - 27		1.584	1.590	
C5		24 - 27		1.543	1.552	1.560
C6		24 - 27		1.541	1.552	
C3		C1 & C2	3/31/80	1.541	1.539	
C4		C1 & C2		1.583	1.581	
C5		C1 & C2		1.541	1.544	1.552
C6		C1 & C2		1.539	1.544	
C3		37 & 38	4/02/80	1.529	1.536	
C4		37 & 38		1.571	1.579	
C5		37 & 38		1.530	1.541	1.549
C6		37 & 38		1.530	1.541	

REFERENCES

Bell, M. J. 1973. ORIGEN - The ORNL Isotope Generation and Depletion Code. ORNL-4628, Oak Ridge National Laboratory, Oak Ridge, Tennessee.

Beyer, N. S., R. B. Perry and R. N. Lewis. 1976. "Fast Response Fuel Rod Calorimeter." In Safeguarding Nuclear Materials. II:541-549.

Croff, A. G. 1980. A User's Manual for the ORIGEN2 Computer Program. ORNL-TM-7175, Oak Ridge National Laboratory, Oak Ridge, Tennessee.

Cross, A. G., R. L. Haese and N. B. Gove. 1976. Updated Decay and Photon Libraries for the ORIGEN Code. ORNL-TM-6050, Oak Ridge National Laboratory, Oak Ridge, Tennessee.

Schenck, H., Jr. 1971. Theories of Engineering Experimentation. McGraw-Hill Book Company, New York, NY.

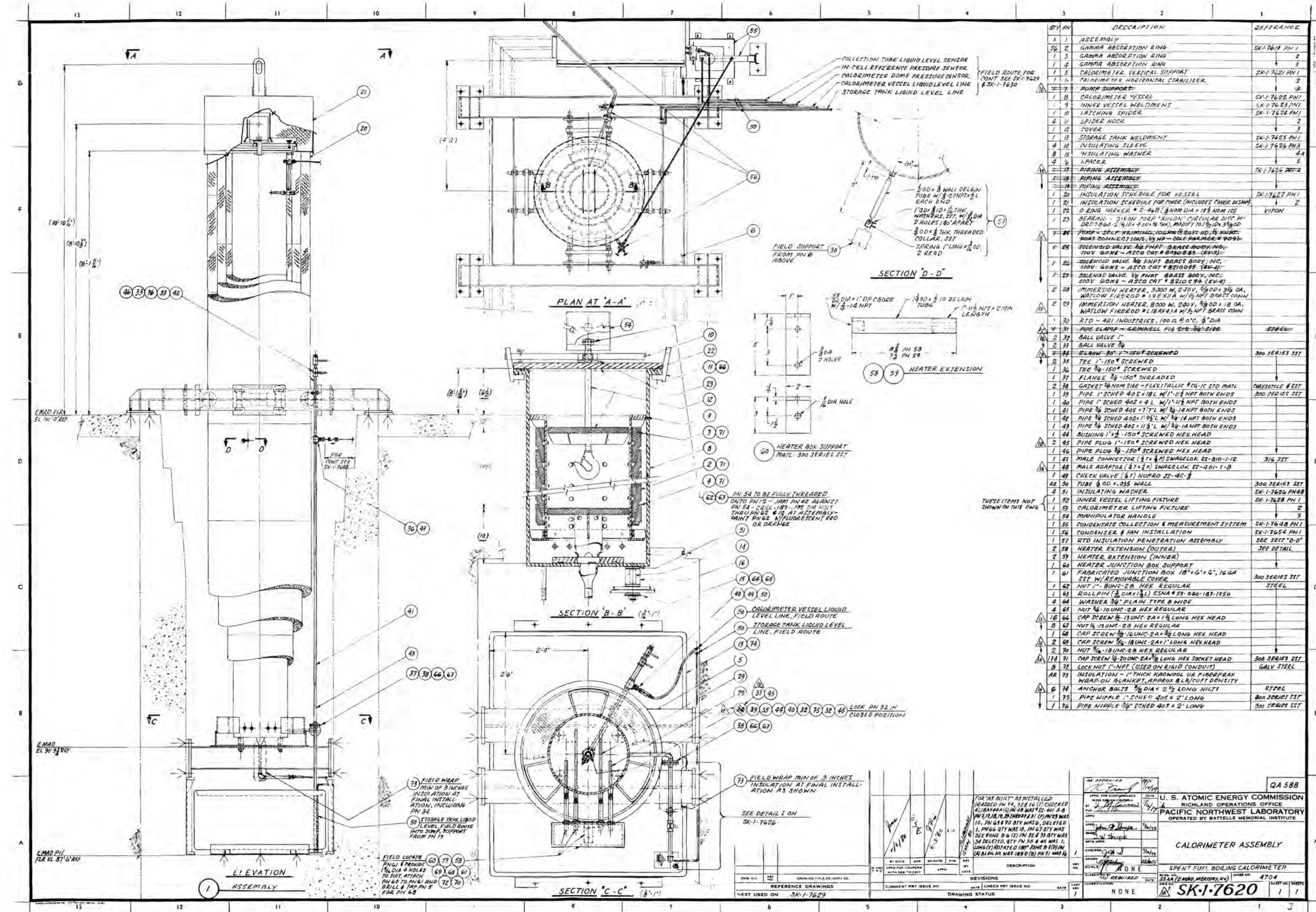
Turner, W. D., D. C. Elrod and I. I. Simon-Tov. 1977. HEATING5 - An IBM 360 Heat Conduction Program. ORNL/CSD/TM-15, Union Carbide Corporation, Nuclear Division, Oak Ridge, Tennessee.

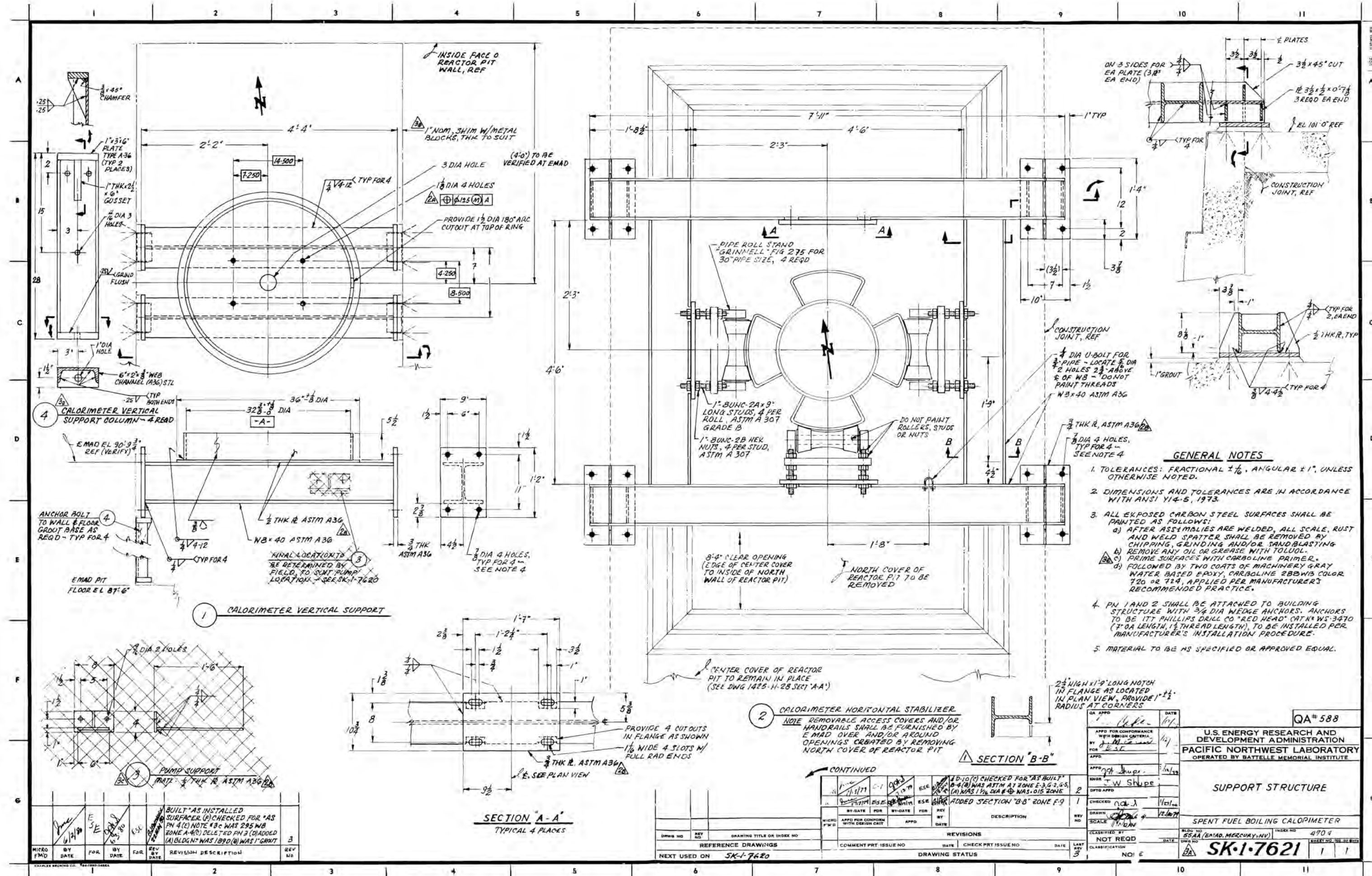
Westinghouse E-MAD Capabilities Manual. Westinghouse Electric Corporation, Advanced Energy Systems Division, Mercury, Nevada.

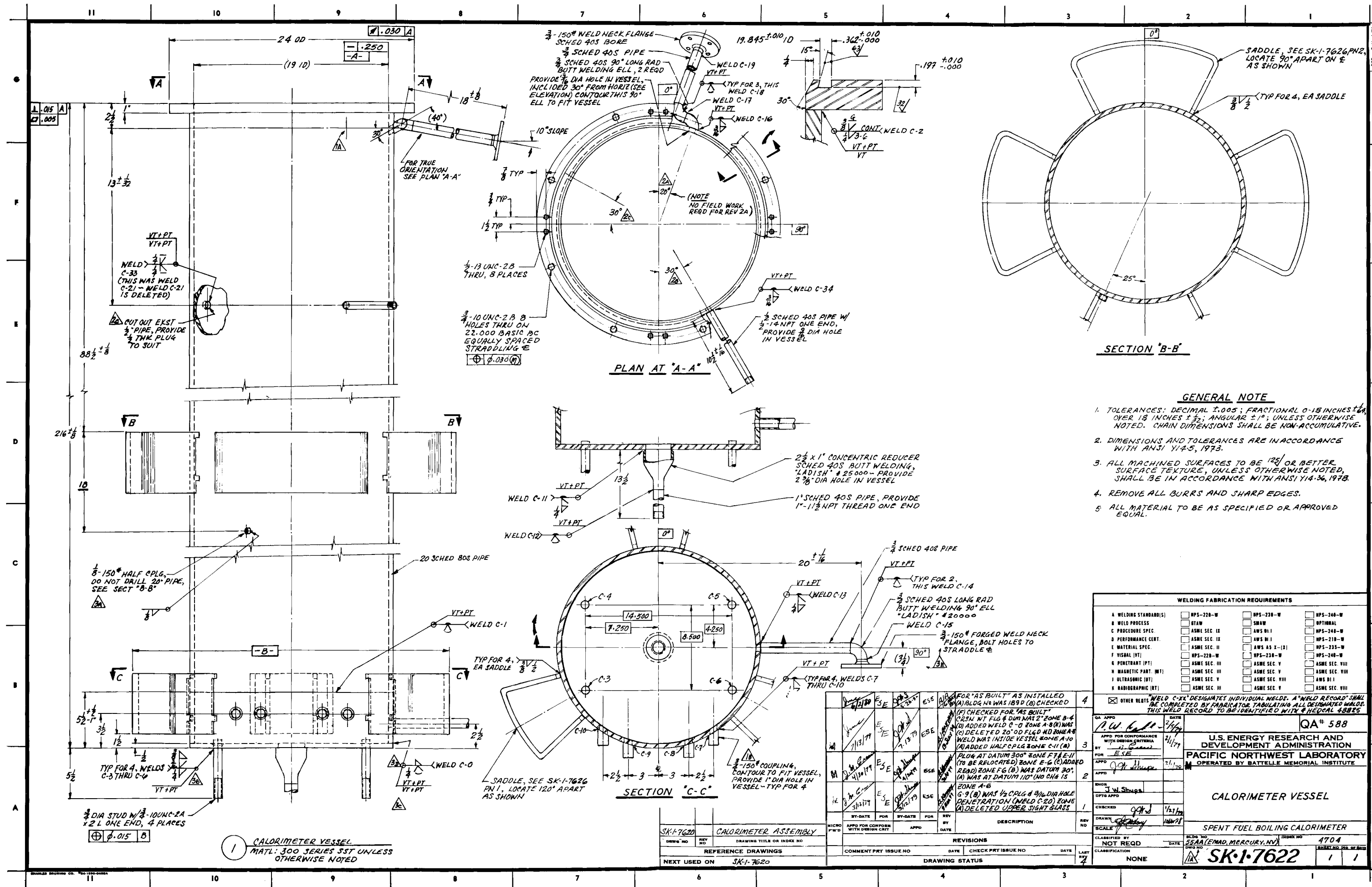
Yarnell, J. L., and P. J. Bendt. 1977. Decay Heat From Products of ^{235}U Thermal Fission By Fast-Response Boil-Off Calorimetry. LA-NURGE-6713, Los Alamos Scientific Laboratory of the University of California, Los Alamos, New Mexico.

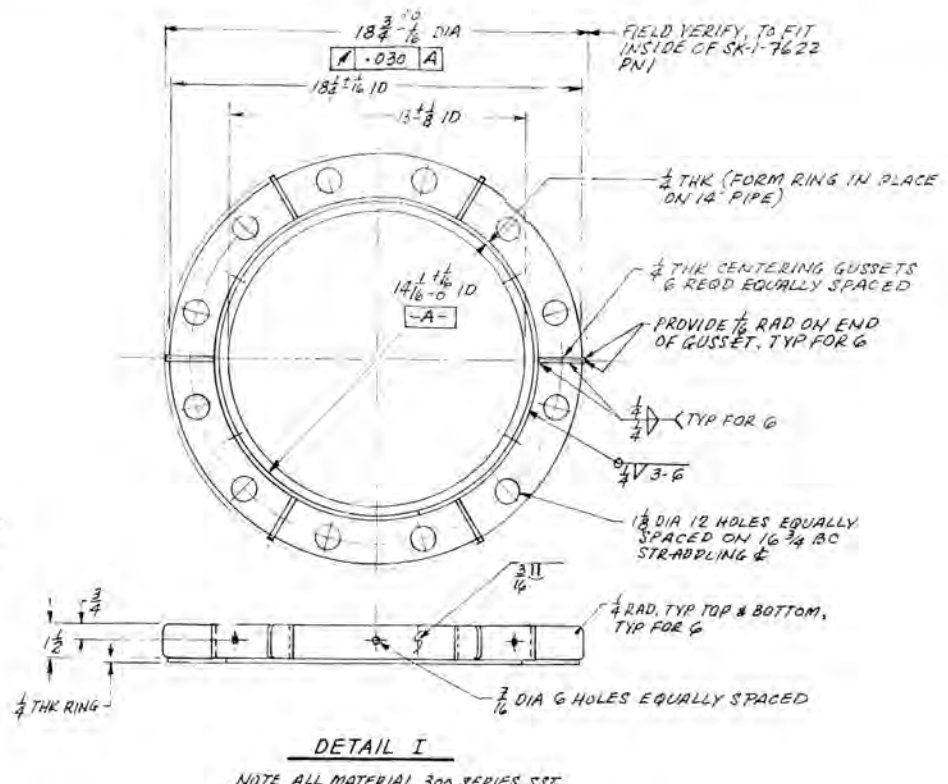
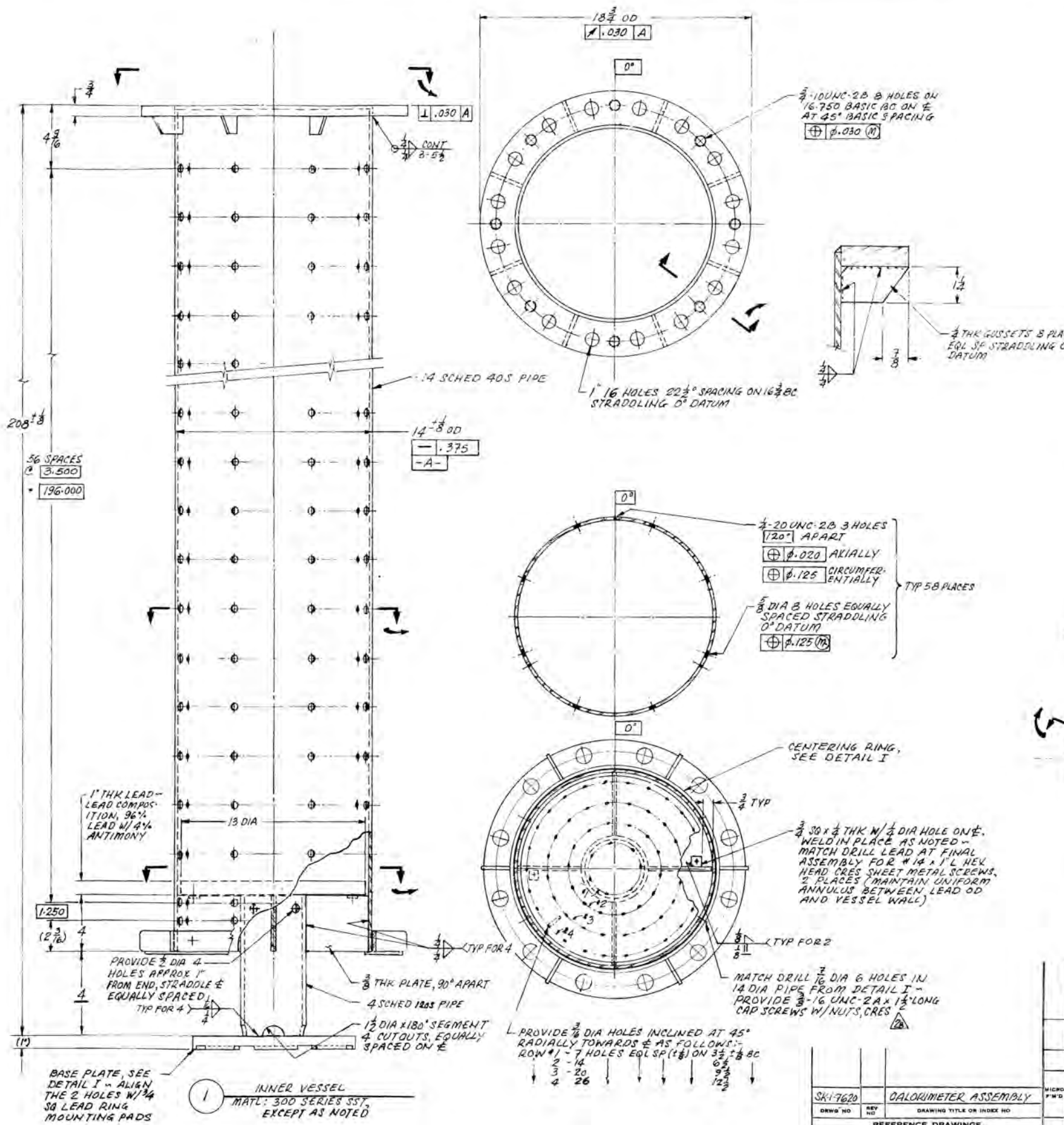


APPENDIX A
DESIGN DRAWINGS





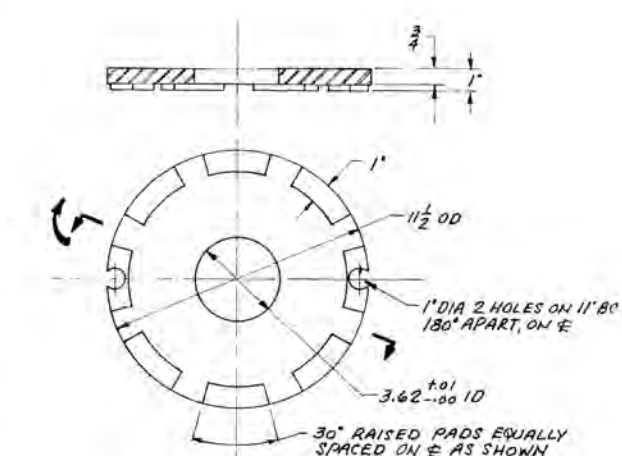




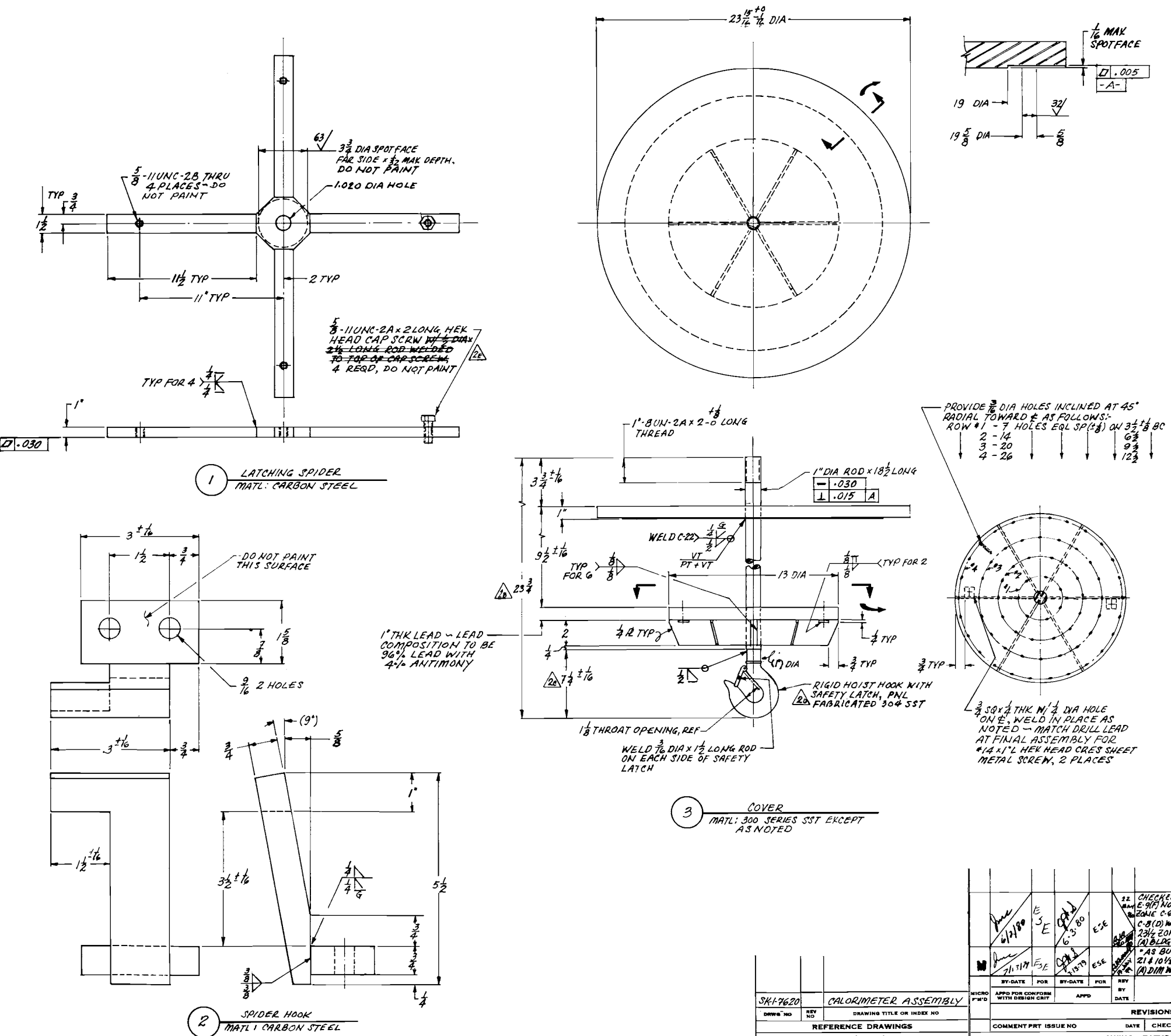
DETAIL I

GENERAL NOTES

1. TOLERANCES: DECIMAL $\pm .005$; FRACTIONAL 0.18 INCHES $\pm \frac{1}{64}$, OVER 1/16 INCHES $\pm \frac{1}{32}$; ANGULAR $\pm 1^\circ$, UNLESS OTHERWISE NOTED. CHAIN DIMENSIONS SHALL BE NON-ACCUMULATIVE.
2. DIMENSIONS AND TOLERANCES ARE IN ACCORDANCE WITH ANSI Y14.5, 1973.
3. ALL MACHINED SURFACES TO BE 120 OR BETTER SURFACE TEXTURE IN ACCORDANCE WITH ANSI Y14.36, 1978.
4. REMOVE ALL BURRS AND SHARP EDGES.



DETAIL II



GENERAL NOTES

TOLERANCES: DECIMAL $\pm .005$; FRACTIONAL 0-18 INCHES $\pm \frac{1}{64}$, OVER 18 INCHES $\pm \frac{3}{32}$; ANGULAR $\pm 1^\circ$; UNLESS OTHERWISE NOTED. CHAIN DIMENSIONS SHALL BE NON-ACCUMULATIVE.

1. DIMENSIONS AND TOLERANCES ARE IN ACCORDANCE WITH ANSI Y14.5, 1973.

2. ALL MACHINED SURFACES TO BE $125/12$ OR BETTER SURFACE TEXTURE, UNLESS OTHERWISE NOTED, SHALL BE IN ACCORDANCE WITH ANSI Y14.36, 1978.

3. REMOVE ALL BURRS AND SHARP EDGES.

4. ALL EXPOSED CARBON STEEL SURFACES SHALL BE PAINTED AS FOLLOWS, UNLESS OTHERWISE NOTED:

a) REMOVE ALL RUST, SCALE AND WELD SPATTER BY CHIPPING, GRINDING AND/OR SANDBLASTING

b) REMOVE ANY OIL OR GREASE WITH TOLUOL.

c) PRIME SURFACES WITH CARBOLINE PRIMER.

d) FOLLOWED BY TWO COATS OF MACHINERY GRAY WATER BASED EPOXY, CARBOLINE 288WB COLOR 720 OR 724, APPLIED PER MANUFACTURER'S RECOMMENDED PRACTICE.

WELDING FABRICATION REQUIREMENTS

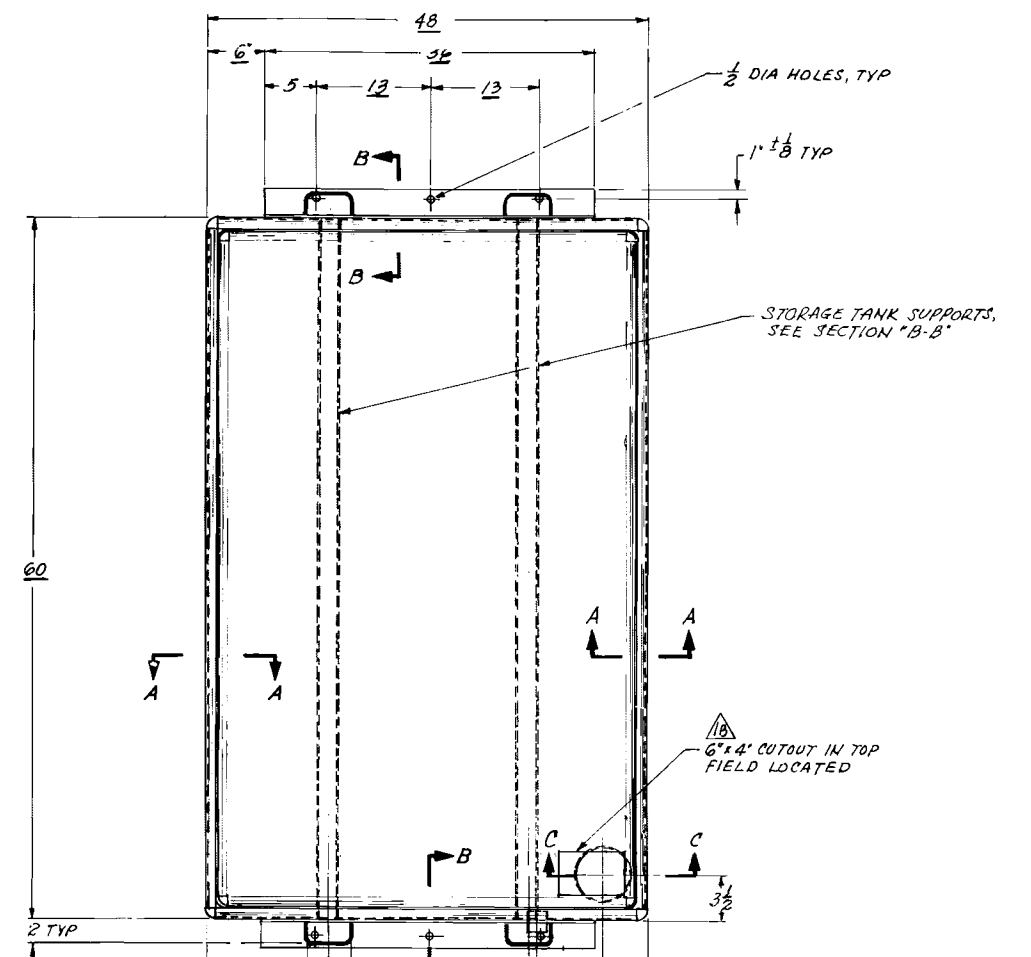
A WELDING STANDARD(S)	<input type="checkbox"/> NPS-228-W	<input type="checkbox"/> NPS-230-W	<input type="checkbox"/> NPS-240-W
B WELD PROCESS	<input type="checkbox"/> GTAW	<input type="checkbox"/> SMAW	<input type="checkbox"/> OPTIONAL
C PROCEDURE SPEC	<input type="checkbox"/> ASME SEC. IX	<input type="checkbox"/> AWS D1.1	<input type="checkbox"/> NPS-240-W
D PERFORMANCE CERT.	<input type="checkbox"/> ASME SEC. IX	<input type="checkbox"/> AWS D1.1	<input type="checkbox"/> NPS-210-W
E MATERIAL SPEC.	<input type="checkbox"/> ASME SEC. II	<input type="checkbox"/> AWS AS-X-(X)	<input type="checkbox"/> NPS-235-W
F VISUAL (VT)	<input type="checkbox"/> NPS-228-W	<input type="checkbox"/> NPS-230-W	<input type="checkbox"/> NPS-240-W
G PENETRANT (PT)	<input type="checkbox"/> ASME SEC. III	<input type="checkbox"/> ASME SEC. V	<input type="checkbox"/> ASME SEC. VIII
H MAGNETIC PART. (MT)	<input type="checkbox"/> ASME SEC. III	<input type="checkbox"/> ASME SEC. V	<input type="checkbox"/> ASME SEC. VIII
J ULTRASONIC (UT)	<input type="checkbox"/> ASME SEC. V	<input type="checkbox"/> ASME SEC. VIII	<input type="checkbox"/> AWS D1.1
K RADIOGRAPHIC (RT)	<input type="checkbox"/> ASME SEC. III	<input type="checkbox"/> ASME SEC. V	<input type="checkbox"/> ASME SEC. VIII

OTHER REQS. "WELD C-XX" DESIGNATES INDIVIDUAL WELDS. A "WELD RECORD" SHALL BE COMPLETED BY FABRICATOR TACKLING ALL DESIGNATED WELDS. THIS WELD RECORD TO BE IDENTIFIED WITH # HEDCAL 48825

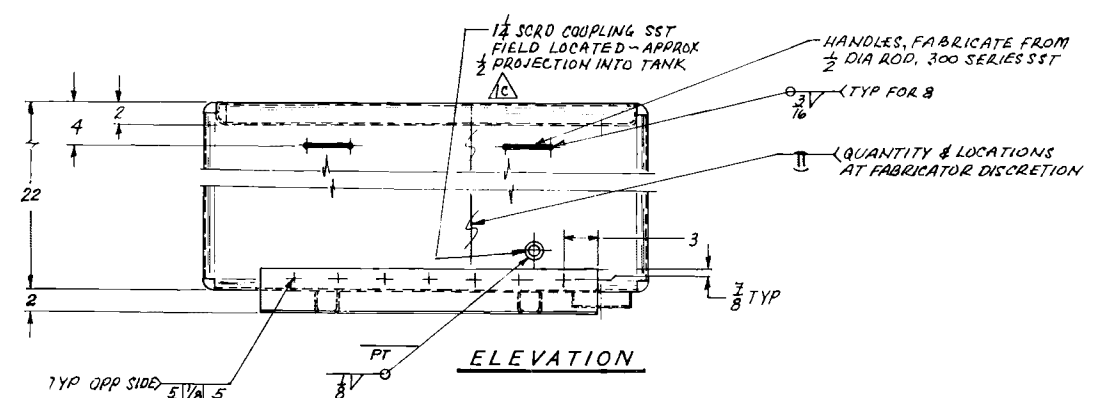
QA# 588

11-397
312177 U.S. ENERGY RESEARCH AND
DEVELOPMENT ADMINISTRATION
PACIFIC NORTHWEST LABORATORY
PORTLAND, OREGON 97234

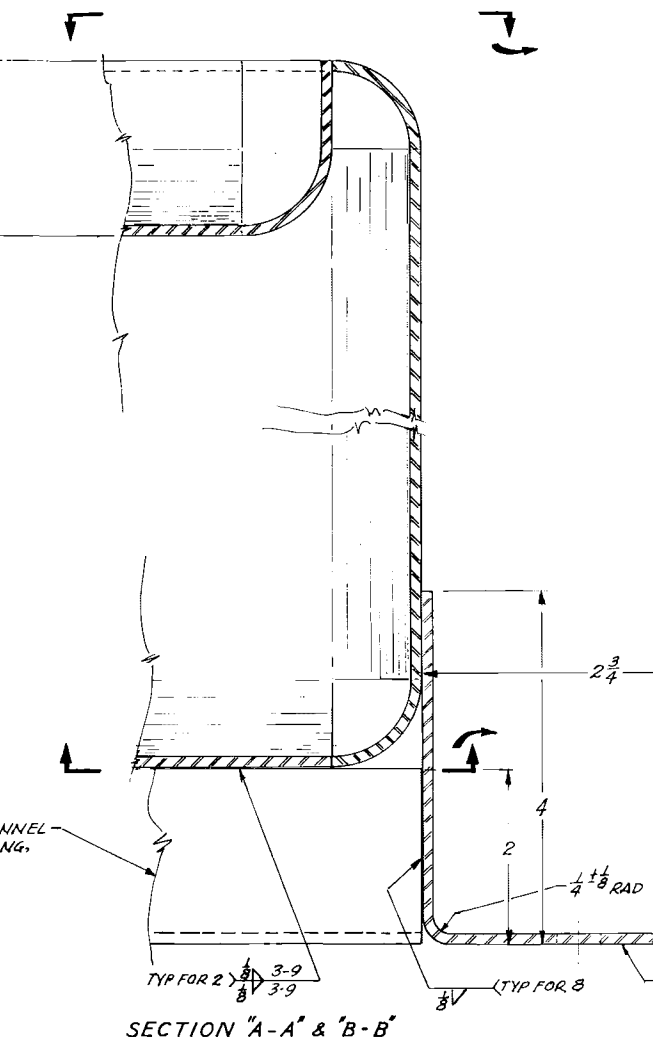
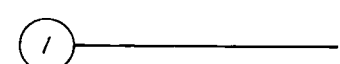
VESSEL COVER & DETAILS



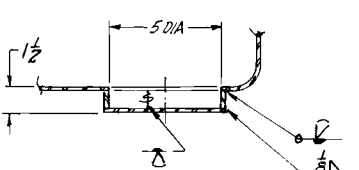
PLAN



ELEVATION.



SECTION "A-A" & "B-B"



SECTION "C-C"

SK-1-7620	CALORIMETER ASSEMBLY			MICRO
DRWG NO	REV NO	DRAWING TITLE OR INDEX NO		
REFERENCE DRAWINGS				
NEXT USED ON		SK-1-7620		

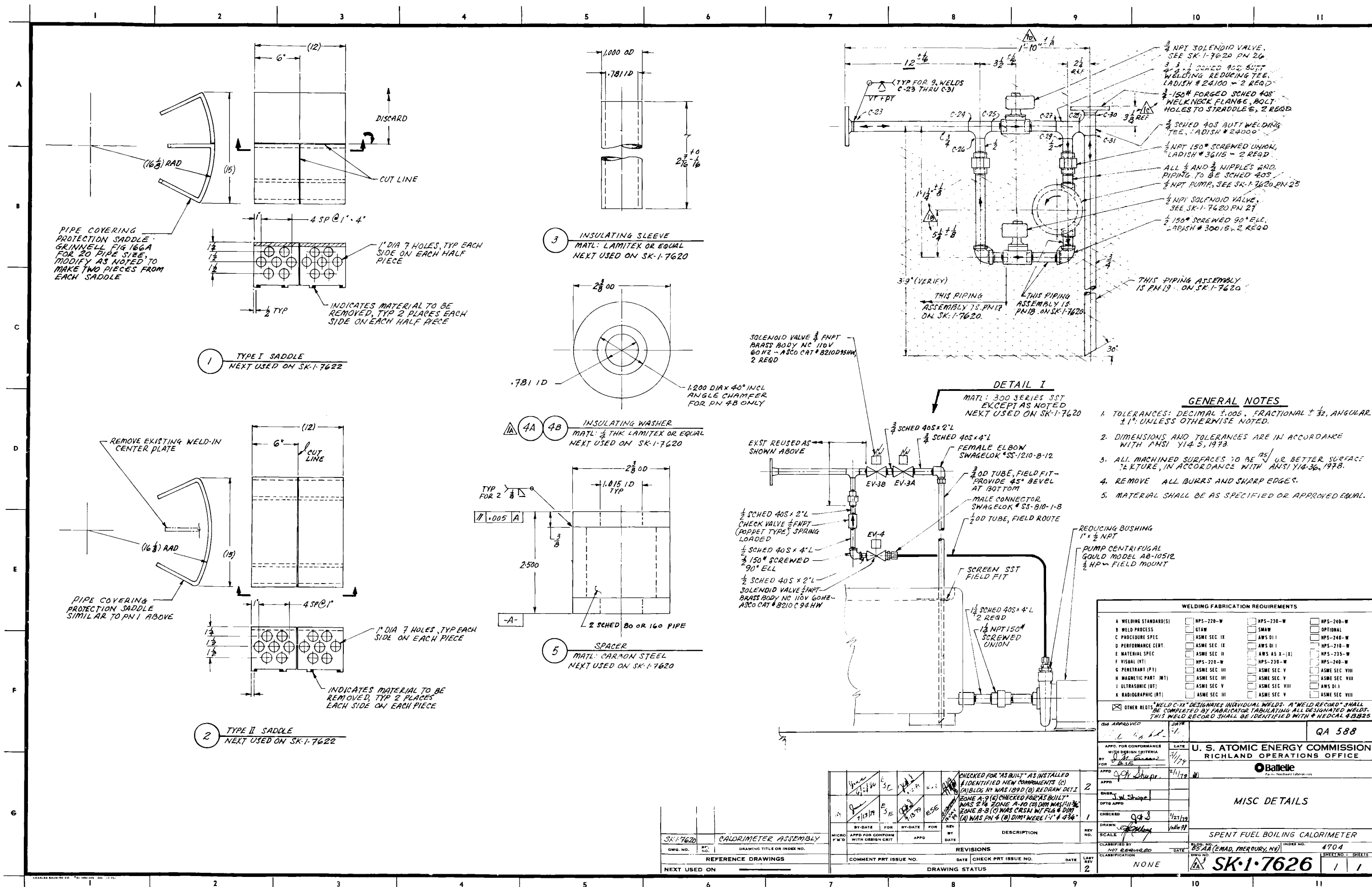
STORAGE TANK WELDMENT

SPENT FUEL BOILING CALORIMETER

SPENT FUEL BURNING CALORIMETER

AA (EMAD, MERCURY, NV) 4704
SK-1-3625 SHEET NO. NO 0

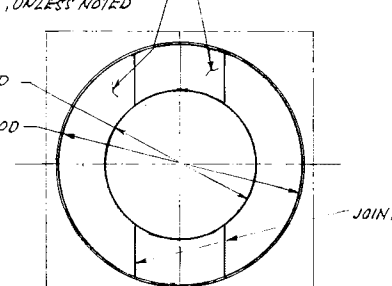
SA-7-7625



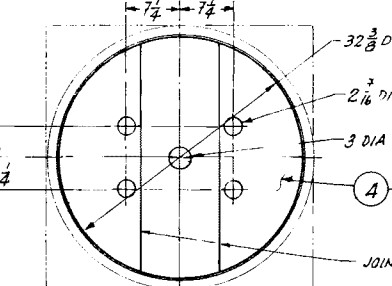
QTY	PN	DESCRIPTION	REMARKS
X	1	INSULATION SCHEDULE FOR VESSEL	
X	2	INSULATION SCHEDULE FOR COVER	
1	3	BLOCK INSULATION $36 \times 18 \times \frac{1}{2}$, SEE SECT "A-A"	SEE NOTE #2
2	4	BLOCK INSULATION $36 \times 18 \times 3$, SEE SECT "B-B"	
3	5	PIPE INSULATION 2010×2 THK $\times 36$ " LONG	
1	6	PIPE INSULATION 2010×2 THK $\times 36$ " LONG (SEE NOTE)	
1	7	PIPE INSULATION 2010×2 THK $\times 36$ " LONG (SEE NOTE)	
1	8	PIPE INSULATION 2010×2 THK $\times 33\frac{1}{2}$ " LONG	
3	9	PIPE INSULATION 2410×3 THK $\times 36$ " LONG	
1	10	PIPE INSULATION 2410×3 THK $\times 36$ " LONG (SEE NOTE)	
1	11	PIPE INSULATION 2410×3 THK $\times 36$ " LONG (SEE NOTE)	
1	12	PIPE INSULATION 2410×3 THK $\times 34$ " LONG	
5	13	PIPE INSULATION $3010 \times 3\frac{1}{2}$ THK $\times 36$ " LONG	
1	14	PIPE INSULATION $3010 \times 3\frac{1}{2}$ THK $\times 6$ " LONG	
1	15	PIPE INSULATION $3010 \times 3\frac{1}{2}$ THK $\times 16$ " LONG (SEE NOTE)	
2	16	BLOCK INSULATION $16'00 \times 8\frac{1}{2}'0 \times 3$ THK	
3	17	BLOCK INSULATION $16'00 \times 8\frac{1}{2}'0 \times 3$ THK	
1	18	PIPE INSULATION 1610×3 THK $\times 15\frac{1}{2}$ " LONG (VERIFY)	
1	19	PIPE INSULATION 2210×3 THK $\times 15\frac{1}{2}$ " LONG (VERIFY)	
1	20	PIPE INSULATION $2810 \times 2\frac{1}{2}$ THK $\times 20\frac{1}{2}$ " LONG (SEE DET I)	
1	21	PIPE INSULATION $3310 \times 3\frac{1}{2}$ THK $\times 20\frac{1}{2}$ " LONG (SEE DET I)	

GENERAL NOTES

1. DIMENSIONS AND TOLERANCES TO BE IN ACCORDANCE WITH ANSI Y14.5, 1973.
2. BLOCK INSULATION AND PIPE INSULATION SEGMENTS TO BE SILICA LIME WITH REINFORCING FIBERS AS MANUFACTURED BY JOHNS-MANVILLE "THERMO-12" TYPE.
3. THE AXIAL BUTT JOINTS BETWEEN SUCCESSIVE LAYERS OF PIPE INSULATION SHALL BE STAGGERED A MINIMUM OF $1\frac{1}{2}$ INCHES.
4. THE INSULATION PARTS OF THE REMOVABLE COVER (PNS 16 THRU 21) SHALL BE BONDED INTO ONE HOMOGENEOUS ASSEMBLY WITH BORDEN ARABOL LAGGING CEMENT.
DIMENSIONED TOLERANCE PROVIDED FOR MAK THK FOR EACH CEMENTED JOINT BETWEEN PNS 16 AND 17.



SECTION "A-A"



SECTION 'B-B

CALORIMETER

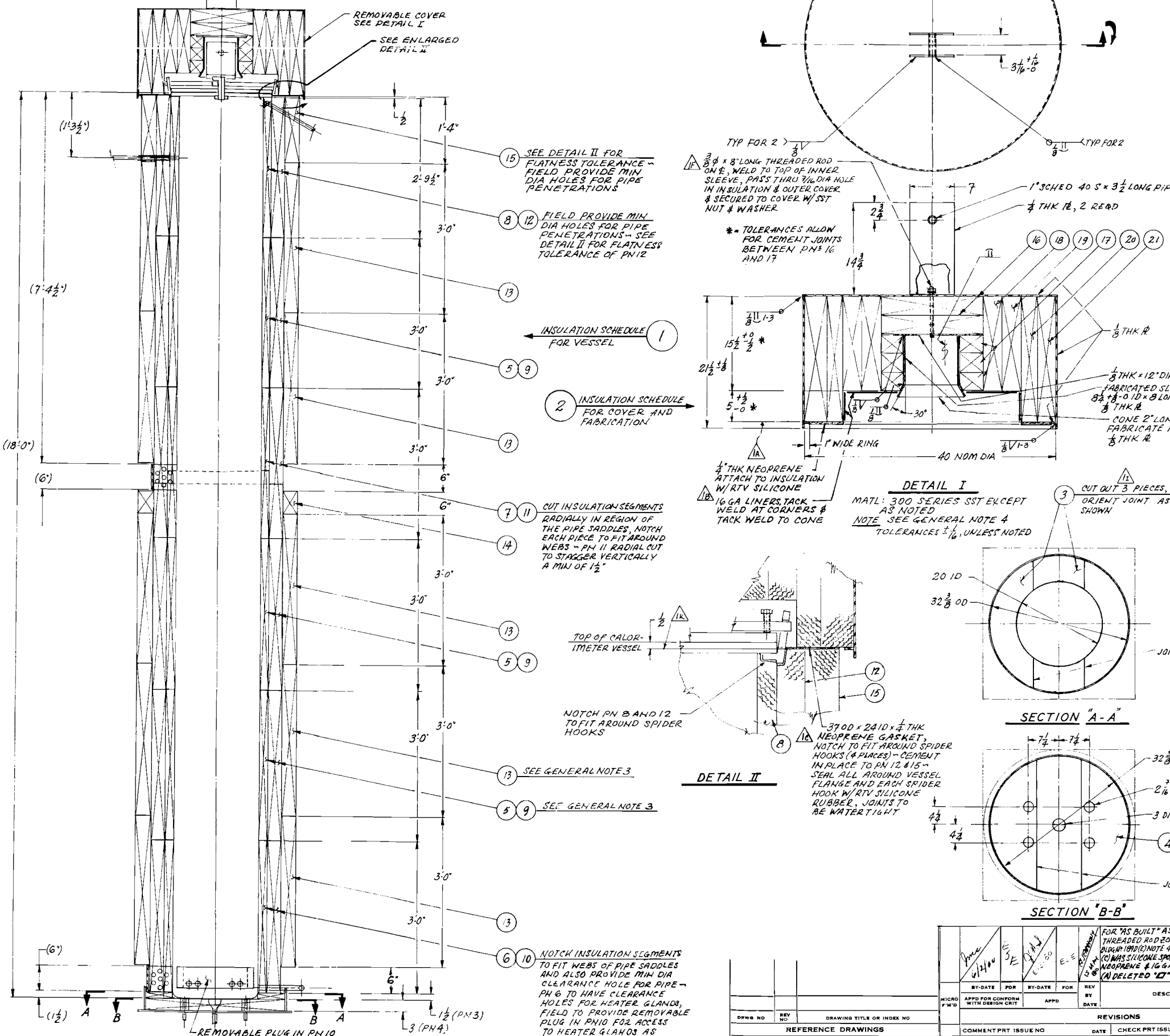
CALORIMETER

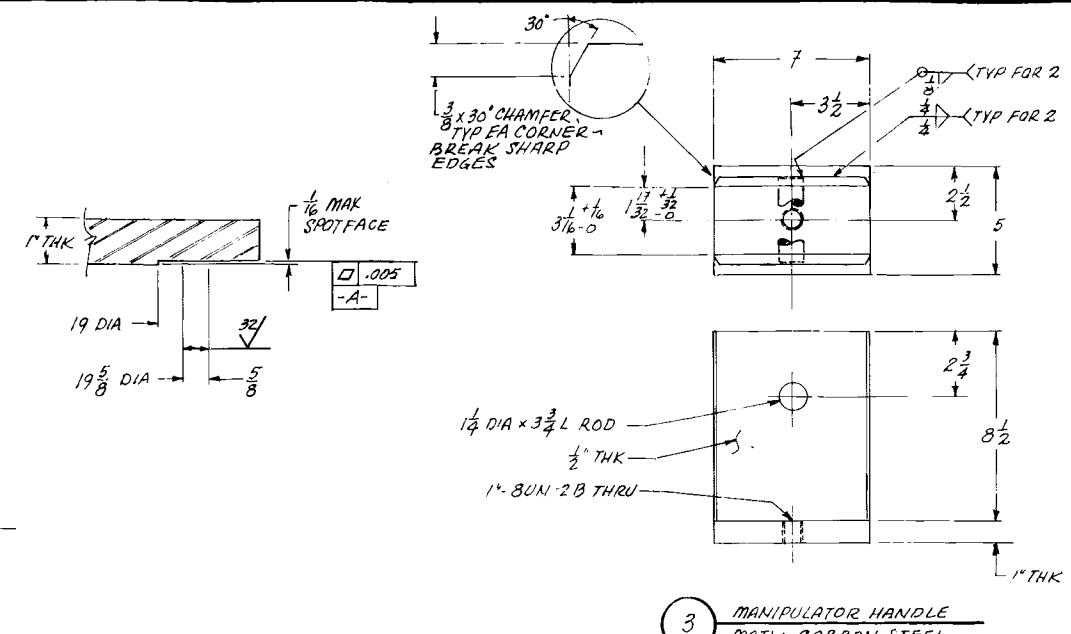
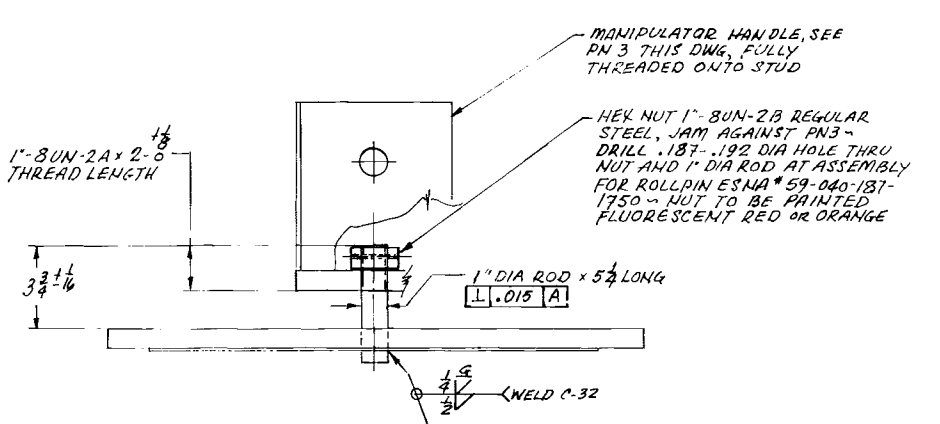
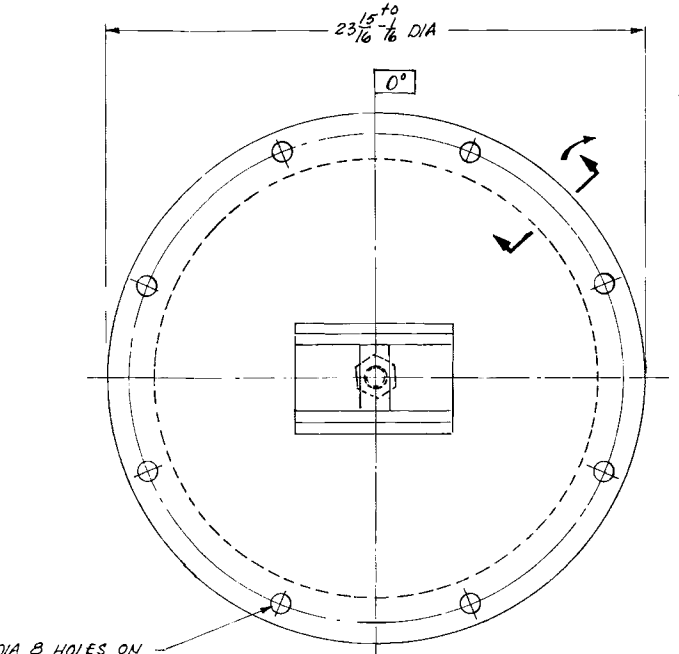
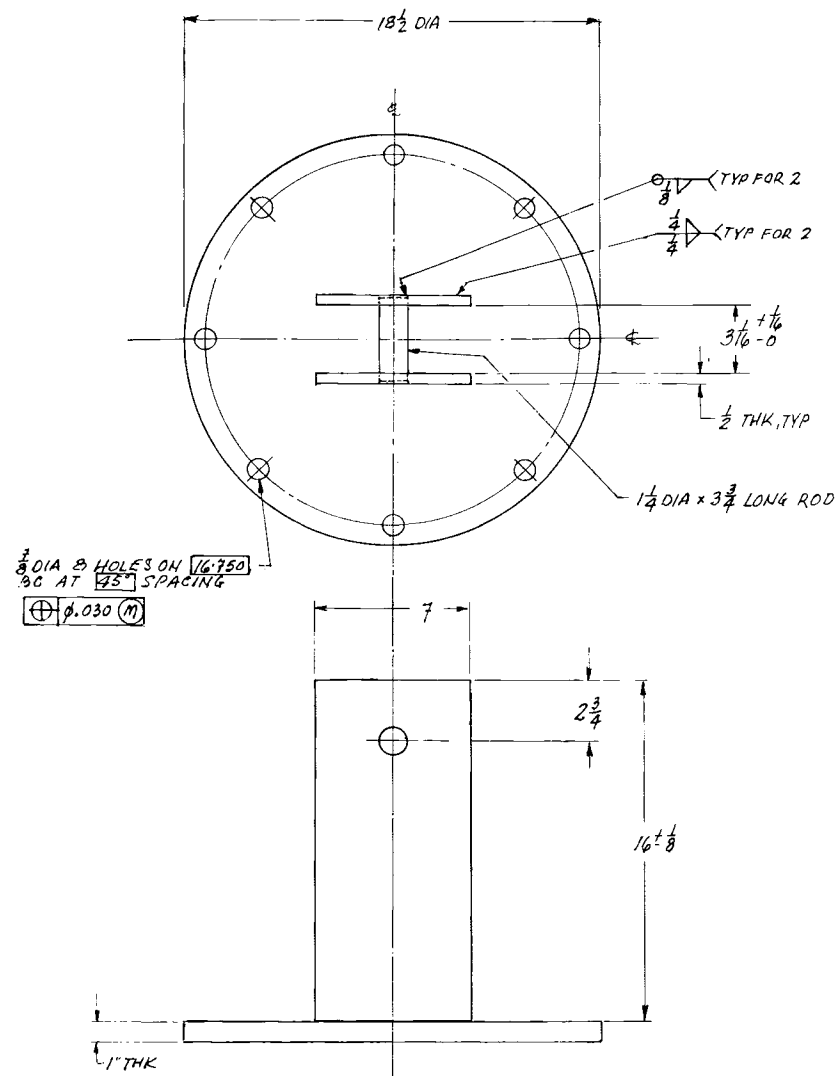
**CALORIMETER
INSULATION SCHEDULE**

ENT FUEL BOILING CALORIMETER

MAO, MERCURY, NV) 4704
SK 17627 SHEET NO 1 NO

SK·I·7027 | 1





GENERAL NOTES

TOLERANCES: DECIMAL $\pm .005$, FRACTIONAL $\pm \frac{1}{32}$,
ANGULAR $\pm 1^\circ$, UNLESS OTHERWISE NOTED.

1. DIMENSIONS AND TOLERANCES ARE IN ACCORDANCE WITH ANSI Y14.5, 1973.
2. ALL MACHINED SURFACES TO BE $\frac{125}{125}$ OR BETTER SURFACE TEXTURE, UNLESS OTHERWISE NOTED, SHALL BE IN ACCORDANCE WITH ANSI Y14.36, 1978.
3. REMOVE ALL BURRS AND SHARP EDGES.
4. PROVIDE $\frac{3}{8}$ -10UNC-2A X 2 LONG 8 HEK HEAD CAP SCREWS ASTM A 325. THESE CAP SCREWS TO BE USED WITH PN 2 WHEN IT IS USED AS A LIFTING FIXTURE.
5. PN 2 MAY ALSO BE USED AS A CALORIMETER COVER DURING CALORIMETER HEAT UP PRIOR TO INSERTION OF SPENT FUEL. IN THIS CASE A LATCHING SPIDER PN 1 ON SK-17624 WITH THRUST BEARING PN 23 ON SKI-3620 SHOULD BE INSTALLED.

WELDING FABRICATION REQUIREMENTS

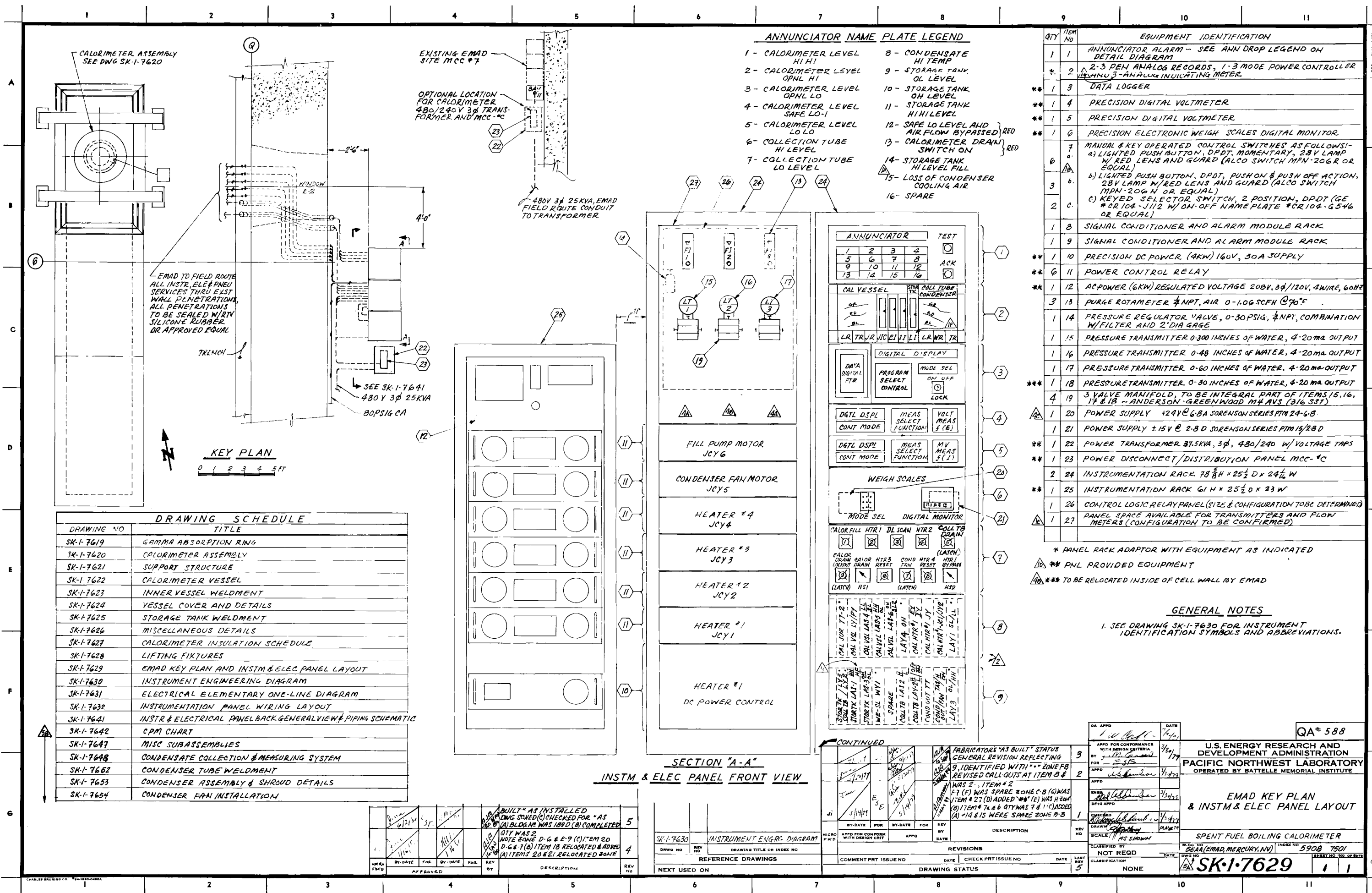
A WELDING STANDARD(S)	<input type="checkbox"/> NPS-220-W	<input type="checkbox"/> NPS-230-W	<input type="checkbox"/> NPS-240-W
B WELD PROCESS	<input type="checkbox"/> GTAW	<input type="checkbox"/> SMAW	<input type="checkbox"/> OPTIONAL
C PROCEDURE SPEC	<input type="checkbox"/> ASME SEC. IX	<input type="checkbox"/> AWS D1.1	<input type="checkbox"/> NPS-240-W
D PERFORMANCE CERT.	<input type="checkbox"/> ASME SEC. IX	<input type="checkbox"/> AWS D1.1	<input type="checkbox"/> NPS-210-W
E MATERIAL SPEC	<input type="checkbox"/> ASME SEC. II	<input type="checkbox"/> AWS AS-X [X]	<input type="checkbox"/> NPS-235-W
F VISUAL [VT]	<input type="checkbox"/> NPS-220-W	<input type="checkbox"/> NPS-230-W	<input type="checkbox"/> NPS-240-W
G PENETRANT (PTI)	<input type="checkbox"/> ASME SEC. III	<input type="checkbox"/> ASME SEC. V	<input type="checkbox"/> ASME SEC. VIII
H MAGNETIC PART. (MT)	<input type="checkbox"/> ASME SEC. III	<input type="checkbox"/> ASME SEC. V	<input type="checkbox"/> ASME SEC. VIII
I ULTRASONIC (UT)	<input type="checkbox"/> ASME SEC. V	<input type="checkbox"/> ASME SEC. VIII	<input type="checkbox"/> AWS D11
K RADIOGRAPHIC (RT)	<input type="checkbox"/> ASME SEC. III	<input type="checkbox"/> ASME SEC. V	<input type="checkbox"/> ASME SEC. VIII

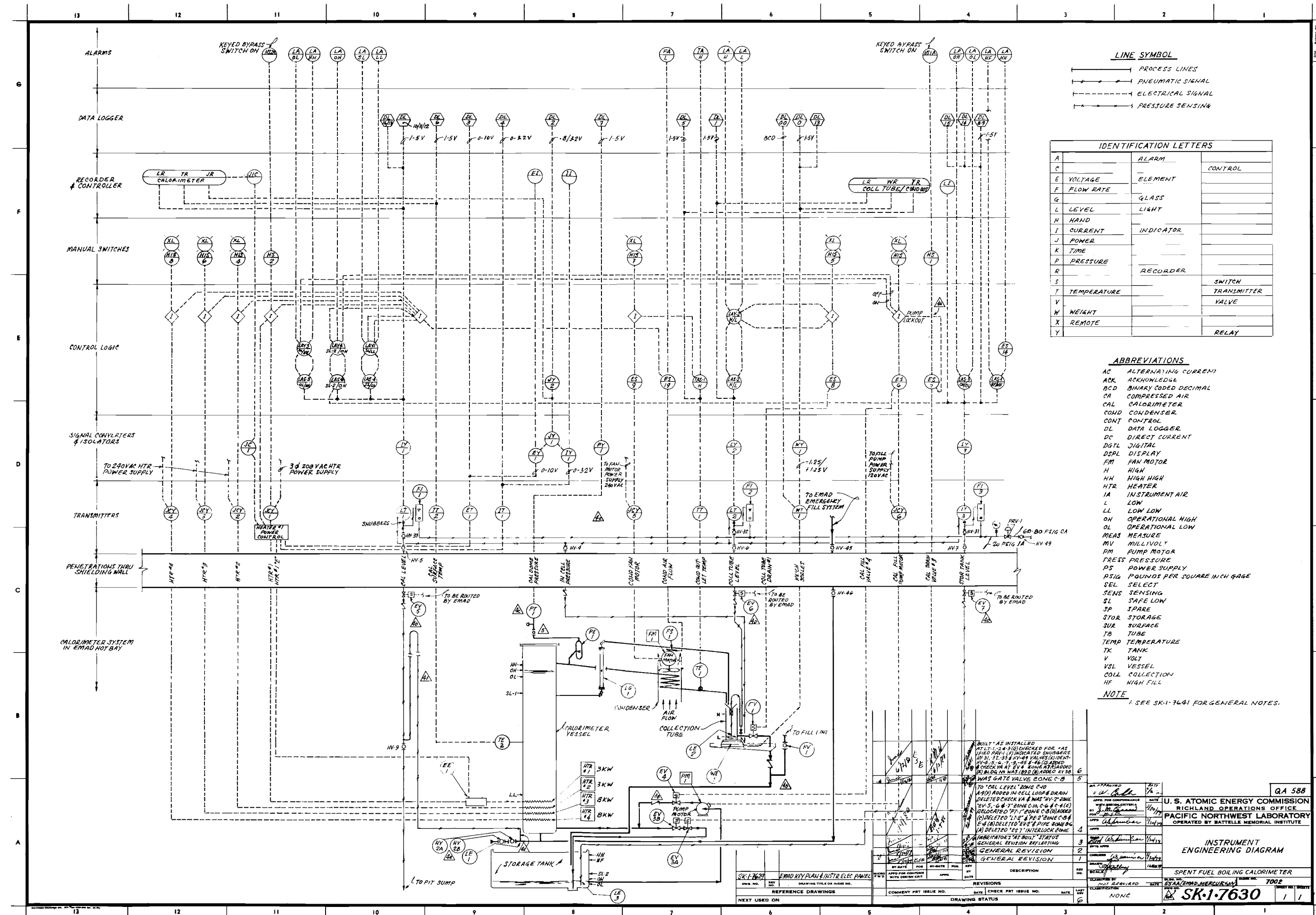
OTHER REQS "WELD C-XX" DESIGNATES INDIVIDUAL WELDS. A "WELD RECORD" SHALL BE COMPLETED BY FABRICATOR TABULATING ALL DESIGNATED WELDS. THIS WELD RECORD TO BE IDENTIFIED WITH A HEAT/LOT NUMBER.

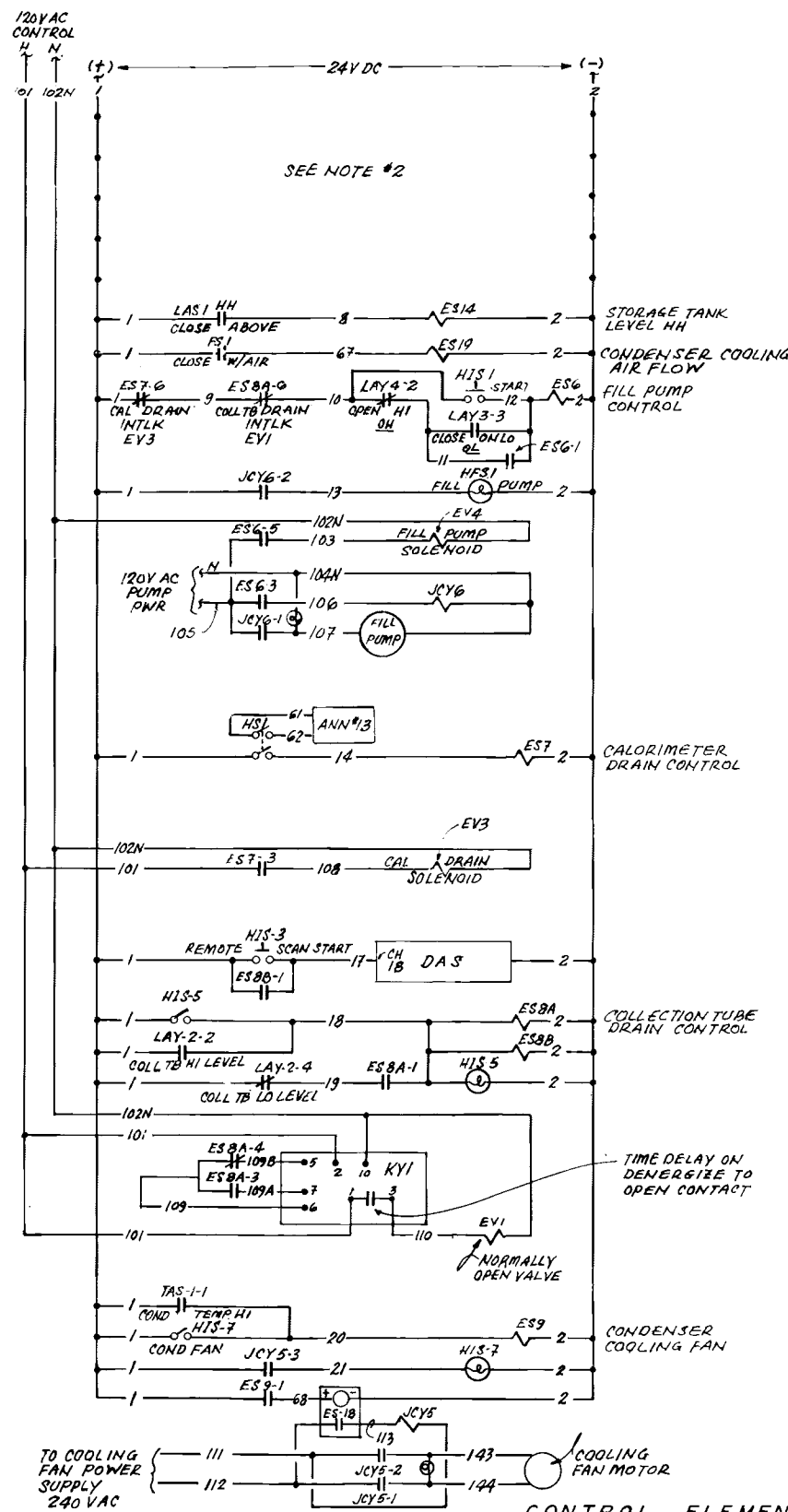
DATE 1/1/81	U.S. ENERGY RESEARCH AND DEVELOPMENT ADMINISTRATION PACIFIC NORTHWEST LABORATORY	QA # 588
		1/12/81

LIFTING FIXTURES

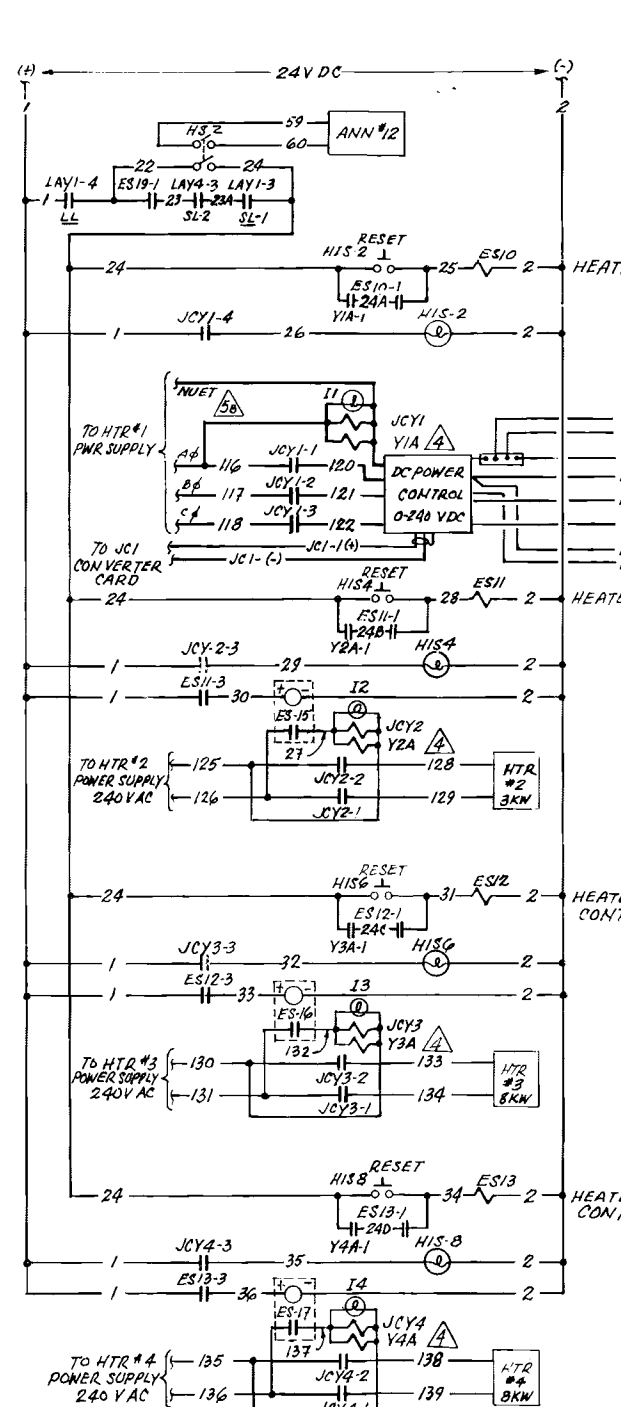
SPENT FUEL BOWLING CALIBRIMETERS



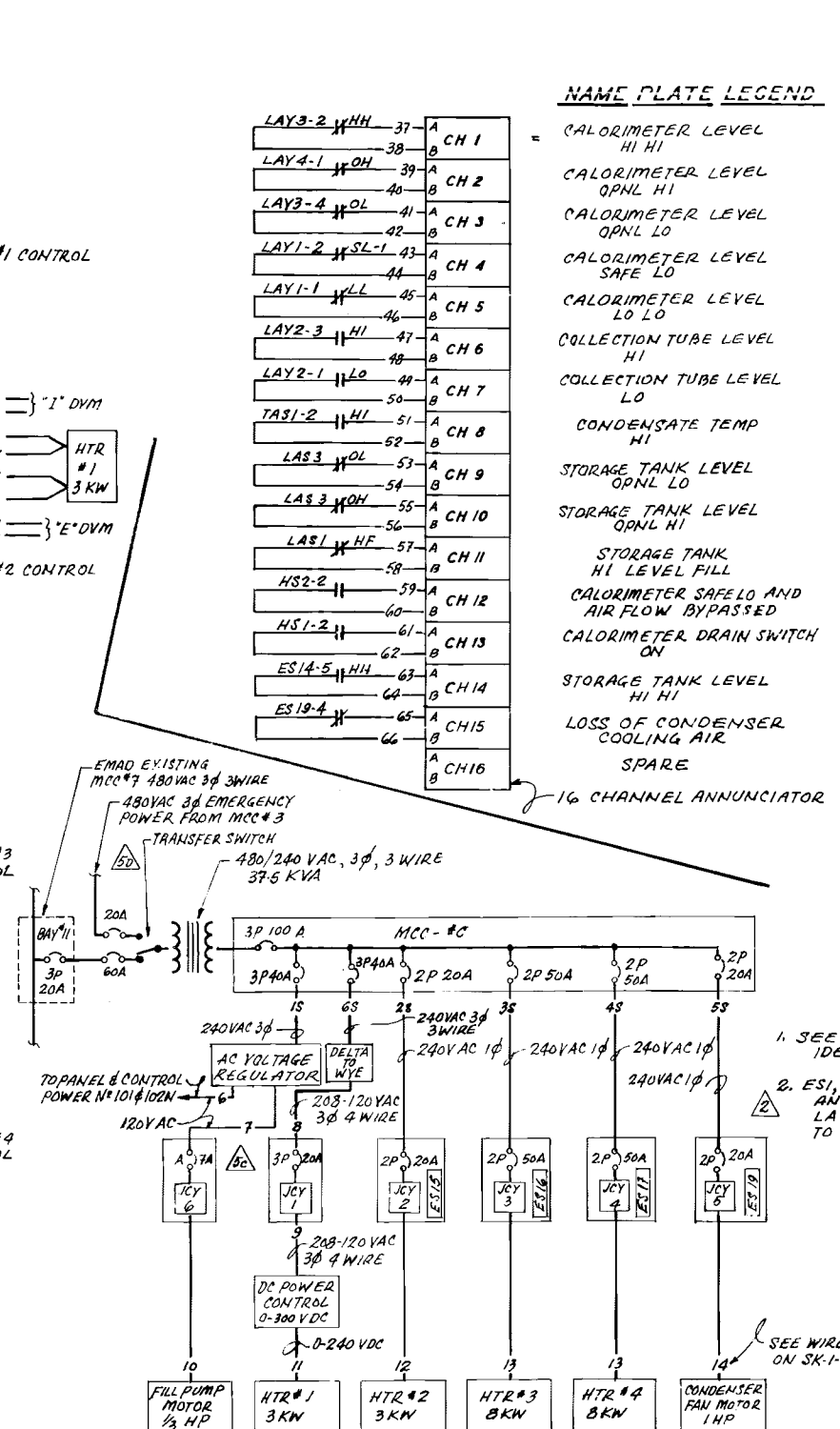




CONTROL ELEMENTAR

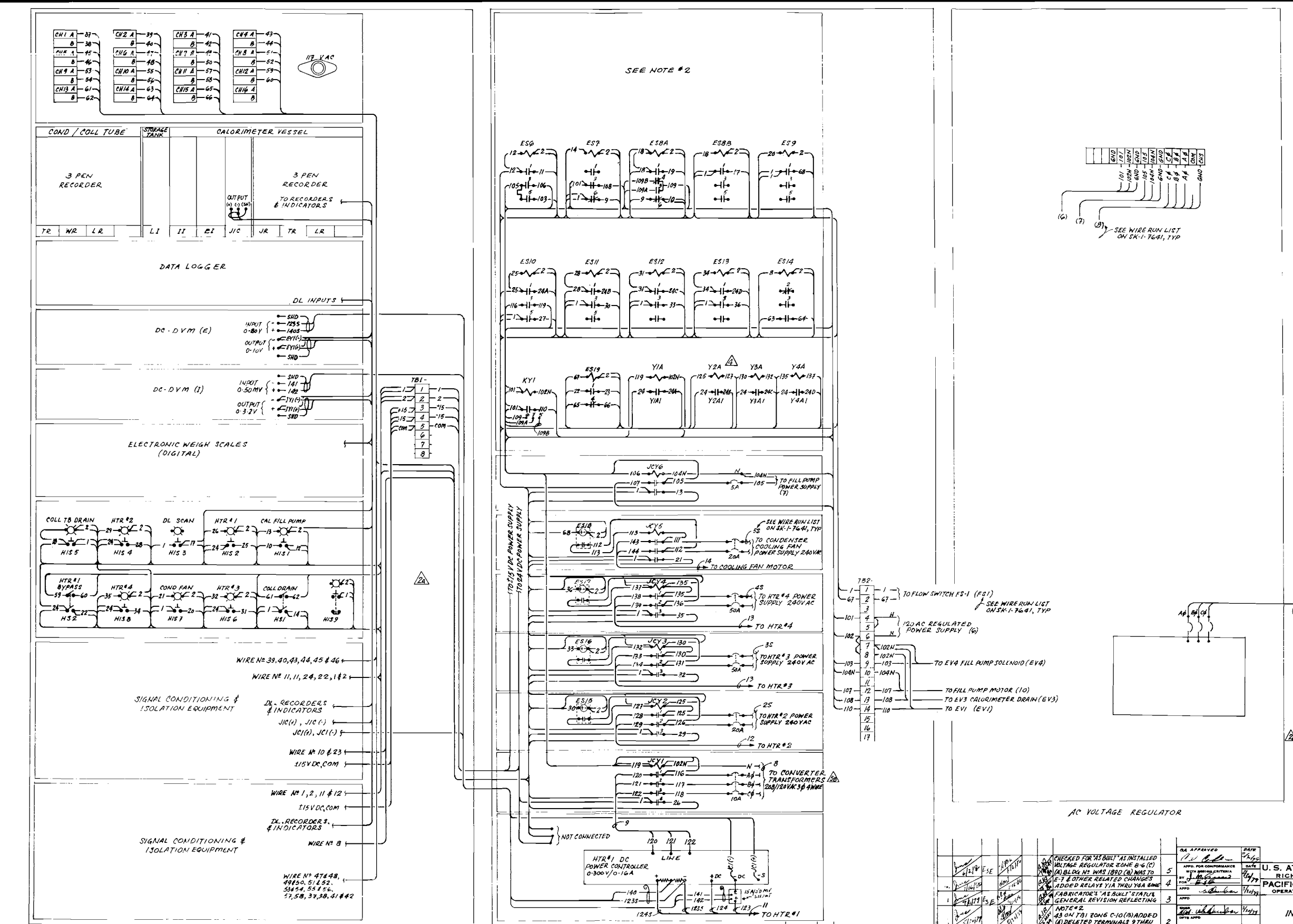


TYPICAL RT

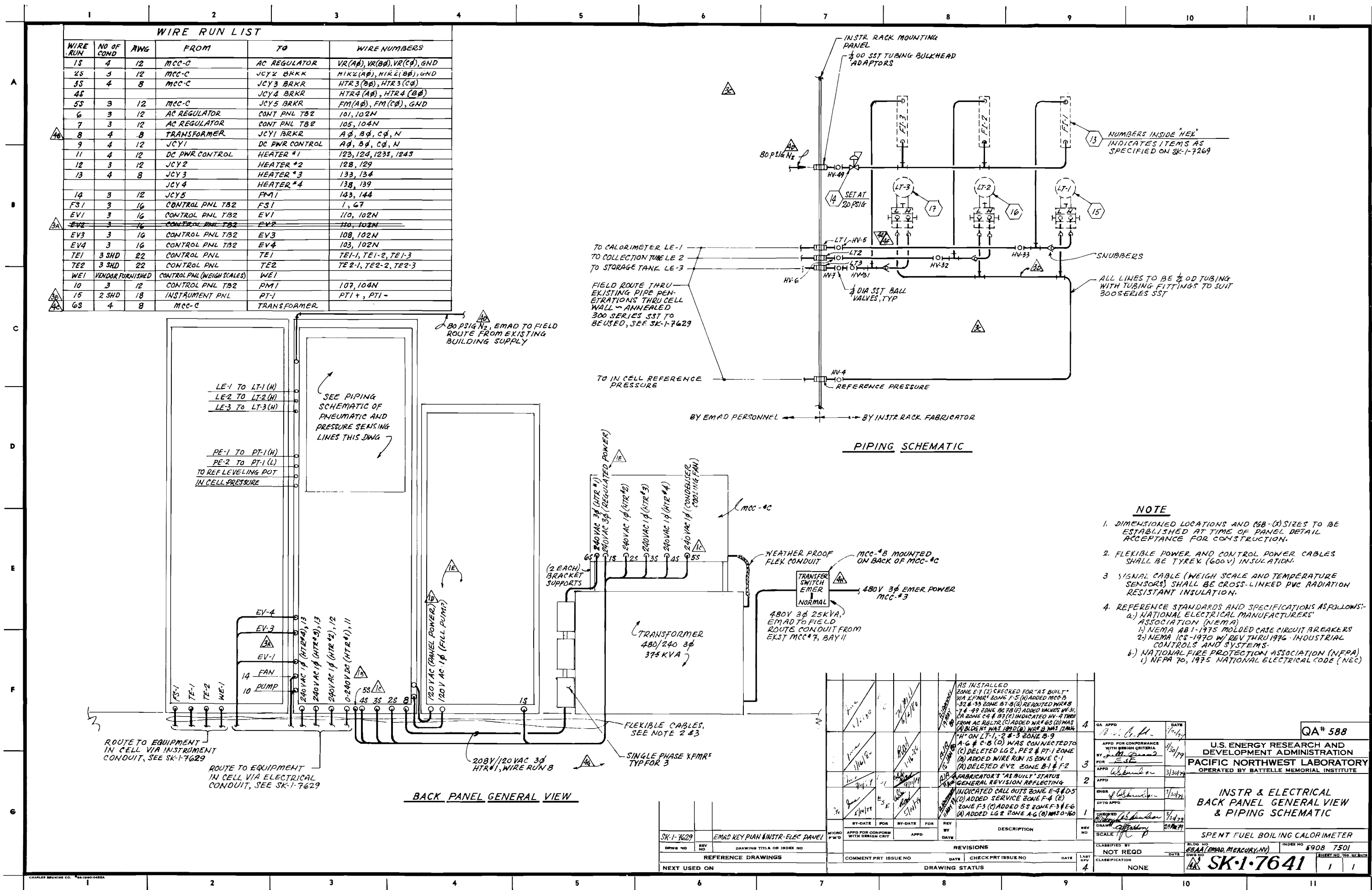


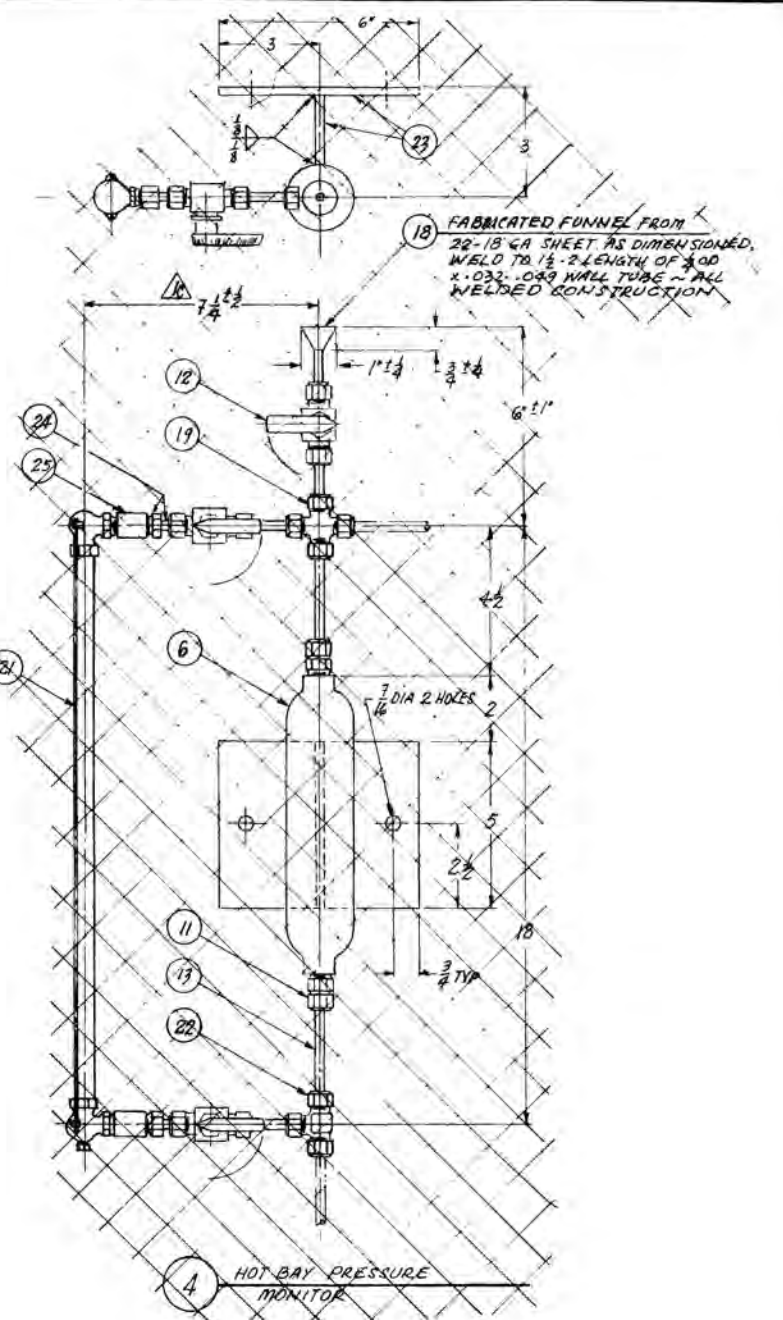
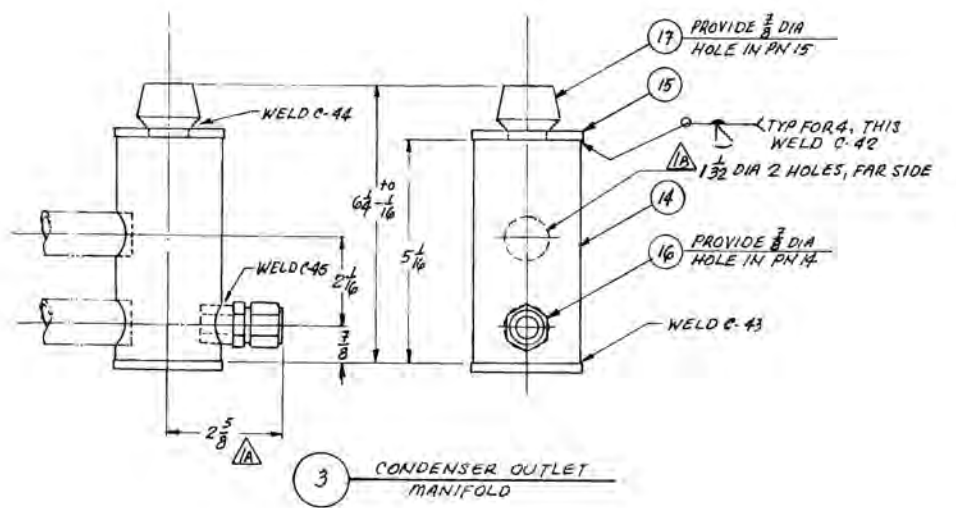
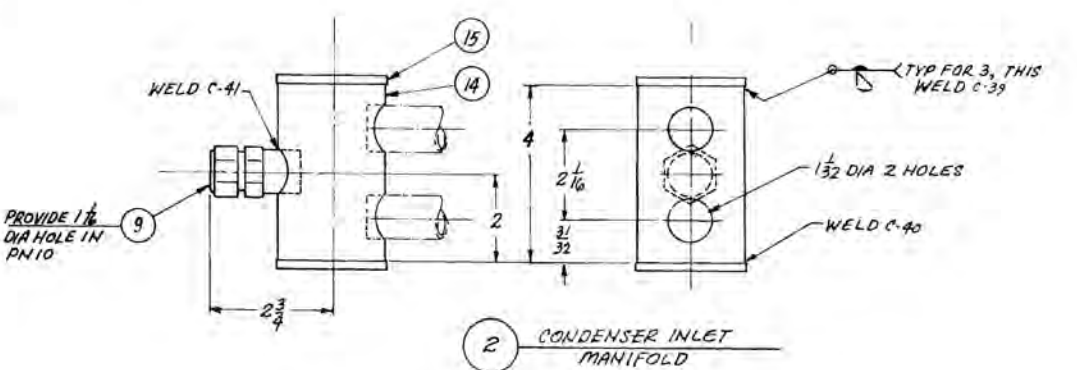
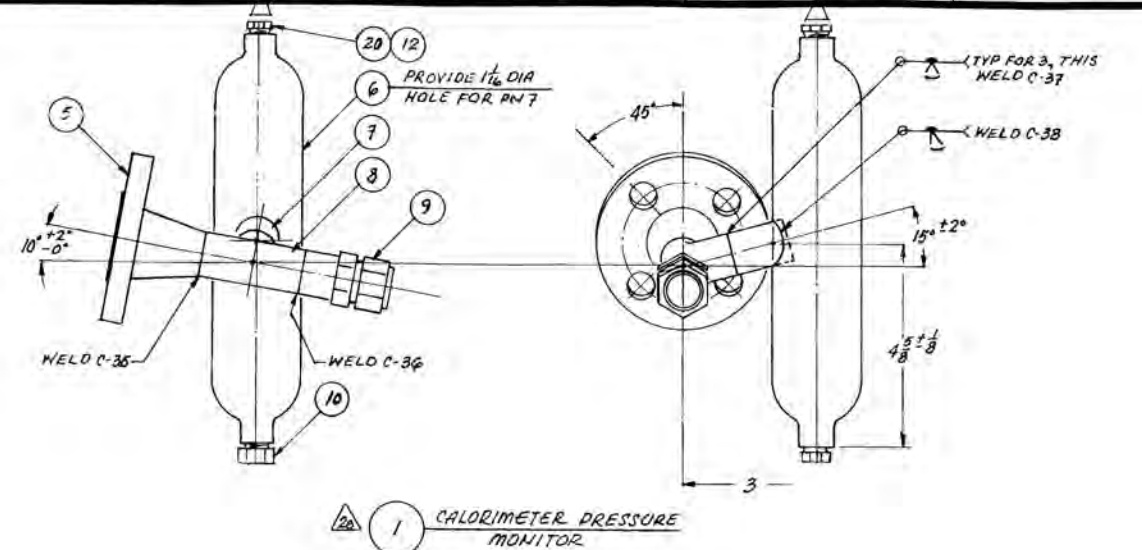
ELECTRICAL POWER

<u>ELECTRICAL POWER</u>									
CONTINUED									
BY-DATE	FOR	BY-DATE	FOR	REV BY DATE	DESCRIPTION	REV NO	REVISIONS		
							APPD FOR CONFORM WITH DESIGN CRIT	APPD	REVISION NO
11/11/73	11/11/73	11/11/73	11/11/73		16. DG & FG & OTHER RELATED CHANGED ADDED RELAYS VIA THRU YARZONES B.G.	4			
11/11/73	11/11/73	11/11/73	11/11/73		18. FABRICATOR'S AS BUILT STATUS GENERAL REVISION REFLECTING	3			
11/11/73	11/11/73	11/11/73	11/11/73		18. ADDED NOTE #2	2			
11/11/73	11/11/73	11/11/73	11/11/73		18. GENERAL REVISION	1			
COMMENT PRT ISSUE NO DATE CHECK PRT ISSUE NO DATE LAST REV									
DRAWING STATUS 5									



QA 586		U. S. ATOMIC ENERGY COMMISSION RICHLAND OPERATIONS OFFICE PACIFIC NORTHWEST LABORATORY OPERATED BY Battelle Memorial Institute	
INSTRUMENT PANEL WIRING LAYOUT			
SPENT FUEL BOILING CALORIMETER			
SK-17632			





QTY	PN	DESCRIPTION	MATERIAL
	x 1	CALORIMETER PRESSURE MONITOR	
x	x 2	CONDENSER INLET MANIFOLD	
x	x 3	CONDENSER OUTLET MANIFOLD	
x	x 4	HOT BAY PRESSURE MONITOR	
	x 5	3/4-150# FLANGE WELD NECK RAISED FACE	300 SERIES SST
1	x 6	CYLINDER 2"OD x 3" NPT ENDS 9 1/2" "WHITEY" #304-HD14-300	
1	x 7	PIPE 3/4 SCHED 40 5' x 1 1/2 L	
1	x 8	TEE 3/4 SCHED 40 S	
1	x 9	WELD CONNECTOR 3/4OD x 3/4 P "SWAGELOK" #SS-1010-1-BMPN	
1	x 10	PLUG 3/4-18NPT HEK HEAD	
2	x 11	MALE CONNECTOR 3/4OD x 3/4 P "SWAGELOK" #SS-400-1-4	
3	x 12	BALL VALVE 3/4OD "WHITEY" #SS-4354	
AR	x 13	TUBE 3/4OD x .032-.049 WALL	
AR	AR 14	PIPE 2 SCHED 40 S	
2	2 15	END PLATE 2 1/2 OD x 3/16 THK	
1	16	WELD CONNECTOR 3/4OD x 3/4 P "SWAGELOK" #SS-810-1-BMPN	
1	17	THREDOLET 1/2-18NPT 3000#	
1	18	FABRICATED FUNNEL, SEE ASSEMBLY	
1	19	UNION CROSS 3/4OD "SWAGELOK" #SS-400-4	
1	20	MALE ADAPTOR 3/4OD x 3/4 P "CAJON" #SS-4-TA-1-4	
1	21	SIGHT GLASS W/ SHUT OFF VALVES 3/4-18NPT MALE ENDS 1/8" CENTER TO CENTER W/ DRAIN PLUG "ERNST" #5-0-33	
1	22	UNION TEE 3/4OD "SWAGELOK" #SS-400-3	
AR	23	PLATE 3/4" THK, SEE ASSEMBLY	
2	24	MALE ADAPTOR 3/4OD x 3/4 P "CAJON" #SS-4-TA-1-6	
2	25	COUPLING 3/4-18NPT 150# SERVICE	

GENERAL NOTES

1. TOLERANCES: FRACTIONAL $\pm \frac{1}{16}$, UNLESS OTHERWISE NOTED.
2. ALL MACHINED SURFACES TO BE $\frac{125}{100}$ OR BETTER
SURFACE TEXTURE IN ACCORDANCE WITH ANSI B46.1,
1962.
3. REMOVE ALL BURRS AND SHARP EDGES.
4. ALL MATERIAL TO BE AS SPECIFIED OR APPROVED EQUAL.

WELDING FABRICATION REQUIREMENTS			
A WELDING STANDARD(S)	<input type="checkbox"/> AWS-220-W	<input type="checkbox"/> AWS-230-W	<input type="checkbox"/> AWS-240-W
B WELD PROCESS	<input type="checkbox"/> GTAW	<input type="checkbox"/> SMAW	<input type="checkbox"/> OPTIONAL
C PROCEDURE SPEC.	<input type="checkbox"/> AWS SEC. IX	<input type="checkbox"/> AWS DI	<input type="checkbox"/> AWS-240-W
D PERFORMANCE CERT.	<input type="checkbox"/> AWS SEC. IX	<input type="checkbox"/> AWS DI	<input type="checkbox"/> AWS-210-W
E MATERIAL SPEC.	<input type="checkbox"/> AWS SEC. II	<input type="checkbox"/> AWS AS 5-X-(X)	<input type="checkbox"/> AWS-235-W
F VISUAL (VT)	<input type="checkbox"/> AWS-220-W	<input type="checkbox"/> AWS-230-W	<input type="checkbox"/> AWS-240-W
G PENETRANT (PT)	<input type="checkbox"/> AWS SEC. III	<input type="checkbox"/> AWS SEC. V	<input type="checkbox"/> AWS SEC. VIII
H MAGNETIC PART (MT)	<input type="checkbox"/> AWS SEC. III	<input type="checkbox"/> AWS SEC. VII	<input type="checkbox"/> AWS SEC. VIII
J ULTRASONIC (UT)	<input type="checkbox"/> AWS SEC. V	<input type="checkbox"/> AWS SEC. VIII	<input type="checkbox"/> AWS DI
K RADIOPHASIC (RT)	<input type="checkbox"/> AWS SEC. III	<input type="checkbox"/> AWS SEC. V	<input type="checkbox"/> AWS SEC. VIII

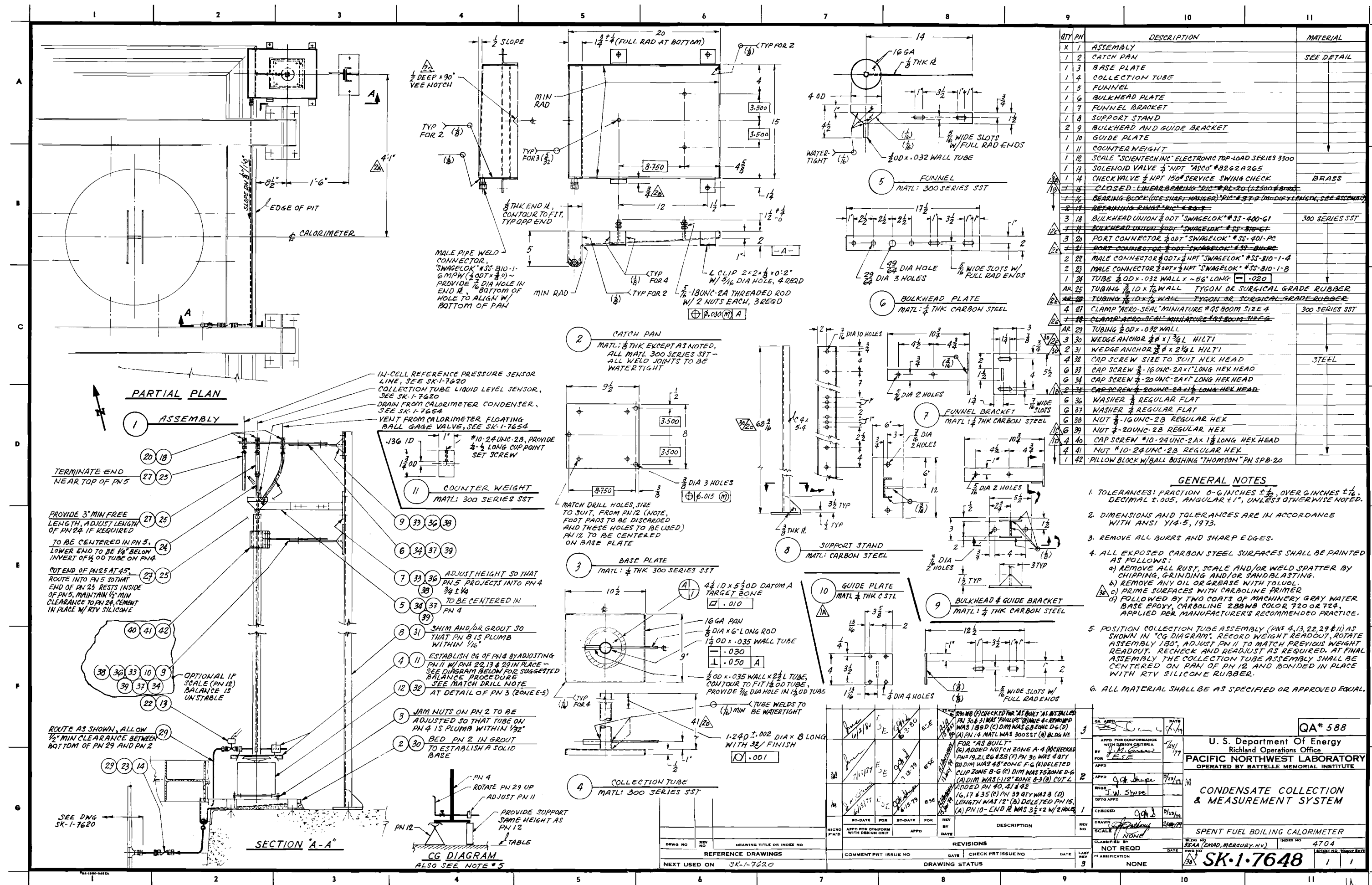
OTHER REQS. "WELD C-XX" DESIGNATES INDIVIDUAL WELDS. A "WELD RECORD" SHALL BE COMPLETED BY FABRICATOR TABULATING ALL DESIGNATED WELDS. THIS WELD RECORD TO BE IDENTIFIED WITH # HEDCAL 48825.

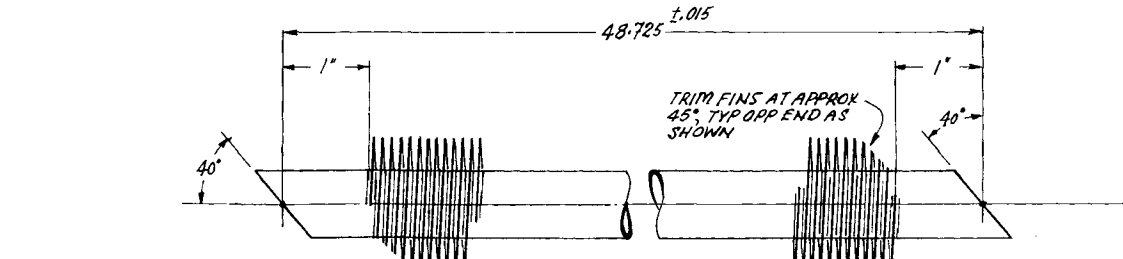
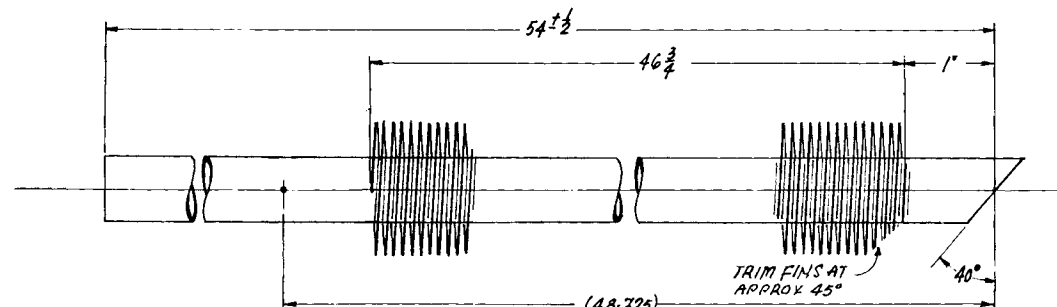
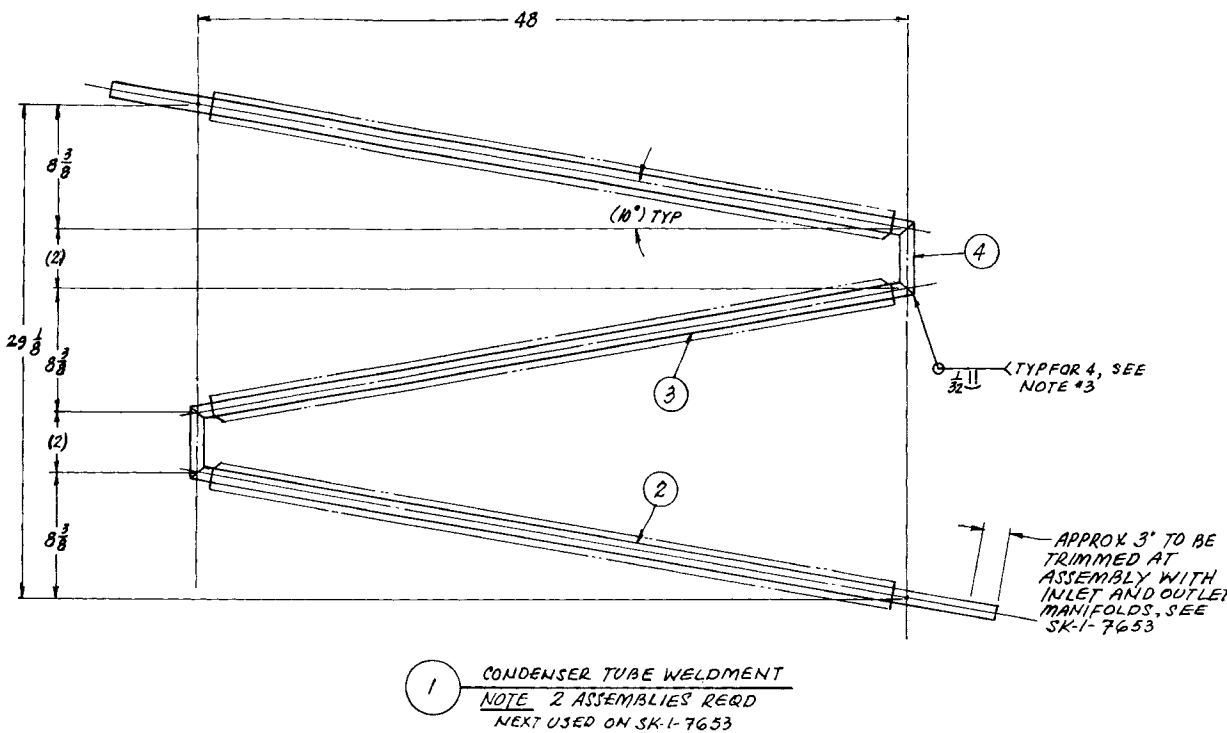
MISC SURASSEMBLIES

PRESENTATION DRAWINGS © 2013 BY THE AUTHOR

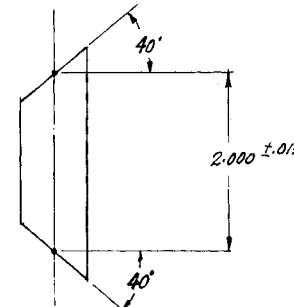
SPENT FUEL BOILING CALORIMETER

AA (EMAO, MERCURY, NY) 4704
NO. SK-1-7647 1 1

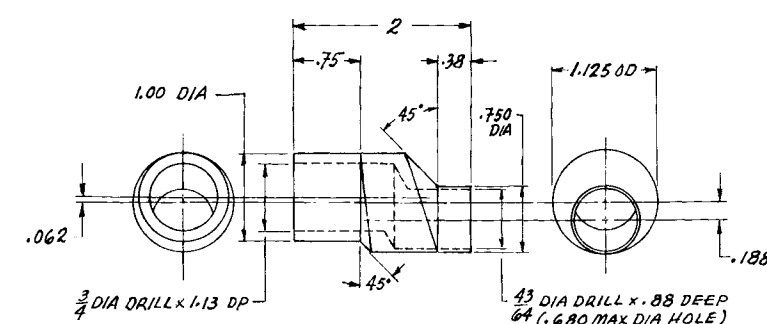




3 FINNED TUBE, SEE NOTE #2
NOTE ONE REQD PER ASSEMBLY



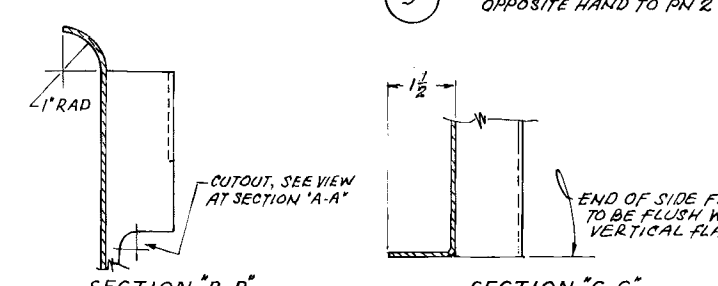
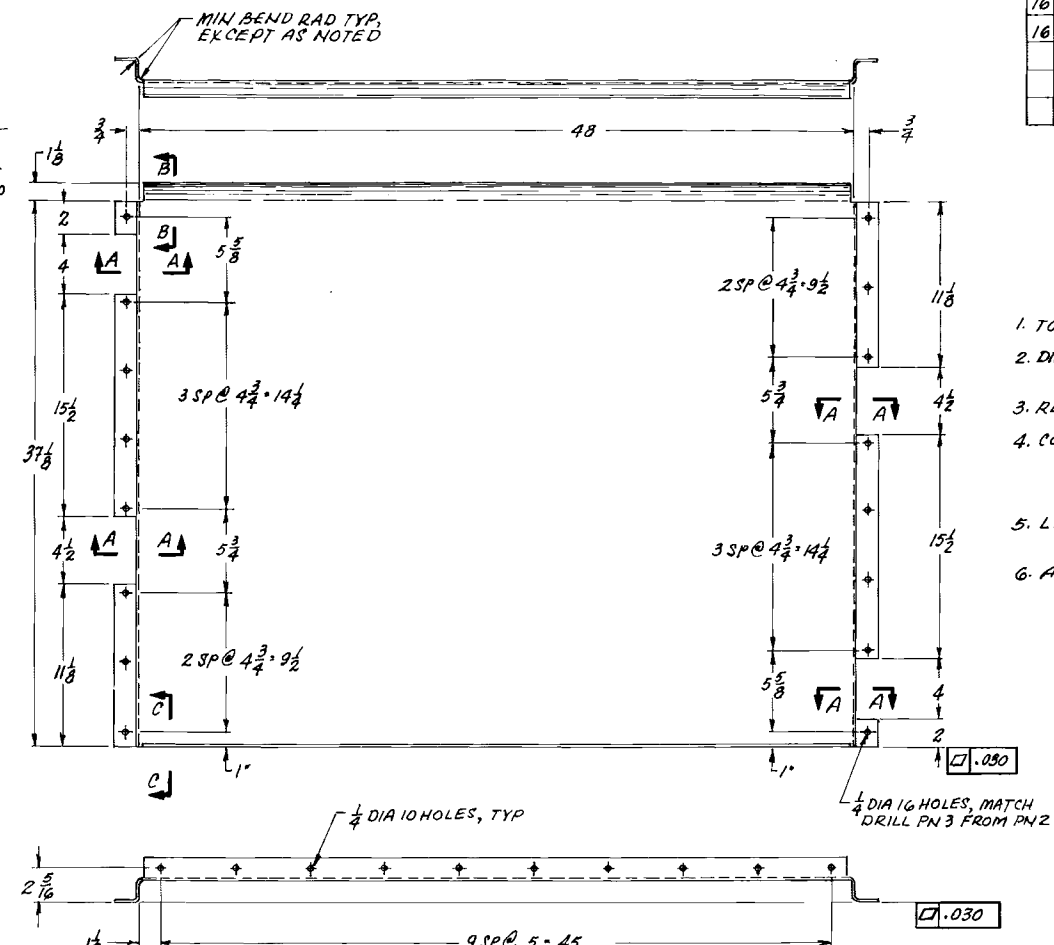
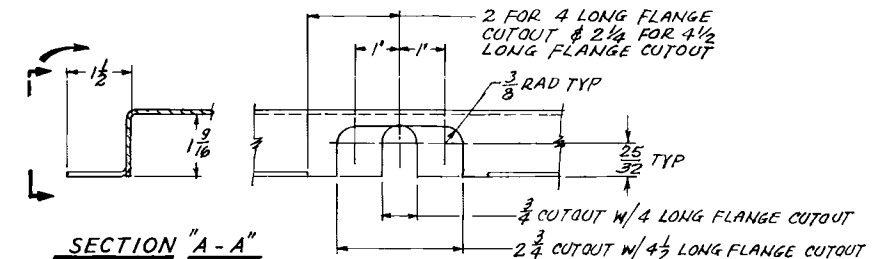
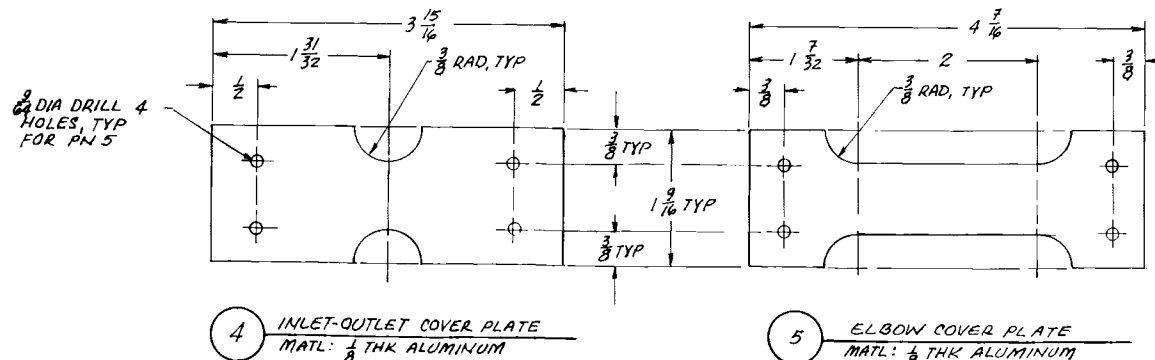
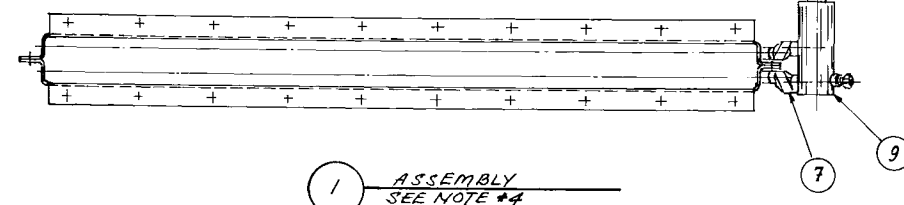
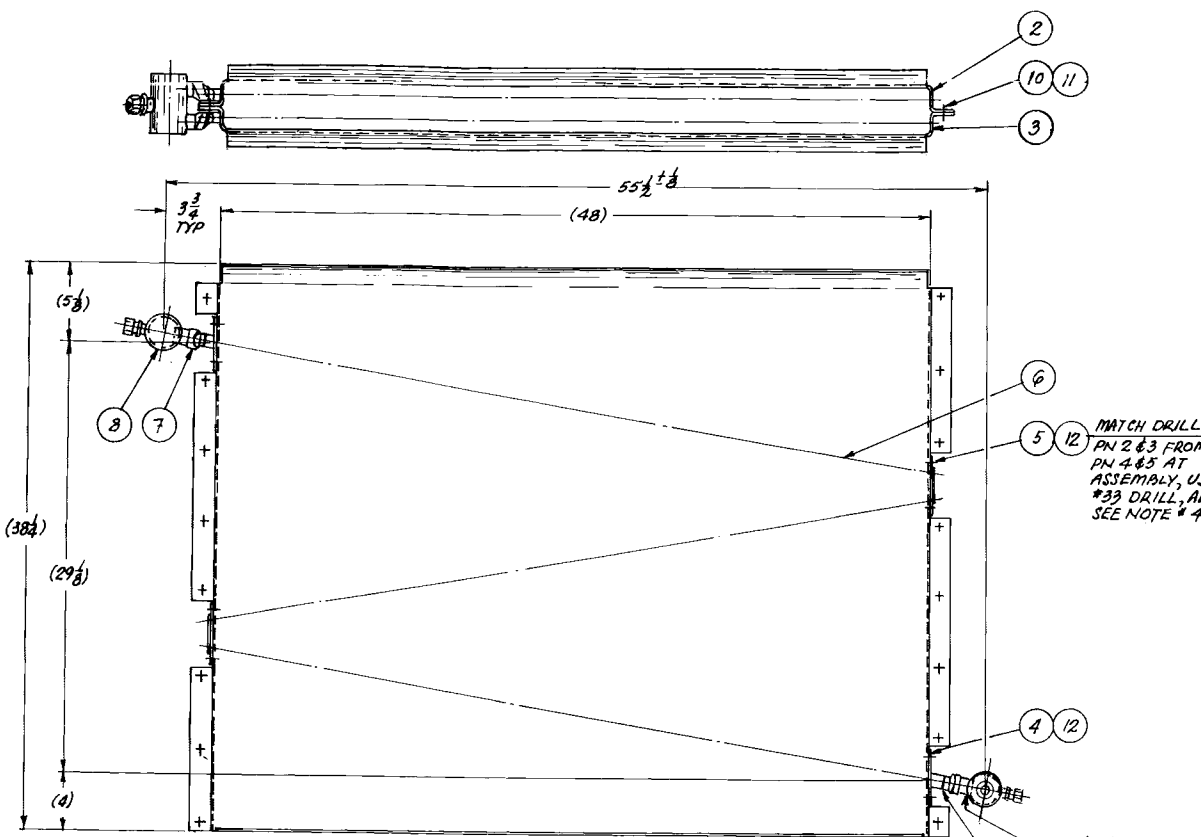
4 3/4 OD X .035 WALL TUBE
MATL: 300 SERIES SST
NOTE 2 REQD PER ASSEMBLY

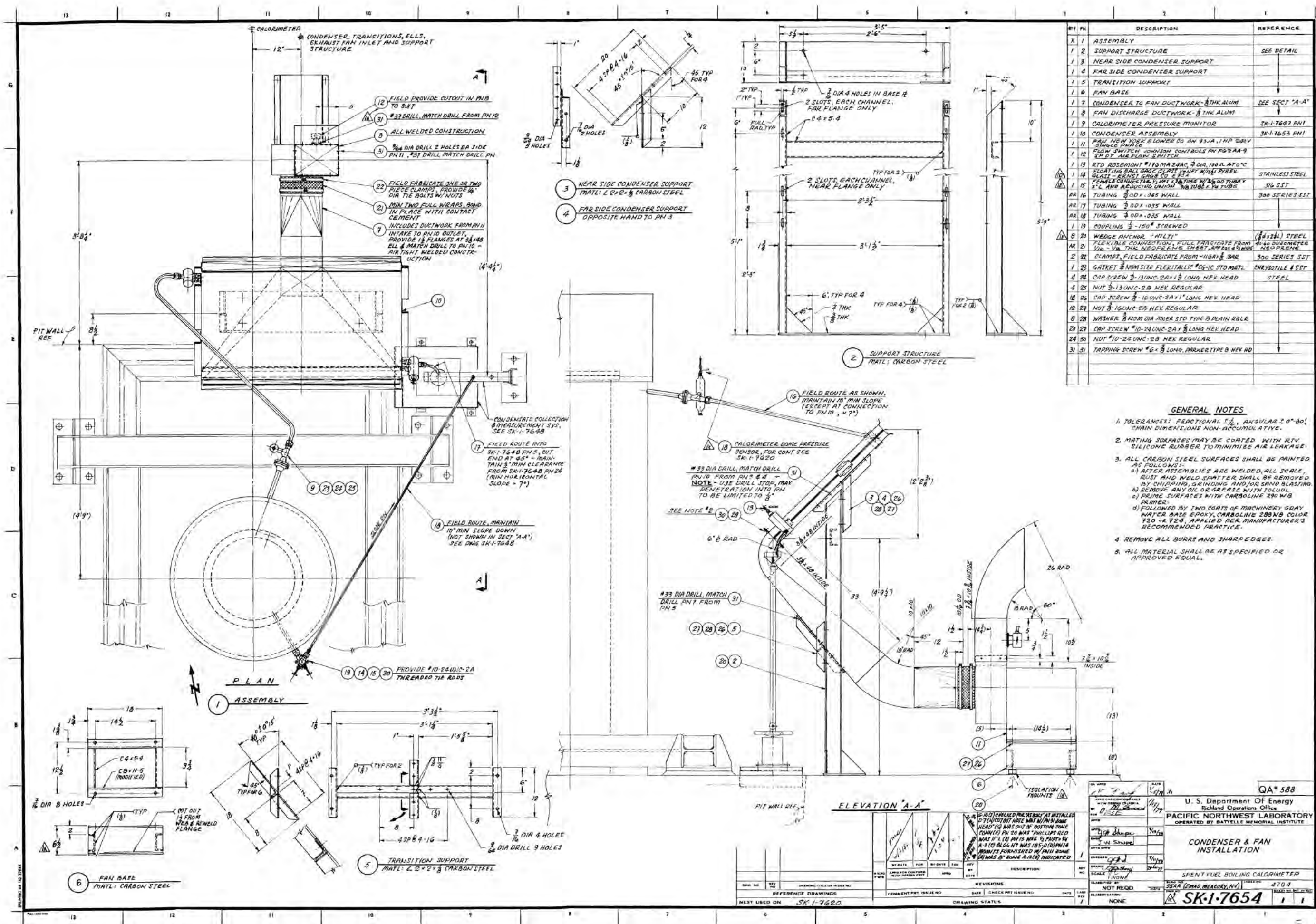


5 MANIFOLD-CONDENSER TUBE ADAPTOR
MATL: 300 SERIES SST
NOTE FOUR REQUIRED
NEXT USED ON SK-17463

GENERAL NOTE

1. TOLERANCES: FRACTIONAL $\pm \frac{1}{16}$, DECIMAL .XX $\pm .010$, .XXX $\pm .005$, ANGULAR $\pm 0^\circ 30'$, UNLESS OTHERWISE NOTED.
2. FINNED TUBING SHALL BE $\frac{3}{8}$ OD X .035 WALL TYPE 304 STAINLESS STEEL WITH SPIRAL WOUND FINS, 10 PER INCH, .375" FIN HEIGHT, .01" FIN THICKNESS, 110 H14 ALUMINUM, AS MANUFACTURED BY MODINE MFG CO., RACINE, WI.
3. LEAK TEST CONDENSER WELDMENTS WITH $\frac{1}{2}$ IN. ID HOOP, OR EQUAL, AT 30 PSIG.





APPENDIX B
RAW DATA

RAW DATA

EXPERIMENTAL RUN SUMMARY

The following table presents a summary of the important experimental runs completed during acceptance testing and calorimetry of spent fuel assemblies.

TABLE B.1. Experimental Run Summary

Run #	Heater Power, kW	Objective
5 and 6	~2.5	Measure q_{cal}
7, 8, and 9	~2.0	Measure q_{cal}
12, 13, and 14	~3.0	Measure q_{cal}
18, 19, 20, and 21	~1.5	Measure q_{cal}
24, 25, 26, and 27	~1.0	Measure q_{cal} and reference run for spent fuel assembly D-34
28, 29, and 30	~0.9	Measure q_{cal}
33 and 34	~3.0	Measure q_{cal} with no insulation cap
37 and 38	~1.0	Measure q_{cal} and reference run for spent fuel assembly D-34
C1 and C2	~1.0	Reference run for spent fuel assembly D-34
C3, C4, C5, and C6	~1.0	Measure q_{SF} of spent fuel assembly D-34

DATA LOGGER CHANNEL NOMENCLATURE

The following table presents the data logger channel nomenclature and units required to reduce the raw data presented in the following section to engineering units.

TABLE B.2. Data Logger Channel Nomenclature

Channel	Parameter	Units
0	Condensate Weight	g
1	Collection Tube Head	in. H ₂ O σ 68°F
2	Reference Heater Power	kW
3	Reference Heater Voltage	volts/24.615
4	Reference Heater Current	amps/4.808
5	Condenser Outlet Temp	°C
6	Calorimeter "Skin" Temp	°C
7	Calorimeter "Dome" Pressure	psia/0.25
8 & 9	Storage Tank Water Level	inches/0.22
10, 11, & 12	Calorimeter Water Level	inches/2.16
13	Condensate plus Tare Weight	g/50
14 & 15	Storage Tank Water Level	inches/0.22
16 & 17	Calorimeter Water Level	inches/2.16
18 & 19	Data Run Initiate and Reset	--

RAW DATA PRINTOUTS

The following pages present data obtained with the data logger throughout testing.

19	<	00002	V	19	<	00002	V
13		0001	V	18		0001	V
17		9538	%	17		9513	%
16		9539	%	16		9513	%
15		2209	%	15		2217	%
14		2209	%	14		2217	%
13		6646	%	13		6646	%
12		9537	%	12		9514	%
11		9537	%	11		9516	%
10		9537	%	10		9517	%
9		2207	%	9		2218	%
8		2207	%	8		2217	%
7		5194	%	7		5183	%
6		8943	%	6		8945	%
5		2922	%	5		2919	%
4		23760	V	4		23783	V
3		8903	V	3		8906	V
2		25435	W	2		25500	W
1	>	3713	tw	1	>	3716	tw
0		13159	G	0		13162	G

0 06538
000003
072:12:39:32

1 > 3703 tw
072:12:39:31

0 06539
000003
072:12:53:01

1 > 3705 tw
072:12:53:01

19	<	00003	V	19	<	00001	V
18		0001	V	18		0001	V
17		9541	%	17		9530	%
16		9541	%	16		9529	%
15		2213	%	15		2219	%
14		2213	%	14		2219	%
13		5520	%	13		5517	%
12		9540	%	12		9521	%
11		9540	%	11		9518	%
10		9540	%	10		9519	%
9		2213	%	9		2219	%
8		2213	%	8		2219	%
7		5186	%	7		5184	%
6		8943	%	6		8944	%
5		2905	%	5		2909	%
4		23777	V	4		23781	V
3		8906	V	3		8903	V
2		25531	W	2		25427	W
1		514	tw	1		517	tw
0		7542	G	0		7520	G

0 00908 R#5
000003
072:12:23:46 3/12/80

1 503 tw
072:12:26:45 02.5kw

0 00899 R#6
000003
072:12:42:19 3/12/80

1 507 tw
072:12:42:18 02.5kw

19	< 00003	V	19	< 00002	V	19	< 00001	V
18	0001	V	18	0001	V	18	0001	V
17	9529	%	17	9517	%	17	9509	%
16	9530	%	16	9517	%	16	9508	%
15	2218	%	15	2223	%	15	2231	%
14	2218	%	14	2223	%	14	2231	%
13	6644	%	13	6640	%	13	6642	%
12	9530	%	12	9516	%	12	9509	%
11	9529	%	11	9514	%	11	9509	%
10	9529	%	10	9514	%	10	9509	%
9	2218	%	9	2223	%	9	2231	%
8	2218	%	8	2223	%	8	2231	%
7	5188	%	7	5191	%	7	5187	%
6	8941	%	6	8941	%	6	8941	%
5	2874	%	5	2873	%	5	2861	%
4	21333	V	4	21333	V	4	21330	V
3	7984	V	3	7981	V	3	7980	V
2	20452	%	2	20453	%	2	20537	%
1	> 3710	tw	1	> 3715	tw	1	> 3709	tw
0	13156	G	0	13161	G	0	13144	G

0	06543		0	06545		0	06532	
	000003			000003			000003	
072:17:04:54			072:17:22:44			072:17:40:55		
1	> 3702	tw	1	> 3707	tw	1	> 3701	tw
072:17:04:53			072:17:22:43			072:17:40:54		

19	< 00001	V	19	< 00001	V	19	< 00002	V
18	0001	V	18	0001	V	18	0001	V
17	9535	%	17	9525	%	17	9515	%
16	9535	%	16	9525	%	16	9515	%
15	2216	%	15	2224	%	15	2229	%
14	2217	%	14	2224	%	14	2229	%
13	5513	%	13	5515	%	13	5515	%
12	9533	%	12	9526	%	12	9515	%
11	9533	%	11	9522	%	11	9517	%
10	9533	%	10	9525	%	10	9517	%
9	2217	%	9	2224	%	9	2229	%
8	2217	%	8	2224	%	8	2229	%
7	5186	%	7	5187	%	7	5187	%
6	8943	%	6	8943	%	6	8941	%
5	2853	%	5	2874	%	5	2857	%
4	21339	V	4	21348	V	4	21330	V
3	7981	V	3	7979	V	3	7976	V
2	20487	%	2	20506	%	2	20491	%
1	508	tw	1	513	tw	1	513	tw
0	7489	G	0	7510	G	0	7520	G

0	00884	R#7	0	00896	R#8	0	00899	R#9
	000003	3/12/80		000003	3/12/80		000003	3/12/80
072:16:50:11			072:17:08:17			072:17:26:14		
501	tw		504	tw		504	tw	
072:16:50:10			072:17:08:16			072:17:26:13		
220 kro			220 kro			220 kro		

19	< 00002	V	19	< 00001	V	19	< 00001	V
18	0001	V	18	0002	V	18	0002	V
17	9434	%	17	9415	%	17	9417	%
16	9435	%	16	9412	%	16	9416	%
15	2253	%	15	2259	%	15	2268	%
14	2253	%	14	2259	%	14	2258	%
13	6671	%	13	6669	%	13	6663	%
12	9438	%	12	9423	%	12	9409	%
11	9438	%	11	9424	%	11	9410	%
10	9428	%	10	9424	%	10	9410	%
9	2253	%	9	2259	%	9	2268	%
8	2253	%	8	2259	%	8	2267	%
7	5174	%	7	5173	%	7	5173	%
6	8961	%	6	8961	%	6	8961	%
5	3219	%	5	3207	%	5	3209	%
4	26024	V	4	26016	V	4	26025	V
3	9750	V	3	9749	V	3	9754	V
2	30249	W	2	30242	W	2	30256	W
1	> 3725	tw	1	> 3720	tw	1	> 3716	tw
0	13264	G	0	13261	G	0	13241	G

0	06529		0	06536		0	06564	
	000003			010003			000003	
073:14:06:43			073:14:17:48			073:14:28:46		
1	> 3709	tw	1	> 3707	tw	1	> 3702	%
073:14:06:46			073:14:17:48			073:14:23:46		

19	< 00003	V	19	< 00003	V	19	< 00001	V
18	0001	V	18	0001	V	18	0001	V
17	9438	%	17	9419	%	17	9419	%
16	9436	%	16	9424	%	16	9423	%
15	2254	%	15	2260	%	15	2269	%
14	2254	%	14	2259	%	14	2258	%
13	5526	%	13	5527	%	13	5529	%
12	3436	%	12	9430	%	12	9427	%
11	9438	%	11	9430	%	11	9427	%
10	9437	%	10	9431	%	10	9427	%
9	2254	%	9	2259	%	9	2268	%
8	2254	%	8	2259	%	8	2268	%
7	5176	%	7	5173	%	7	5173	%
6	8960	%	6	8962	%	6	8961	%
5	3201	%	5	3253	%	5	3204	%
4	26019	V	4	26019	V	4	26032	V
3	9752	V	3	9748	V	3	9759	V
2	30280	W	2	30231	W	2	30245	W
1	518	tw	1	517	tw	1	519	tw
0	7545	G	0	7550	G	0	7567	G

0	00875	R#12	0	00876	R#13	0	00886	R#14
	000003	03ku		000003	03ku		000003	03ku
073:13:58:07		3/13/80	073:14:09:00		3/13/80	073:14:20:09		3/13/80
1	505	tw	1	504	tw	1	504	tw
073:13:58:06			073:14:08:59			073:14:20:09		

19	00002	V	19	00034	V
18	0001	V	18	> 24663	V
17	9600	V	17	9599	V
16	9599	V	16	9593	V
15	2302	V	15	2304	V
14	2302	V	14	2304	V
13	6066	V	13	6075	V
12	9599	V	12	9597	V
11	9599	V	11	9596	V
10	9599	V	10	9597	V
9	2301	V	9	2304	V
8	2301	V	8	2304	V
7	5135	V	7	5134	V
6	8873	V	6	8875	V
5	2713	V	5	2706	V
4	18366	V	4	18385	V
3	6885	V	3	6883	V
2	15074	V	2	15126	V
1	> 2109	tw	1	> 2108	tw
0	10284	G	0	10270	G

0 03669

000003

084:14:47:51

1 > 2104 tw

084:14:47:50

0 03655

000003

084:15:05:03

1 > 2103 tw

084:15:05:02

19	-00001	V	19	00002	V
18	0001	V	18	0001	V
17	9601	V	17	9598	V
16	9601	V	16	9598	V
15	2299	V	15	2304	V
14	2299	V	14	2304	V
13	5495	V	13	5499	V
12	9594	V	12	9598	V
11	9594	V	11	9598	V
10	9594	V	10	9597	V
9	2295	V	9	2304	V
8	2295	V	8	2304	V
7	5134	V	7	5135	V
6	8870	V	6	8874	V
5	2719	V	5	2711	V
4	18366	V	4	18374	V
3	6886	V	3	6876	V
2	15078	V	2	15106	V
1	505	tw	1	505	tw
0	7434	G	0	7433	G

0 00814 R#18
000003 21.5kw
084:14:35:42 3/24/80

1 500 tw
084:14:35:41

00621 R#19
000003 21.5kw
084:14:52:46 3/24/80

1 500 tw
084:14:52:45

19	20001	V	19	00002	V
18	0001	V	18	0001	V
17	9592	S	17	9586	S
16	9592	S	16	9588	S
15	2307	S	15	2309	S
14	2307	S	14	2309	S
13	6068	S	13	6066	S
12	9592	S	12	9588	S
11	9592	S	11	9588	S
10	9592	S	10	9587	S
9	2307	S	9	2310	S
8	2307	S	8	2310	S
7	5134	S	7	5133	S
6	8877	S	6	8869	S
5	2700	S	5	2694	S
4	18374	V	4	18378	V
3	6864	V	3	6865	V
2	15026	S	2	15064	S
1	> 2108	SW	1	> 2108	SW
0	10280	S	0	10264	S

0 03663

000003

084:15:20:53

1 > 2103 SW

084:15:20:52

0 63653

000003

084:15:39:27

1 > 2103 SW

084:15:39:26

19	-00001	V
18	0001	V
17	9590	S
16	9591	S
15	2310	S
14	2310	S
13	5499	S
12	9588	S
11	9584	S
10	9588	S
9	2309	S
8	2309	S
7	5133	S
6	8876	S
5	2700	S
4	18373	V
3	6862	V
2	15061	S
1	508	SW
0	7436	S

0 00824 R#20

000003 21.5kw

084:15:09:08 3/24/80

1 509 SW

084:15:09:07

19	00002	V
18	0001	V
17	9589	S
16	9591	S
15	2309	S
14	2309	S
13	5492	S
12	9594	S
11	9593	S
10	9593	S
9	2309	S
8	2309	S
7	5134	S
6	8879	S
5	2693	S
4	18373	V
3	6860	V
2	15065	S
1	507	SW
0	7436	S

0 00838 R#21

000003 21.5kw

084:15:27:27 3/24/80

1 501 SW

084:15:27:26

19	00001	V	19	00002	V
18	0001	V	18	0001	V
17	9567	%	17	9564	%
16	9568	%	16	9564	%
15	2315	%	15	2317	%
14	2315	%	14	2317	%
13	5874	%	13	5879	%
12	9566	%	12	9562	%
11	9566	%	11	9562	%
10	9565	%	10	9562	%
9	2315	%	9	2318	%
8	2315	%	8	2318	%
7	5138	%	7	5138	%
6	8894	%	6	8892	%
5	2692	%	5	2685	%
4	14949	V	4	14946	V
3	5594	V	3	5594	V
2	10020	V	2	10023	V
1	> 1604	%W	1	> 1603	%W
0	9320	G	0	9323	G

0 02736

000015

085:13:28:46

1 > 1602 %W
085:13:28:45

0 02717

000015

085:13:55:02

1 > 1601 %W
085:13:55:01

19	00002	V	19	00002	V
18	2221	V	18	0001	V
17	9569	%	17	9564	%
16	9569	%	16	9563	%
15	2314	%	15	2318	%
14	2314	%	14	2318	%
13	5494	%	13	5492	%
12	9568	%	12	9560	%
11	9568	%	11	9560	%
10	9568	%	10	9559	%
9	2314	%	9	2319	%
8	2313	%	8	2319	%
7	5137	%	7	5138	%
6	8891	%	6	8893	%
5	2679	%	5	2685	%
4	14948	V	4	14948	V
3	5589	V	3	5591	V
2	10029	V	2	10054	V
1	503	%W	1	503	%W
0	7417	G	0	7411	G

0 00729 R# 24
000015 1.0kW
085:13:11:15 3/25/80

1 501 %W
085:13:11:15

0 00781 R# 25
000015 1.0kW
085:13:37:27 3/25/80

1 500 %W
085:13:37:26

19	20002	V	19	00000	V
18	2201	V	18	0001	V
17	9560	%	17	9556	%
16	9560	%	16	9556	%
15	2319	%	15	2323	%
14	2319	%	14	2323	%
13	5384	%	13	5382	%
12	9559	%	12	9555	%
11	9559	%	11	9554	%
10	9559	%	10	9554	%
9	2319	%	9	2323	%
8	2319	%	8	2323	%
7	5135	%	7	5134	%
6	6391	%	6	6391	%
5	2685	%	5	2684	%
4	14349	V	4	14349	V
3	5595	V	3	5594	V
2	10006	%	2	10016	%
1	> 1604	%	1	> 1604	%
0	9361	G	0	9362	G

0 02732
000015
035:14:22:23

1 > 1602 %W
035:14:22:27

0 02730
001000
035:14:49:53

1 > 1602 %W
035:14:49:52

19	20001	V	19	20001	V
18	2201	V	18	0001	V
17	9557	%	17	9560	%
16	9555	%	16	9559	%
15	2321	%	15	2324	%
14	2321	%	14	2324	%
13	5392	%	13	5394	%
12	9554	%	12	9559	%
11	9555	%	11	9559	%
10	9556	%	10	9559	%
9	2321	%	9	2324	%
8	2321	%	8	2324	%
7	5138	%	7	5135	%
6	6392	%	6	6392	%
5	2687	%	5	2686	%
4	14341	V	4	14345	V
3	5592	V	3	5595	V
2	10001	%	2	10009	%
1	502	%	1	502	%
0	7409	G	0	7426	G

0 00762 R#26
000015 21.0kW
035:14:04:46 3/25/80

1 500 %W
035:14:04:45

0 00300 R#27
001000 21.0kW
035:14:32:05 3/25/80

1 500 %W
035:14:32:04

19	-00000	V	19	00004	V	19	00002	V
18	0001	V	18	0001	V	18	0001	V
17	9609	%	17	9601	%	17	9602	%
16	9609	%	16	9600	%	16	9602	%
15	2285	%	15	2287	%	15	2289	%
14	2285	%	14	2287	%	14	2290	%
13	5877	%	13	5876	%	13	5879	%
12	9609	%	12	9599	%	12	9601	%
11	9609	%	11	9598	%	11	9600	%
10	9609	%	10	9598	%	10	9600	%
9	2285	%	9	2288	%	9	2290	%
8	2285	%	8	2289	%	8	2290	%
7	5143	%	7	5143	%	7	5141	%
6	8885	%	6	8884	%	6	8883	%
5	2752	%	5	2752	%	5	2755	%
4	14220	V	4	14215	V	4	14216	V
3	5320	V	3	5319	V	3	5315	V
2	9056	W	2	9056	W	2	9056	W
1	> 1603	tw	1	> 1603	tw	1	> 1603	tw
0	9331	G	0	9339	G	0	9345	G

0	02759		0	02767		0	02778	
	001000			001000			001000	
086:14:41:23			086:15:13:29			086:15:45:45		
1	> 1601	tw	1	> 1601	tw	1	> 1602	tw
086:14:41:22			086:15:13:29			086:15:45:45		

19	-00000	V	19	00001	V	19	00001	V
18	0001	V	18	0001	V	18	0001	V
17	9605	%	17	9604	%	17	9594	%
16	9608	%	16	9604	%	16	9594	%
15	2284	%	15	2290	%	15	2290	%
14	2284	%	14	2290	%	14	2290	%
13	5489	%	13	5489	%	13	5489	%
12	9611	%	12	9603	%	12	9603	%
11	9612	%	11	9602	%	11	9604	%
10	9612	%	10	9602	%	10	9604	%
9	2284	%	9	2290	%	9	2291	%
8	2284	%	8	2290	%	8	2291	%
7	5144	%	7	5143	%	7	5141	%
6	8885	%	6	8884	%	6	8883	%
5	2753	%	5	2753	%	5	2754	%
4	14211	V	4	14214	V	4	14214	V
3	5320	V	3	5320	V	3	5322	V
2	9056	W	2	9056	W	2	9056	W
1	502	tw	1	503	tw	1	503	tw
0	7393	G	0	7397	G	0	7401	G

0	00828	R#28	0	00831	R#29	0	00829	R#30
	001000	D 0.9kw		001000	D 0.9kw		001000	D 0.9kw
086:14:19:33		3/26/80	086:14:51:44		3/26/80	086:15:23:38		3/26/80
1	500	%	1	500	%	1	500	%
086:14:19:32			086:14:51:44			086:15:23:37		

19	20002	✓
18	00001	✓
17	9526	✓
16	9525	✓
15	2336	✓
14	2335	✓
13	6517	✓
12	9524	✓
11	9523	✓
10	9522	✓
9	2331	✓
8	8331	✓
7	5144	✓
6	2334	✓
5	3164	✓
4	26014	✓
3	2770	✓
2	26013	✓
1	> 3718	SW
0	13208	✓

0 00001
01000

087:14:32:24

1 > 3704 SW
087:14:32:23

19	00002	✓
18	0001	✓
17	9534	✓
16	9533	✓
15	2349	✓
14	2348	✓
13	6563	✓
12	9518	✓
11	9517	✓
10	9516	✓
9	2349	✓
8	2348	✓
7	5161	✓
6	8365	✓
5	3160	✓
4	26019	✓
3	3771	✓
2	29634	✓
1	> 3715	SW
0	13208	✓

0 06543
001000

087:14:44:41

1 > 3702 SW
087:14:44:40

19	00001	✓
18	0001	✓
17	9534	✓
16	9533	✓
15	2347	✓
14	2346	✓
13	6520	✓
12	9549	✓
11	9548	✓
10	9546	✓
9	2347	✓
8	2346	✓
7	5143	✓
6	8346	✓
5	3177	✓
4	26017	✓
3	3753	✓
2	29634	✓
1	512	SW
0	7503	✓

R#33
000044
001000
087:14:32:45 with No
Ins Cap
3/27/80

1 501 SW
087:14:32:44

R#34
0 00852
001000
087:14:33:07 with No
Ins Cap
3/27/80

1 504 SW
087:14:33:06

18	0001	V	18	0001	V
17	9562	%	17	9564	%
16	9562	%	16	9564	%
15	2224	%	15	2229	%
14	2224	%	14	2230	%
13	5890	%	13	5887	%
12	9559	%	12	9564	%
11	9559	%	11	9563	%
10	9559	%	10	9564	%
9	2225	%	9	2230	%
8	2224	%	8	2230	%
7	5155	%	7	5154	%
6	8898	%	6	8899	%
5	2784	%	5	2785	%
4	14963	V	4	14958	V
3	5602	V	3	5607	V
2	10059	W	2	10049	W
1	> 1605	tw	1	> 1605	tw
0	9395	G	0	9394	G

0	02822		0	02820	
	000001			000001	
093:15:24:26			093:15:50:35		
1	> 1602	tw	1	> 1602	tw
093:15:24:25			093:15:50:34		

18	0001	V	18	0001	V
17	9570	%	17	9566	%
16	9569	%	16	9566	%
15	2225	%	15	2228	%
14	2225	%	14	2228	%
13	5498	%	13	5496	%
12	9569	%	12	9565	%
11	9569	%	11	9564	%
10	9569	%	10	9564	%
9	2225	%	9	2227	%
8	2225	%	8	2227	%
7	5155	%	7	5156	%
6	8899	%	6	8898	%
5	2785	%	5	2787	%
4	14953	V	4	14955	V
3	5606	V	3	5606	V
2	10050	W	2	10050	W
1	504	tw	1	503	tw
0	7431	G	0	7444	G

0	00867	R# 37	0	00873	R# 38
	000001	21kw		000001	21kw
093:15:07:20		4/2/80	093:15:33:20		4/2/80
1	501	tw	1	501	tw
093:15:07:19			093:15:33:19		

SPENT FUEL CALORIMETER TEST

ENGINEER: WEEKS PAGE: 1 REF: D-34 (1Kw)
 TECHNICIAN: DELEE DATE: 31 MAR 1980 FINAL:

19	00001	V
18	00001	V
17	00001	V
16	9530	X
15	2312	X
14	2312	X
13	5882	X
12	9528	X
11	9528	X
10	9529	X
9	2312	X
8	2312	X
7	5419	X
6	8839	X
5	2729	X
4	14961	V
3	14961	V
2	10041	W
1	> 1604	W
0	9336	G
0	02768	
0	000001	
091:16:51:21		

19	00001	V
18	00001	V
17	00001	V
16	9528	X
15	2312	X
14	2312	X
13	5492	X
12	9527	X
11	9527	X
10	9526	X
9	2308	X
8	2312	X
7	5427	X
6	8839	X
5	2312	X
4	14954	V
3	14954	V
2	10040	W
1	> 1602	W
0	7422	G
0	00851	R# C1
0	000001	D 1 Kw
091:16:34:05 R# Run		

19	00001	V
18	00001	V
17	00001	V
16	9531	X
15	2312	X
14	2312	X
13	5376	X
12	9529	X
11	9528	X
10	9528	X
9	2313	X
8	2313	X
7	5419	X
6	8841	X
5	2725	X
4	14961	V
3	14961	V
2	10041	W
1	> 1604	W
0	9336	G
0	02751	
0	000001	
091:17:17:00		

19	00001	V
18	00001	V
17	9528	X
16	9528	X
15	2306	X
14	2309	X
13	5492	X
12	9527	X
11	9527	X
10	9526	X
9	2308	X
8	2308	X
7	5427	X
6	8839	X
5	2730	X
4	14959	V
3	14959	V
2	10040	W
1	> 1602	W
0	7422	G
0	00841	R# C2
0	000001	D 1 Kw
091:16:59:41 R# Run		
091:16:59:41 R# Run		
091:16:59:41 R# Run		

SPENT FUEL CALORIMETER TEST

ENGINEER: WEEKS
TECHNICIAN: DELEE

PAGE: 2

DATE: 2 APRIL 1980

REF:

FINAL: 0-34

19	00012	V
18	0001	V
17	9523	%
16	9524	%
15	3009	%
14	3009	%
13	6571	%
12	9525	%
11	9525	%
10	9525	%
9	3008	%
8	3007	%
7	5125	%
6	8912	%
5	2357	%
4	14959	V
3	5603	V
2	10046	V
1	> 3721	TW
0	13255	G

0	06630	
	000001	
	092:16:24:01	
1	> 3708	TW
	092:16:24:00	

19	00001	V
18	0001	V
17	9526	%
16	9527	%
15	3011	%
14	3011	%
13	5524	%
12	9533	%
11	9536	%
10	9534	%
9	3010	%
8	3010	%
7	5121	%
6	8912	%
5	2459	%
4	14957	V
3	5599	V
2	10043	V
1	> 510	TW
0	7542	G

RFC3
0 00919
000001 Fuel Assam
092:16:13:24 D-34 with
092:16:13:24 D-34 with
092:16:13:24 D-34 with
092:16:13:23 4/1/80
092:16:13:23 4/1/80
092:16:13:23 4/1/80
092:16:13:23 4/1/80

RFC4
0 00999 Fuel Assam
000001 Fuel Assam
092:16:13:46 D-34 with
092:16:13:46 D-34 with
092:16:13:46 D-34 with
092:16:13:46 4/1/80
092:16:13:46 4/1/80
092:16:13:46 4/1/80

SPENT FUEL CALORIMETER TEST

ENGINEER: WEEKS PAGE: 3 REF:
TECHNICIAN: DELEE DATE: 1 APRIL 1980 FINAL: D-34

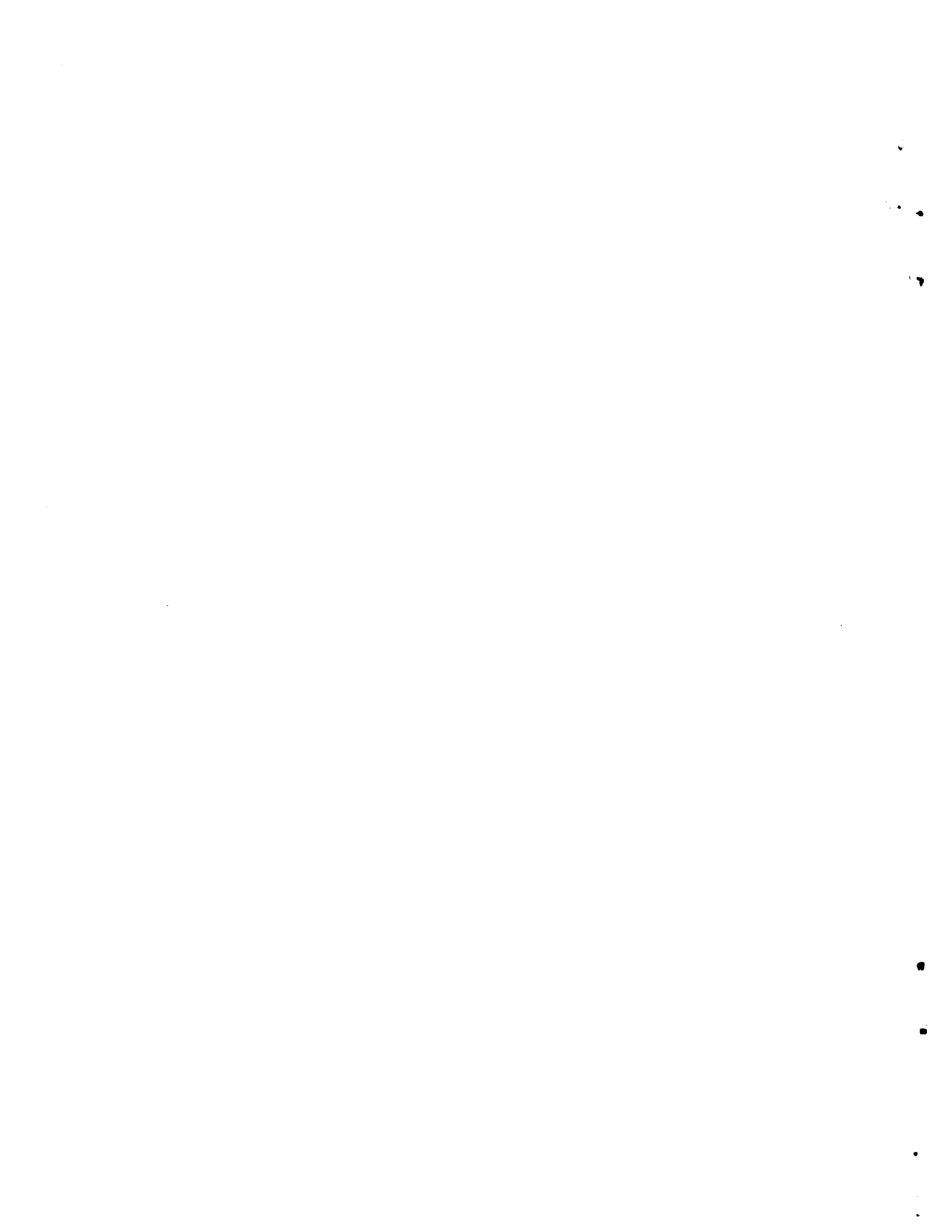
19	30301	Y	3	19	30302	V
18	30301	Y	3	18	30301	V
17	3493	Z	3	17	3493	V
16	3493	Z	3	16	3493	V
15	3023	X	3	15	3023	V
14	3023	X	3	14	3023	V
13	3023	X	3	13	6572	V
12	3493	Z	3	12	3493	V
11	9500	Z	3	11	2531	V
10	9500	Z	3	10	9490	V
9	3023	X	3	9	3023	V
8	3023	X	3	8	3023	V
7	3123	X	3	7	5120	V
6	8313	Z	3	6	5310	V
5	2363	Z	3	5	2357	V
4	14961	V	3	4	14963	V
3	5606	V	3	3	5607	V
2	10026	W	2	2	10054	V
1	> 3714	W	1	>	3717	V
0	13259	G.	0	0	13265	V

0 06632 06633
000001 000001
032:16:50:21 032:17:03:49
1 > 3702 tw 1 > 3705 t4
032:16:50:20 032:17:03:48

19	20002	V	19	-20000
18	0031	V	18	0001
17	9511	V	17	9499
16	9512	V	16	9498
15	9025	V	15	9030
14	3025	V	14	3031
13	5529	V	13	5537
12	9514	V	12	9493
11	9514	V	11	9492
10	9515	V	10	9492
9	3026	V	9	3030
8	3026	V	8	3030
7	5124	V	7	5125
6	8911	V	6	8912
5	2987	V	5	2958
4	14357	V	4	14360
3	5600	V	3	5600
2	10039	V	2	10036
1	518	V	1	521
0	7570	V	0	7600

0 60933 R#C5
000001 Final Return
092:16:39:47 D-34 with
water 0.01m
1 506 4/18/80
092:16:39:46

0 60972 R#C6
000001 Final Return
092:16:53:13 D-34 with
water 0.01m
1 509 4/18/80
092:16:53:14



APPENDIX C
DATA REDUCTION METHOD

DATA REDUCTION METHOD

The following sections present the method used in the data reduction process. The parameter of primary interest was the determination of the heat generation rate of the spent fuel assembly.

CALORIMETER PRESSURE

The pressure at the top of the calorimeter, i.e., in the "dome" above the water level, was printed out in Channel 7 by the data logger. Refer to Appendix B for raw data nomenclature and printouts. The unit of the Channel 7 printout was percent of full scale. The absolute pressure transducer used to measure "dome" pressure had a full-scale range of 25 psia. Therefore, pressure was computed as follows:

$$P_{cal} = (\text{Chan 7 Reading}/100) \cdot 25 \text{ psia} \quad (\text{C-1})$$

LATENT HEAT OF VAPORIZATION

The latent heat of vaporization, h_{fg} Btu/lb, was obtained from the steam tables at P_{cal} psia.

MASS ACCUMULATION RATE

Two methods were used to obtain mass accumulation rates. The primary method was measurement of the head accumulation rate in a precision collection tube with a differential pressure transmitter. The secondary or backup method was direct measurement of the weight of condensate accumulated. The equations required to calculate mass accumulation rates using these two methods are presented in the following sections.

Head Accumulation Measurement

The time to accumulate a selected amount of condensate in the collection apparatus was determined by subtracting the time of the initial data scan (empty collection tube) from the time of the final data scan (full or partially full tube), i.e., $\Delta t = (t_f - t_i)$ sec. The times are shown on the printouts in Appendix B.

The differential head of condensate collected during the accumulation time, Δt , was determined by differencing the final (H_f) and initial (H_i) heads (Channel 1) as shown below:

$$\Delta H = (H_f - H_i) \text{ in. H}_2\text{O} \quad (\text{C-2})$$

The differential pressure transducer indicated head at standard conditions 68°F.

The mass accumulation rate was obtained using the following equation:

$$\dot{m}_H = (K_H A_T \Delta H / \Delta t) \text{ lb/hr} \quad (\text{C-3})$$

where

K_H is a constant used to convert standard in. $H_2\text{O}$ to psi and seconds to hours: i.e., $K_H = (0.0361 \text{ psi/in. H}_2\text{O})(3600 \text{ sec/hr}) = 129.96 \text{ psi-sec/in. H}_2\text{O-hr}$

A_T is the area of the collection tube containing condensate, which is equal to the internal area of the collection tube, 1.094 in.^2 , minus the outer area of the "bubble" or "dip" tube, which extends into the collection tube, 0.049 in.^2 : $A_T = 1.094 - 0.049 = 1.045 \text{ in.}^2$

The equation reduces to

$$\dot{m}_H = (135.81 \Delta H / \Delta t) \text{ lb/hr} \quad (\text{C-4})$$

Weight Accumulation Measurement

The collection time for the weight accumulation measurement was obtained in the same manner as that previously discussed for the head accumulation measurement. The weight accumulated was determined by differencing the final weight accumulated (W_f) and the initial tare weight (W_i) printed out in Channel 0, and correcting for the buoyancy force created by the air-filled dip tube ($W_B = \rho_C A_D \Delta H$)

$$\Delta W = (W_f - W_i - W_B)g \quad (\text{C-5})$$

$$\dot{m}_W = (K_W \Delta W / \Delta t) \text{lb/hr} \quad (C-6)$$

where

K_W is a constant used to convert grams to pounds and seconds to hours;

$$\text{i.e., } K_W = (3600 \text{ sec/hr})(454 \text{ g/lb}) = 7.929 \text{ g.sec/(1b hr)}$$

The equation reduces to

$$\dot{m}_W = (7.929 \Delta W / \Delta t) \text{lb/hr} \quad (C-8)$$

CALORIMETER HEAT GENERATION MEASUREMENT

Heat generated in the calorimeter that produced boiling was determined using the mass accumulation rates measured with the differential head transmitter (\dot{m}_H) and the weigh scales (\dot{m}_W). Note that the calorimeter heat generation measurement was the total heat generated in the calorimeter minus heat losses, i.e., $q_{cal} = (q_{tot} - q_L) \text{kW}$. Equations used to determine calorimeter heat generation measurements from the two mass accumulation rate methods were

$$q_{cal,H} = (\dot{m}_H h_{fg} / 3412) \text{ kW, and} \quad (C-9)$$

$$q_{cal,W} = (\dot{m}_W h_{fg} / 3412) \text{ kW.} \quad (C-10)$$

CALORIMETER HEAT LOSSES

Heat losses from the calorimeter were determined by accurately measuring power to the reference dc heater and subtracting these values from the heat generation rates measured with the calorimeter. The equations used to calculate heat losses using the two mass accumulation rate measurement methods were

$$q_{L,H} = (q_h - q_{cal,H}) \text{ kW, and} \quad (C-11)$$

$$q_{L,W} = (q_h - q_{cal,W}) \text{ kW} \quad (C-12)$$

where q_h is the accurately measured reference heater power (Chan 3 x Chan 4), kW.

SPENT FUEL ASSEMBLY HEAT GENERATION RATES

The heat generation rates of spent fuel assemblies were determined using the equations identified in the following steps:

- 1) The system was brought to boiling and the dc reference heater was set at ~1.0 kW. After the system reached steady state, the mass accumulation rate (\dot{m}_R , lb/hr) resulting from the heat being generated by the reference heater (q_h , kW) less any heat losses ($q_{L,R}$, kW) from the system was measured. This reference heat generation rate was determined using the equation

$$q_R = q_h - q_{L,R} = (\dot{m}_R h_{fg,R} / 3412) \text{ kW} \quad (\text{C-13})$$

- 2) The heater power was maintained constant and a spent fuel assembly was inserted in the calorimeter. The final mass accumulation rate (\dot{m}_f lb/hr) was measured. This mass accumulation rate resulted from the heat generated by the reference heater, plus the heat generated by the spent fuel assembly (q_{SF}), minus any heat losses. The following equation was used to describe the final heat generation rate

$$q_f = q_{SF} + q_h - q_{L,SF} = (\dot{m}_f h_{fg,f} / 3412) \text{ kW} \quad (\text{C-14})$$

- 3) The heat generated by the spent fuel assembly was determined by subtracting the reference heat generation rate from the final rate as shown below:

$$\begin{aligned} q_f - q_R &= (q_{SF} + q_h - q_{L,SF}) - (q_h - q_{L,R}) \\ &= [(\dot{m}_f h_{fg,f} - \dot{m}_R h_{fg,R}) / 3412] \text{ kW} \end{aligned} \quad (\text{C-15})$$

$$\therefore q_{SF} = [(\dot{m}_f h_{fg,f} - \dot{m}_R h_{fg,R}) / 3412 + q_{L,SF} - q_{L,R}] \text{ kW} \quad (\text{C-16})$$

If the calorimeter heat losses were constant and if the calorimeter dome pressure was the same during the reference run (q_R) and the

final run (q_f), the latent heat of vaporization was also the same and the equation reduces to

$$q_{SF} = \left[(\dot{m}_f - \dot{m}_R) h_{fg} / 3412 \right] \text{ kW} \quad (C-17)$$

Because there were two methods used to measure mass accumulation rates, equations can be written for both the head accumulation method and the weight accumulation method, as follows:

$$q_{SF,H} = \left[(\dot{m}_{f,H} - \dot{m}_{R,H}) h_{fg} / 3412 \right] \text{ kW, and} \quad (C-18)$$

$$q_{SF,W} = \left[(\dot{m}_{f,W} - \dot{m}_{R,W}) h_{fg} / 3412 \right] \text{ kW.} \quad (C-19)$$

APPENDIX D

UNCERTAINTY ANALYSIS

UNCERTAINTY ESTIMATES

The following sections present details of the uncertainty analysis.

THEORETICAL APPROACH

Accuracies of the results of the calorimeter measurements were estimated using the uncertainty method presented by Schenck (1961, p. 40).^(a)

Consider the general case of a result R , which is a function of the two measured variables X and Y :

$$R_c + r_1 = f(X_c + x_1, Y_c + y_1) \quad (D-1)$$

If this function is continuous and has derivatives, it can be expanded in a "Taylor series", using the first two terms only:

$$R_c + r_1 = f(X_c, Y_c) + \left[\left(\frac{\partial R}{\partial X_c} \right)_y \frac{X_c + x_1 - X_c}{1} + \left(\frac{\partial R}{\partial Y_c} \right)_x \frac{Y_c + y_1 - Y_c}{1!} \right] \quad (D-2)$$

Or, since $R_c = f(X_c, Y_c)$:

$$r_1 = \left(\frac{\partial R}{\partial X_c} \right)_y x_1 + \left(\frac{\partial R}{\partial Y_c} \right)_x y_1 \quad (D.3)$$

where the lower case letters (r_1 , x_1 , and y_1) apply to deviations from the correct readings, and

$$\sum r^2 = \left(\frac{\partial R}{\partial X_c} \right)_y^2 \sum x^2 = 2 \left(\frac{\partial R}{\partial X_c} \right)_y \left(\frac{\partial R}{\partial Y_c} \right)_x \sum x y + \left(\frac{\partial R}{\partial Y_c} \right)_x^2 \sum y^2 \quad (D-4)$$

$\sum x y$ tends to zero and $s_r^2 = \sum r^2/n$ (standard deviation) so that

$$s_r^2 = \left(\frac{\partial R}{\partial X_c} \right)_y^2 s_x^2 + \left(\frac{\partial R}{\partial Y_c} \right)_x^2 s_y^2 \quad (D-4)$$

(a) This reference refers to main text reference list.

and, for any uncertainty interval ω ,

$$\omega_r^2 = \left(\frac{\partial R}{\partial X_c} \right)_y^2 \omega_x^2 + \left(\frac{\partial R}{\partial X_c} \right)_x^2 \omega_y^2. \quad (D-6)$$

ANALYSIS DETAILS

The uncertainty analysis presented in the following sections provides estimates of the uncertainties of each primary parameter measured or calculated from a combination of measured values. These uncertainty estimates were conservative and should enclose 95% of all measurements.

Collection Tube Wetted Area

The collection tube is a precision 1.25-in.-OD tube with a 0.035-in. wall. The tube contains a "bubble" tube 0.25 in. in diameter. The wetted cross sectional area, that area containing water during mass accumulation, is equal to

$$A_T = A_{1.18} - A_{0.25}$$

$$A_T = \pi(d_{1.18}^2 - d_{0.25}^2)/4$$

The diameters of the tubes are known within ± 0.002 inches. The uncertainty in A_T is

$$\omega_{A_T}^2 = \left(\frac{\partial A_T}{\partial d_{1.18}} \right)^2 \omega_{d_{1.18}}^2 + \left(\frac{\partial A_T}{\partial d_{0.25}} \right)^2 \omega_{d_{0.25}}^2$$

$$\omega_{A_T}^2 = \left(2\pi d_{1.18}/4 \right)^2 \cdot 0.002^2 + \left(-2\pi d_{0.25}/4 \right)^2 \cdot 0.002^2$$

$$\omega_{A_T}^2 = 1.4 \times 10^{-5} + 1.0 \times 10^{-6}$$

$$\omega_{A_T} = \pm 3.87 \times 10^{-3} \text{ in.}$$

In percent

$$\omega_{A_T} / A_T = \pm \frac{0.00387}{1.045} \approx \pm 0.4\%$$

Collection Tube Differential Head

The head accumulated in the collection tube during a data run was

$$\Delta H = (H_f - H_i) \text{ in. H}_2\text{O}$$

The final head (H_f) and the initial head (H_i) were measured within $\pm 0.5\%$ of full scale; i.e., ω_{H_f} and $\omega_{H_i} = \pm 0.005 \cdot 50 = \pm 0.25$ in. $H_2\text{O}$.

The uncertainty in ΔH can be determined using the uncertainty equation

$$\omega_{\Delta H}^2 = \left(\frac{\partial \Delta H}{\partial H_f} \right)^2 \omega_{H_f}^2 + \left(\frac{\partial \Delta H}{\partial H_i} \right)^2 \omega_{H_i}^2$$

$$\omega_{\Delta H}^2 = \omega_{H_f}^2 + \omega_{H_i}^2$$

During most of the data runs the initial head was 5 in. $H_2\text{O}$ and the final head was 16, 21, or 37 in. $H_2\text{O}$. Therefore,

$$\omega_{\Delta H} = (0.25^2 + 0.25^2)^{1/2} = \pm 0.35 \text{ in. H}_2\text{O}$$

In percentages

$$\omega_{\Delta H, 11} / \Delta H_{11} = \pm 0.35 / 11 = \pm 3.2\%$$

$$\omega_{\Delta H, 16} / \Delta H_{16} = \pm 0.35 / 16 = \pm 2.2\%$$

$$\omega_{\Delta H, 32} / \Delta H_{32} = \pm 0.35 / 32 = \pm 1.1\%$$

Mass Accumulation Time

The initial and final times of condensate accumulation were measured with the Fluke data logger. Each time was measured within ± 1 sec. The accumulation time is the difference between the final time (t_f) and the

initial time (t_i) as shown below.

$$\Delta t = (t_f - t_i) \text{ sec}$$

The uncertainty of Δt is

$$\omega_{\Delta t}^2 = \omega_{t_f}^2 + \omega_{t_i}^2$$

$$\omega_{\Delta t} = (1.0^2 + 1.0^2)^{1/2} = \pm 1.4 \text{ sec}$$

The shortest accumulation time was ~ 525 sec. The percent uncertainty is

$$\omega_{\Delta t}/\Delta t = 1.4/525 = \pm 0.27\%$$

Weight Accumulation

A weigh scale was used to obtain the weight of condensate accumulated over a period of time (Δt). The scale had an accuracy of $\pm 0.1\%$; however, an accuracy of $\pm 1\%$ was assumed because of the uncertainties resulting from contact between the "bubble" tube and collection tube, the resistance to movement caused by the collection tube alignment bearing, and the uneven loading on the scale platform caused by vibration from the collection tube solenoid drain valve during actuation. The uncertainty in the buoyancy force created by the air-filled dip tube, $W_B = \rho A_{DT} \Delta H$, was estimated to be $\pm 2\%$ using these uncertainty analysis methods.

The uncertainty in ΔW can be determined as follows:

$$\Delta W = W_f - W_i - W_B$$

$$\omega_{\Delta W}^2 = \omega_{W_f}^2 + \omega_{W_i}^2 + \omega_{W_B}^2$$

During most of the runs the initial weight was between ~ 740 or 755 g and the final weights were ~ 935 , 1030 , or 1325 g, depending on heat generation rates. Therefore, at $935 - 750 = 185$ g (~ 1 kW, $W_B = 8.8$ g),

$$\omega_{\Delta W} = (9.350^2 + 7.500^2 + 0.176^2)^{1/2} = \pm 11.99 \text{ g}$$

$$\text{or } \omega_{\Delta W} / 185 = 11.99 / 185 = \pm 6.5\%$$

$$\text{At } 1030 - 75 = 280 \text{ g } (\sim 1.5 \text{ kW}, W_B = 12.79 \text{ g}),$$

$$\omega_{\Delta W} = (10.300^2 + 7.500^2 - 0.256^2) = \pm 12.74 \text{ g}$$

$$\text{or } \omega_{\Delta W} / 280 = (12.74 / 280 = \pm 4.6\%)$$

$$\text{At } 1325 - 750 = 575 \text{ g } (\sim 2 \text{ to } 3 \text{ kW}, W_B = 25.58 \text{ g}),$$

$$\omega_{\Delta W} = (13.250^2 + 7.500^2 + 0.512^2) = \pm 15.23 \text{ g}$$

$$\text{or } \omega_{\Delta W} / 575 = 15.23 / 575 = \pm 2.6\%$$

Mass Accumulation Rate

The mass accumulation rate determined using the differential head method required the following equation:

$$\dot{m}_H = K_H A_T \Delta H / \Delta t$$

The uncertainty of \dot{m}_H was estimated as follows:

$$\omega_{\dot{m}_H}^2 = \left(\frac{\partial \dot{m}_H}{\partial A_T} \right)^2 \omega_{A_T}^2 + \left(\frac{\partial \dot{m}_H}{\partial \Delta H} \right)^2 \omega_{\Delta H}^2 + \left(\frac{\partial \dot{m}_H}{\partial \Delta t} \right)^2 \omega_{\Delta t}^2$$

$$\omega_{\dot{m}_H}^2 = (K_H \Delta H / \Delta t)^2 \omega_{A_T}^2 + (K_H A_T / \Delta t)^2 \omega_{\Delta H}^2 + (-1 K_H A_T \Delta H \Delta t^{-2})^2 \omega_{\Delta t}^2$$

For a typical $\Delta H = 11$ in. H_2O run (~ 1 kW)

$$\omega_{\dot{m}_H, 11}^2 = (129.96 \cdot 11 / 1055)^2 \cdot (3.87 \times 10^{-3})^2$$

$$+ (129.96 \cdot 1.045 / 1055)^2 \cdot 0.35^2$$

$$+ (129.96 \cdot 1.045 \cdot 11 / 1055)^2 \cdot 2.85^2$$

$$\omega_{\dot{m}_H, 11}^2 = 2.7 \times 10^{-5} = 2.03 \times 10^{-3} + 1.5 \times 10^{-5}$$

$$\omega_{\dot{m}_{H,11}} = \pm 0.046 \text{ lb/hr}$$

In percentage

$$\omega_{\dot{m}_{H,11}} / \dot{m}_{H,11} = \pm 0.046 / 1.413 = \pm 3.2\%$$

For an ~3 kW run ($\Delta H = 32$ in. H₂O and $\Delta t = 522$ sec) the uncertainty is

$$\omega_{\dot{m}_{H,32}}^2 = (129.96 \cdot 32/522)^2 \cdot (3.87 \times 10^{-3})^2$$

$$+ (129.96 \cdot 1.045/522)^2 \cdot 0.35^2$$

$$+ (129.96 \cdot 1.045 \cdot 32/522^2)^2 \cdot 1.4^2$$

$$\omega_{\dot{m}_{H,32}}^2 = 9.51 \times 10^{-4} + 8.29 \times 10^{-3} + 5.0 \times 10^{-4}$$

$$\omega_{\dot{m}_{H,32}} = \pm 0.099 \text{ lb/hr}$$

$$\text{or } \omega_{\dot{m}_{H,32}} / \dot{m}_{H,32} = 0.099 / 8.3 = \pm 1.2\%$$

The following equations are used to determine the uncertainty in the mass accumulation rate obtained from weight accumulation measurements:

$$\dot{m}_w = 7.929 \Delta W / \Delta t \text{ lb/hr}$$

$$\omega_{\dot{m}_w}^2 = \left(\frac{\partial \dot{m}_w}{\partial \Delta W} \right)^2 \omega_{\Delta W}^2 + \left(\frac{\partial \dot{m}_w}{\partial \Delta t} \right)^2 \omega_{\Delta t}^2$$

$$\omega_{\dot{m}_w}^2 = (7.929 / \Delta t)^2 \omega_{\Delta W}^2 + (-7.929 \Delta t^{-2})^2 \omega_{\Delta t}^2$$

For a typical run at 1 kW, $\Delta W \approx 193$ g, $\Delta t \approx 1035$ sec, and

$$\omega_{\dot{m}_w}^2 = (7.929 / 1035)^2 \cdot 12^2 + (-7.929 \cdot 1035^{-2})^2 \cdot 2.79^2$$

$$\omega_{\dot{m}_W}^2 = 0.0085 + 4.26 \times 10^{-10}$$

$$\omega_{\dot{m}_W} = \pm 0.092 \text{ lb/hr}$$

or $\omega_{\dot{m}_W} / \dot{m}_W = 0.92/1.45 \approx \pm 6.3\%$

Note the time uncertainty term is negligible.

For a $\Delta W \sim 572 \text{ g}$ run ($\sim 3 \text{ kW}$), $\Delta t \approx 522 \text{ sec}$ and

$$\omega_{\dot{m}_W}^2 = (7.929/522)^2 \cdot 15.23^2 + (-7.929 \cdot 522^{-2})^2 \cdot 1.4^2$$

$$\omega_{\dot{m}_W}^2 = 0.054 + 1.66 \times 10^{-9}$$

$$\omega_{\dot{m}_W} = \pm 0.23 \text{ lb/hr}$$

or $\omega_{\dot{m}_W} / \dot{m}_W = 0.23/8.7 = \pm 2.7\%$

The time uncertainty term is again negligible.

Pressure

The absolute pressure transmitter used to measure the calorimeter "dome" pressure (P_{cal}) above the water level was accurate within $\pm 0.25\%$ of full scale (25 psia). The signal from the transmitter was passed through a signal conditioner and read out on the Fluke data logger. Therefore, it was assumed that the accuracy of pressure measurements was $\pm 0.5\%$ of full scale ($\pm 0.125 \text{ psia}$).

Latent Heat of Vaporization

The latent heat of vaporization was obtained from the steam tables at the "dome" pressure. The absolute pressure ranged between 12.5 and 13.0 psia during testing. The range of the latent heat (h_{fg}) corresponding to this pressure range was 975.4 Btu/lb to 974.2 Btu/lb, respectively. The uncertainty of the latent heat can be estimated using the accuracy of the

pressure measurement as follows:

$$\Delta h_{fg}/\Delta P_{cal} = (975.4 - 974.2)/(13.0 - 12.5)$$

$$\Delta h_{fg}/\Delta P_{cal} = 2.4 \text{ Btu}/(1 \text{b} \cdot \text{psia})$$

The uncertainty of P_{cal} was $\pm 0.125 \text{ psia}$, therefore,

$$\omega_{h_{fg}} = \omega_{P_{cal}} \cdot \Delta h_{fg}/\Delta P = \pm 0.125 \text{ psia} \cdot 2.4 \text{ Btu}/(1 \text{b} \cdot \text{psia})$$

$$\omega_{h_{fg}} = \pm 0.3 \text{ Btu}/1 \text{b}$$

In percentage

$$\omega_{h_{fg}}/h_{fg} = \pm 0.3/974.8 = \pm 0.03\%$$

Calorimeter Heat Generation Measurement

The calorimeter measurements of heat generation rates using the head accumulation method required the following equation:

$$q_{cal,H} = (\dot{m}_H h_{fg}/3412) \text{ kW}$$

The uncertainty in $q_{cal,H}$ can be estimated as follows:

$$\omega_{q_{cal,H}}^2 = (h_{fg}/3412)^2 \omega_{\dot{m}_H}^2 + (\dot{m}_H/3412)^2 \omega_{h_{fg}}^2$$

For a low heat generation rate the uncertainty in $q_{cal,H}$ ($\omega_{q_{cal,H}}$) is relatively large because $\omega_{\dot{m}_H}$ is relatively large. The uncertainty in $q_{cal,H}$ is

$$\omega_{q_{cal,H}}^2 = (974.8/3412)^2 \cdot 0.045^2 + (1.413/3412)^2 \cdot 0.3^2$$

$$\omega_{q_{cal,H}}^2 = 1.65 \times 10^{-4} + 1.54 \times 10^{-8} \text{ kW}^2$$

$$\omega_{q_{cal,H}} = \pm 0.0128 \text{ kW}$$

In percentage

$$\omega_{q_{cal,H}}^2 / q_{cal,W} = 0.0128/0.386 = \pm 3.3\%$$

Estimates of heat generation rate measurements using the weigh scale method are identical to those using the head method except \dot{m}_H must be replaced with \dot{m}_W . The uncertainty in $q_{cal,W}$ is estimated below:

$$\omega_{q_{cal,W}}^2 = (h_{fg}/3412)^2 \omega_{\dot{m}_W}^2 + (m_W/3412)^2 \omega_{h_{fg}}^2$$

$$\omega_{q_{cal,W}}^2 = (974.8/3412)^2 \cdot 0.092^2 + (1.45/3412)^2 \cdot 0.3^2$$

$$\omega_{q_{cal,W}}^2 = 6.91 \times 10^{-4} + 1.63 \times 10^{-8} \text{ kW}^2$$

$$\omega_{q_{cal,W}} = \pm 0.026 \text{ kW}$$

In percentage

$$\omega_{q_{cal,W}}^2 / q_{cal,W} = 0.026/0.386 = \pm 6.8\%$$

Heater Power

The heat generated by the dc reference heater was determined by the product of the voltage drop across the heater and the current passing through the heater. The heater voltage drop was measured with a voltmeter which had an accuracy of $\pm 0.0006\%$ of the reading. During testing the signal was observed to fluctuate $\pm 0.2\%$. Because the reading printed by the data logger was instantaneous, this value ($\pm 0.2\%$) was assumed for heater voltage uncertainty.

The current passing through the heater was obtained by measuring the voltage across a series precision resistor. The voltmeter had a quoted accuracy of $\pm 0.0006\%$ of reading, but the signal fluctuated $\sim \pm 0.1\%$ during measurement. Therefore, this value ($\pm 0.1\%$) was assumed for the uncertainty of the resistor voltage drop and the uncertainty of heater current was estimated

as follows:

$$I_R = V_R / R_R = I_h$$

$$\omega_{I_h}^2 = (1/R_R)^2 \omega_{V_R}^2 = (-V_R R_R^{-2}) \omega_{R_R}^2$$

At high heater powers (~ 3 kW) V_R is relatively high so $\omega_{I_h}^2$ will be high:

$$\begin{aligned} \omega_{I_h}^2 &= (1/0.003327)^2 (4.2 \times 10^{-5})^2 \\ &+ (-0.0417 \cdot 0.003327^{-2})^2 \cdot (7 \times 10^{-6})^2 \end{aligned}$$

$$\omega_{I_h}^2 = 1.59 \times 10^{-4} + 6.95 \times 10^{-4} \text{ A}^2$$

$$\omega_{I_h} = \pm 0.029 \text{ A}$$

In percentage

$$\omega_{I_h} / I_h = 0.029 / 12.5 = \pm 0.23\%$$

The uncertainty in heater power can be estimated as shown below:

$$q_h = V_h I_h$$

$$\omega_{q_h}^2 = I_h^2 \omega_{V_h}^2 + V_h^2 \omega_{I_h}^2$$

At relatively high powers (~ 3 kW) I_h and V_h will be high, resulting in a relatively high ω_{q_h} , therefore

$$\omega_{q_h}^2 = 12.52^2 \cdot 0.48^2 + 240.2^2 \cdot 0/125^2$$

$$\omega_{q_h}^2 = 36.12 + 901.5 \text{ W}^2$$

$$\omega_{q_h} = 30.6 \text{ W}$$

In percentage

$$\omega_{q_h} / q_h = 30.6/3000 = \pm 1\%$$

Calorimeter Heat Loss

Heat losses from the calorimeter were determined using results from the head accumulation method and the weight accumulation method as shown in the following two equations:

$$q_{L,H} = (q_h - q_{cal,H})kW$$

$$q_{L,W} = (q_h - q_{cal,W})kW$$

The uncertainty equations are

$$\omega_{q_{L,H}}^2 = \omega_{q_h}^2 + \omega_{q_{cal,H}}^2 \text{ and}$$

$$\omega_{q_{L,W}}^2 = \omega_{q_h}^2 + \omega_{q_{cal,W}}^2$$

At a reference heater power of ~ 2 kW, the uncertainties are

$$\omega_{q_{L,H}}^2 = 0.031^2 + 0.013^2$$

$$\omega_{q_{L,H}}^2 = 9.61 \times 10^{-4} + 1.69 \times 10^{-4}$$

$$\omega_{q_{L,H}} = \pm 0.034 \text{ kW or } 0.034/0.596 = \pm 5.6\%$$

and $\omega_{q_{L,W}}^2 = 0.031^2 + 0.026^2$

$$\omega_{q_{L,W}} = \pm 0.040 \text{ kW or } 0.040/0.553 = \pm 7.2\%$$

Spent Fuel Assembly Heat Generation Rate Measurement

The heat generation rate of a spent fuel assembly was measured with the calorimeter using the head and weight accumulation methods. The equations

used to obtain assembly heat generation rates were

$$q_{SF,H} = \left[(\dot{m}_{f,H} - \dot{m}_{R,H}) h_{fg} / 3412 + q_{L,f,H} - q_{L,R,H} \right] \text{ kW}$$

$$\text{and } q_{SF,W} = \left[(\dot{m}_{f,W} - \dot{m}_{R,W}) h_{fg} / 3412 + q_{L,f,W} - q_{L,R,W} \right] \text{ kW}$$

The resulting uncertainty equations become

$$\begin{aligned} \omega_{q_{SF,H}}^2 &= (h_{fg}/3412)^2 \omega_{\dot{m}_{f,H}}^2 + (-h_{fg}/3412)^2 \omega_{\dot{m}_{R,H}}^2 \\ &+ [(\dot{m}_{f,H} - \dot{m}_{R,H})/3412]^2 \omega_{h_{fg}}^2 + \omega_{q_{L,f,H}}^2 + \omega_{q_{L,R,H}}^2 \end{aligned}$$

and,

$$\begin{aligned} \omega_{q_{SF,W}}^2 &= (h_{fg}/3412)^2 \omega_{\dot{m}_{f,W}}^2 + (-h_{fg}/3412)^2 \omega_{\dot{m}_{R,W}}^2 \\ &+ [(\dot{m}_{f,W} - \dot{m}_{R,W})/3412]^2 \omega_{h_{fg}}^2 + \omega_{q_{L,f,W}}^2 + \omega_{q_{L,R,W}}^2 \end{aligned}$$

The uncertainties can be found as follows:

$$\begin{aligned} \omega_{q_{SF,H}}^2 &= (974.8/3412)^2 \cdot 0.099^2 + (-974.8/3412)^2 \cdot 0.046^2 \\ &+ [(6.875 - 1.442)/3412]^2 \cdot 0.3^2 + 0.035^2 + 0.035^2 \end{aligned}$$

$$\begin{aligned} \omega_{q_{SF,W}}^2 &= (974.8/3412)^2 \cdot 0.23^2 + (-974.8/3412)^2 \cdot 0.92^2 \\ &+ [(7.151 - 1.466)/3412]^2 \cdot 0.3^2 + 0.040^2 + 0.040^2 \end{aligned}$$

$$\begin{aligned} \therefore \omega_{q_{SF,H}}^2 &= 7.6 \times 10^{-4} + 1.65 \times 10^{-4} + 2.28 \times 10^{-7} + 1.2 \times 10^{-3} \\ &+ 1.2 \times 10^{-3} \end{aligned}$$

$$\begin{aligned} \therefore \omega_{q_{SF,W}}^2 &= 4.3 \times 10^{-3} + 6.9 \times 10^{-4} + 2.49 \times 10^{-7} + 1.6 \times 10^{-3} \\ &+ 1.6 \times 10^{-3} \end{aligned}$$

Note that the uncertainties introduced by the latent heat are negligible and the heat loss uncertainties are significant.

$$\omega_{q_{SF,H}} = \pm 0.058 \text{ kW}$$

$$\omega_{q_{SF,W}} = \pm 0.091 \text{ kW}$$

In percentages

$$\omega_{q_{SF,H}} / q_{SF,H} = 0.058 / 1.55 \sim \pm 3.7\%$$

$$\omega_{q_{SF,W}} / q_{SF,W} = 0.091 / 1.55 \sim \pm 5.9\%$$



DISTRIBUTION

<u>No. of Copies</u>	<u>No. of Copies</u>
<u>OFFSITE</u>	
A. A. Churm DOE Chicago Patent Division 9800 South Cass Avenue Argonne, IL 60439	T. E. Cross Westinghouse Advanced Energy System Division P. O. Box 10864 Pittsburgh, PA 15236
342 DOE Technical Information Center	J. B. Wright Westinghouse Advanced Energy System Division P. O. Box 10864 Pittsburgh, PA 15236
5 E. F. Benz Battelle Memorial Institute Office of Nuclear Waste Isolation 505 King Avenue Columbus, OH 43201	J. B. Delee EMAD Facility Westinghouse Advanced Energy Systems Division P. O. Box 708 Mercury, NV 89023
J. A. Carr Battelle Memorial Institute Office of Nuclear Waste Isolation 505 King Avenue Columbus, OH 43201	C. B. Dimmerling EMAD Facility Westinghouse Advanced Energy Systems Division P. O. Box 708 Mercury, NV 89023
J. E. Monsees Battelle Memorial Institute Office of Nuclear Waste Isolation 505 King Avenue Columbus, OH 43201	J. C. Dobbins EMAD Facility Westinghouse Advanced Energy Systems Division P. O. Box 708 Mercury, NV 89023
Beverly Rawls Battelle Memorial Institute Office of Nuclear Waste Isolation 505 King Avenue Columbus, OH 43201	D. C. Durrill EMAD Facility Westinghouse Advanced Energy Systems Division P. O. Box 708 Mercury, NV 89023
Harold Rothstein Ebasco Services Inc. 2 World Trade Center New York, NY 10048	

<u>No. of Copies</u>	<u>No. of Copies</u>	
A. Hakl EMAD Facility Westinghouse Advanced Energy Systems Division P. O. Box 708 Mercury, NV 89023	2 C. R. Cooley U. S. Department of Energy Headquarters Mail Stop B-107 Washington, DC 20545	
B. L. Robbins EMAD Facility Westinghouse Advanced Energy Systems Division P. O. Box 708 Mercury, NV 89023	O. W. Gormley U. S. Department of Energy Headquarters Mail Stop B-107 Washington, DC 20545	
M. R. Secord EMAD Facility Westinghouse Advanced Energy Systems Division P. O. Box 708 Mercury, NV 89023	C. A. Heath U. S. Department of Energy Headquarters Mail Stop B-107 Washington, DC 20545	
A. P. Weber EMAD Facility Westinghouse Advanced Energy Systems Division P. O. Box 708 Mercury, NV 89023	D. Vieth U. S. Department of Energy Headquarters Mail Stop B-107 Washington, DC 20545	
R. M. Nelson U. S. Department of Energy Nevada Operations Office P. O. Box 14100 Las Vegas, Nevada 89114	<u>ONSITE</u>	
A. J. Roberts U. S. Department of Energy Nevada Operations Office P. O. Box 14100 Las Vegas, Nevada 89114	14 <u>Hanford Engineering Development Laboratory</u>	D. M. Bosi (2) R. J. Cash (2) R. E. Einziger R. L. Fish (2) S. E. Girault R. L. Knecht J. C. Krogness R. E. Schenter F. A. Schmitroth W. F. Sheely H. H. Yoshikawa
J. O. Neff U. S. Department of Energy Columbus Program Office Richland Operations Office 505 King Avenue Columbus, Ohio 43201	<u>DOE Richland Operations Office</u>	
	H. E. Ransom	

No. of
Copies

ONSITE

32 Pacific Northwest Laboratory

W. J. Apley
J. M. Creer (12)
K. M. Harmon
A. J. Haverfield
W. W. Laity
L. T. Lakey
R. G. Nelson
A. M. Platt
R. A. Scoggin
J. W. Shupe, Jr.
A. M. Sutey
H. M. Woods
F. R. Zaloudek
G. E. Zima
Publishing Coordination (2)
Technical Information (5)

5 DOE Fast Flux Test Facility
Program Office

Director

